Developing a 3-Dimensional Kinematic Model of the Hand for Ergonomic Analyses of Hand Posture, Hand Space Envelope, and Tendon Excursion

by

Jaewon Choi

A dissertation submitted in partial fulfillment
of the requirements for the degree of
Doctor of Philosophy
(Mechanical Engineering)
in The University of Michigan
2008

Doctoral Committee:

Professor Thomas J. Armstrong, Co-Chair

Research Professor James A. Ashton-Miller, Co-Chair

Professor Kevin C. Chung

Professor Brent Gillespie

To my family

Acknowledgements

This dissertation could not have been possible without the support, guidance, and efforts of many people. Because of them, past years that I spent at the University of Michigan have been the greatest moments that I will cherish forever.

I would like to give my deepest gratitude to my advisor, Professor Thomas Armstrong, for his advice, guidance, and support. His mentorship was paramount in providing great inspiration and gentle guidance, both of which encouraged me to pursue my interests throughout my research. He also showed endless enthusiasm in the research, which incited me to greater effort. I would also like to acknowledge co-chair, Professor James Ashton-Miller, for his stimulating suggestions and encouragement. I am deeply indebted to my other committee members, Dr. Kevin Chung and Professor Brent Gillespie, whose valuable comments and advice made this dissertation better.

I am grateful to faculties in Center for Ergonomics, Professor Don Chaffin, Professor Bernard Martin, Dr. Matt Reed, Dr. Sheryl Ulin, for their continuous interests in my research, support, and advice.

I would like to take this opportunity to thank the staffs in department who contributed to this work in innumerable ways – James Foulke, Charles Woolley, Eyvind Claxton, Randy Rabourn, Mint Rahaman, Christopher Konrad, Rod Capps, and Tina Blay.

My thanks go out to my colleagues, Michael Lau, Chris Grieshaber, Marrissa Ebersole, Najin Seo, Sungchan Bae, and Justin Young, for sharing the precious memory with me. I could enjoy my graduate life because of them.

Most importantly, none of this would have been possible without the love, support, and patience of my family. I thank my mom and dad for praying for me with endless love. I would like to express my loving appreciation to my wife, Jung Hei Kim, my son, Allen Eugene Choi, for their love, patience, and encouragement.

Table of Contents

List of Figures

List of Tables

List of Appendices

Nomenclature

MCP : Metacarpophalangeal Joint

PIP : Proximal Interphalangeal Joint

DIP : Distal Interphalangeal Joint

IP : Interphalangeal Joint (Thumb)

CMC : Carpometacarpal Joint (Thumb)

DOF : Degree of Freedom

F/E : Flexion-Extension

ABD/ABB : Abduction-Adduction

P/S : Pronation-Supination

MCPFE : Flexion-Extension of MCP Joint (Thumb)

MCPAA : Abduction-Adduction of MCP Joint (Thumb)

CMCFE : Flexion-Extension of CMC Joint (Thumb)

CMCAA : Abduction-Adduction of CMC Joint (Thumb)

CMCPS : Pronation-Supination of CMC Joint (Thumb)

FDP : Flexor Digitorum Profundus

FDS : Flexor Digitorum Superficialis

MSD : Musculoskeletal Disorder

WRMSD : Work-Related Musculoskeletal Disorder

Lg : Large (Object Size)

Med : Medium (Object Size)

Sm : Small (Object Size)

R^2 : Coefficient of Determinant

CHAPTER 1

INTRODUCTION

1.1 THESIS STATEMENT

The posture of the hand can be predicted with a 3-D kinematic model that uses a contact algorithm with appropriate finger joint movement patterns. It is the thesis of this work that the 3-D kinematic model can be used for ergonomic analyses of predicting hand posture, estimating hand space envelope, and assessing tendon excursion during specific tasks.

1.2 RESEARCH OBJECTIVES

The goal of this research was to evaluate the above thesis. Towards this end, the following objectives were established.

- Development of a 3-D kinematic model: Develop a 3-D kinematic model of the hand with a contact algorithm to predict hand posture for a given hand size, object properties, and task properties.
- Estimation of a hand space envelope: Simulate the required space for a specific task, using the 3-D kinematic model.
- Quantitative analysis of finger movements during reaching and grasping: Analyze the finger movement patterns which depend on object properties and grip types.

- Investigation of the relationship between tendon excursion and the risk of MSDs (musculoskeletal disorders): Investigate the association of tendon excursion and the risk of MSDs by time-based analysis.

1.3 RATIONALE

The human hand is an essential part of our interactions with the environment during activities of daily living, work, and leisure. We use our hands to grasp, hold, manipulate an object, or support the body (MacKenzie and Iberall 1994; Brand and Hollister 1999). In industrial environments, proper design of work objects and work space that considers the properties of the hand is necessary to increase workers' productivity, safety of workers, and efficiency. In spite of the importance of the hand, models of the hand have not reached the sophisticate level of current models of the whole body (Armstrong, Choi et al. 2008). Considering the usefulness and importance of human modeling for proactive injury prevention, development and improvement of better hand models may be of great value in solving many current ergonomics problems.

Ergonomic analyses of hand function remain a challenge for engineers and designers. The hand strength is closely related to hand posture as different hand postures change the characteristics of the muscles which determine the force and moment at each joint of the hand (Mathiowetz, Kashman et al. 1985; Imrhan and Loo 1989; Crosby, Wehbe et al. 1994; Josty, Tyler et al. 1997; Blackwell, Kornatz et al. 1999; Yan and Downing 2001). The required work envelope for the hand is also determined by hand posture which, in turn, is affected by properties of the grip object and hand size (Choi, Grieshaber et al. 2007; Grieshaber 2007). Knowledge of hand posture is imperative for tendon excursions – which have been implicated in the etiology of repetitive trauma disorders (Moore 2002) - to be predicted, because tendon

displacement is determined by the joint angles of the finger (Landsmeer 1961; Landsmeer 1961; Armstrong and Chaffin 1978).

Many studies have been conducted to qualitatively describe hand posture by relating to object size, required force, and purpose of grip (Napier 1956; Landsmeer 1962; Cutkosky 1989; Grieshaber 2007). Only a few quantitative studies of hand posture have been completed. Buchholz developed a kinematic model using ellipsoids to evaluate prehensile capabilities (Buchholz and Armstrong 1992). The model was used to simulate and predict the prehensile posture of the hand for power grasp of objects that can be described as ellipsoids or elliptical cylinders. Lee and Zhang (2005) suggested a model to predict hand posture using optimization under the premise that the hand configuration in a power prehension best conforms to the shape of the object. These models explained how the grip posture varies in power grip, but were not sufficient to explain other types of postures (e.g., lateral pinch, pulp pinch). Also, they cannot be applied to object shapes that cannot be represented mathematically. Using a contact algorithm to find a posture is effective for complicated object shapes, because the object geometry can be easily imported to the model in the form of an array of points. Recently, some researchers and commercial softwares have used a contact algorithm to predict hand posture (Pollard and Zordan 2005; Endo and Kanai 2006; Miyata, Kouchi et al. 2006); however, posture predictions using these models have not been evaluated. Also, it is not clear how hand movement is modeled, which affects posture prediction (Armstrong, Choi et al. 2008).

A kinematic hand model can be used not only for predicting hand posture but also for estimating the hand space envelope and tendon excursions, both of which are directly related to the hand geometry and movements. Information about hand space envelope can help designers and engineers to design work space and work objects

avoiding obstruction problems. Obstruction problems occurs when performing a task in narrow and confined or crowded space. Examples of obstruction problems are such jobs as joining parts (e.g., hose placement in an engine compartment, connector assembly) or using tools (e.g., vehicle maintenance, oral surgery). Obstructions penetrating hand space often interfere with workers' ability to perform the task and results in loss of productivity and workers' safety. Therefore, a model to estimate hand space envelope for varying hand size, object size, and behaviors is needed to design a work environment minimizing interference from obstructions.

Tendon excursion has been used as one of the measures that indicates the risk of upper extremity musculoskeletal disorders such as carpal tunnel syndrome and tendinitis (Moore, Wells et al. 1991; Marras and Schoenmarklin 1993; Wells, Moore et al. 1994; Wells, Moore et al. 1994; Sommerich, Marras et al. 1996; Marklin and Monroe 1998; Serina, Tal et al. 1999). Highly repetitive motion leads to high tendon excursions which cause biomechanical stress on the tendon and surrounding tissues. Many models to predict tendon displacement for given finger joint angles have been proposed (Landsmeer 1961; Landsmeer 1961; Landsmeer 1962; Armstrong and Chaffin 1978). However, to predict tendon excursions during some specific movements, we first need accurate prediction of hand posture.

In summary, development of a kinematic model that predicts hand posture is fundamental and necessary to estimate hand strength, required space envelopes, and tendon excursions for a specific task. A well-developed model of the hand will be highly helpful to engineers by helping them to approach the ergonomic issues proactively.

1.4 DISSERTATION ORGANIZATION

This dissertation combines a series of four manuscripts, along with introductory and concluding chapters.

Chapter 2 describes the development of a 3-D kinematic model of the hand that predicts hand posture, including a detailed description of the model and validation of the model through experiments, and a discussion of the sensitivity of the model to various input parameters.

Chapter 3 describes the estimation of a hand space envelope during a hose placement task. By prediction of hand posture using the 3-D kinematic model and modeling of behavioral characteristics of the hose placement task, a required space was estimated. The simulated space envelope was validated by comparing it with the measured space envelope.

Chapter 4 presents a quantitative analysis of finger movements during reaching and grasping. Spatial and temporal variables that depict finger motion during grasping were investigated so that the resulting data can be applied to actuation of the 3-D kinematic model.

Chapter 5 addresses the relationship between tendon excursion and the risk of MSDs by investigating hand activity level and tendon excursions at the wrist. Re-analysis of Latko's data (Latko, Armstrong et al. 1999) was performed through a time-based analysis. This study illustrates the potential use of the 3-D kinematic model for estimating tendon excursions caused by finger motions as well as wrist motions.

Finally, Chapter 6 concludes the dissertation with a summary of major findings, general discussions of the results, and suggestions for future studies.

Appendix A includes a detailed description of the model structure in the Visual C++ environment.

1.5 REFERENCES

Armstrong, T. J. and D. B. Chaffin (1978). "An inverstigation of the relationship between displacements of the finger and wrist joints and the extrinsic finger flexor tendons." Journal of biomechanics 11: 119-128.

Armstrong, T. J., J. Choi and V. Ahuja (2008). Development of kinematic and biomechanical hand models for ergonomic applications. Handbook of Digital human Modeling. V. G. Duffy, CRC Press.

Blackwell, J. R., K. W. Kornatz and E. M. Heath (1999). "Effect of grip span on maximal grip force and fatigue of flexor digitorum superficialis." Appl Ergon 30(5): 401-5.

Brand, P. W. and A. M. Hollister (1999). Clinical Mechanics of the Hand. St. Louis, Mosby.

Buchholz, B. and T. J. Armstrong (1992). "A kinematic model of the human hand to evaluate its prehensile capabilities." J Biomech 25(2): 149-62.

Choi, J., C. D. Grieshaber and T. J. Armstrong (2007). Estimation of grasp envelope using a 3-dimensional kinematic model of the hand. Human Factors and Ergonomics Society Annual Meeting, Baltimore, MD.

Crosby, C. A., M. A. Wehbe and B. Mawr (1994). "Hand strength: normative values." J Hand Surg [Am] 19(4): 665-70.

Cutkosky, M. R. (1989). "On grasp choice, grasp models and the design of hands for manufacturing tasks." IEEE Transactions on Robotics and Automation 5(3): 269-279.

Endo, Y. and S. Kanai (2006). An Application of a Digital Hand to Ergonomic Assessment of Handheld Information Appliances. Digital Human Modeling for Design and Engineering Conference, Lyon, France.

Grieshaber, C. D. (2007). Factors affecting hand posture and one-handed push force during flexible rubber hose insertions tasks. Industrial and Operations Engineering. Ann Arbor, University of Michigan.

Imrhan, S. N. and C. H. Loo (1989). "Trends in finger pinch strength in children, adults, and the elderly." Hum Factors 31(6): 689-701.

Josty, I. C., M. P. Tyler, P. C. Shewell, et al. (1997). "Grip and pinch strength variations in different types of workers." J Hand Surg [Br] 22(2): 266-9.

Landsmeer, J. M. (1961). "Studies in the anatomy of articulation. I. The equilibrium of the "intercalated" bone." Acta Morphol Neerl Scand 3: 287-303.

Landsmeer, J. M. (1961). "Studies in the anatomy of articulation. II. Patterns of movement of bi-muscular, bi-articular systems." Acta Morphol Neerl Scand 3: 304-21.

Landsmeer, J. M. (1962). "Power grip and precision handling." Ann Rheum Dis 21: 164-70.

Latko, W. A., T. J. Armstrong, A. Franzblau, et al. (1999). "Cross-sectional study of the relationship between repetitive work and the prevalence of upper limb musculoskeletal disorders." Am J Ind Med 36(2): 248-59.

Lee, S. W. and X. Zhang (2005). "Development and evaluation of an optimization-based model for power-grip posture prediction." J Biomech 38(8): 1591-7.

MacKenzie, C. L. and T. Iberall (1994). The Grasping Hand. Amsterdam, North-Holland.

Marklin, R. W. and J. F. Monroe (1998). "Quantitative biomechanical analysis of wrist motion in bone-trimming jobs in the meat packing industry." Ergonomics 41(2): 227-37.

Marras, W. S. and R. W. Schoenmarklin (1993). "Wrist motions in industry." Ergonomics 36(4): 341-51.

Mathiowetz, V., N. Kashman, G. Volland, et al. (1985). "Grip and pinch strength: normative data for adults." Arch Phys Med Rehabil 66(2): 69-74.

Miyata, N., M. Kouchi and M. Mochimaru (2006). Posture Estimation for Design Alternative Screening by DhaibaHand - Cell Phone Operation. Digital Human Modeling for Design and Engineering Conference, Lyon, France.

Moore, A., R. Wells and D. Ranney (1991). "Quantifying exposure in occupational manual tasks with cumulative trauma disorder potential." Ergonomics 34(12): 1433-53.

Moore, J. S. (2002). "Biomechanical models for the pathogenesis of specific distal upper extremity disorders." Am J Ind Med 41(5): 353-69.

Napier, J. R. (1956). "The prehensile movements of the human hand." J Bone Joint Surg Br 38-B(4): 902-13.

Pollard, N. S. and V. B. Zordan (2005). Physically based grasping control from example. Eurographics/ACM SIGGRAPH Symposium on Computer Animation, Los Angeles.

Serina, E. R., R. Tal and D. Rempel (1999). "Wrist and forearm postures and motions during typing." Ergonomics 42(7): 938-51.

Sommerich, C. M., W. S. Marras and M. Parnianpour (1996). "A quantitative description of typing biomechanics." Journal of Occupational Rehabilitation 6(1): 33-54.

Wells, R., A. Moore and P. Keir (1994). Biomechanical models of the hand. Proc. Marconi Keyboard Research Conference.

Wells, R., A. Moore, J. Potvin, et al. (1994). "Assessment of risk factors for development of work-related musculoskeletal disorders (RSI)." Appl Ergon 25(3): 157-64.

Yan, J. H. and J. H. Downing (2001). "Effects of aging, grip span, and grip style on hand strength." Res Q Exerc Sport 72(1): 71-7.

CHAPTER 2

DEVELOPING A 3-DIMENSIONAL KINEMATIC MODEL OF THE HAND TO PREDICT HAND POSTURES

Abstract

The objective of the study is to develop a 3-dimensional kinematic model of the hand that predicts hand posture. A 3-dimensional kinematic model of the hand was built using Visual C++ environment and OpenGL graphics. The hand was modeled as open chains of rigid bodies with 25 DOF's. The GUI of the model was designed to include human, object , and task attributes. A simple contact algorithm was applied to the model to find contacts between hand segments and object surface while rotating joint angles of fingers. Two different joint angle rotation algorithms – "variable rotation method" in which observed joint rotation rates were used, and "constant rotation method" in which all joints rotate at constant rates – were applied to the model. Joint angles of all fingers and thumb were measured for 16 subjects (11 males, 5 females) with motion capture system during a power grip and a pulp pinch grip. Three differently sized cylindrical objects were used. A sensitivity study was performed to investigate the effects of object size, object location, object orientation, hand size, and skin deformation on predicted postures. The average difference between predicted and measured joint angles ranged from -10.0º to 9.1º. The coefficient of determinant (R^2) between predicted and measured joint angles was 0.76 for the power grip and 0.88 for the pinch grip. The joint rotation algorithm affected prediction accuracy : application of the "variable rotation

method" improved the model's accuracy by 20% compared with the "constant rotation method." The sensitivity study showed that hand posture is more sensitive to object size, orientation, and location than hand size and skin deformation.

2.1 INTRODUCTION

The human hand is essential for the performance of activities of daily living, work and leisure. Interactions between the human and the environment are achieved mainly by using the hand. For example, people use their hand to reach, grasp, hold, and manipulate the object or support the body. Despite the importance of the hand, many aspects of hand biomechanical models have not yet reached the level of whole body models. In an age of electronic controls and devices when endless possibilities are at one's fingertips, the need for the tool that enables designers to evaluate how well an object fits the hand is ever increasing.

The hand posture is known to be directly related to grip strength (Mathiowetz, Kashman et al. 1985; Imrhan and Loo 1989; Crosby, Wehbe et al. 1994; Josty, Tyler et al. 1997; Blackwell, Kornatz et al. 1999; Yan and Downing 2001). Decrease of grip strength will result in decrease of friction force between the hand and the object, and thus the object will be more likely to slip out of the hand. Therefore, it is necessary to understand hand posture before investigating strength and friction forces of the hand. Another important aspect of the hand posture is that it is the major determinant of the required space for the hand (Choi, Grieshaber et al. 2007). Because the information about required space for the hand can enable designers to design work space and parts with minimal obstruction, hand posture should be investigated in the design stage.

Several taxonomies have been developed to categorize hand grip postures based on one or a few variables such as object size and force (Napier 1956; Landsmeer 1962; Cutkosky 1989; Grieshaber 2007). These taxonomies are helpful to account for variation in hand posture qualitatively, but they cannot give quantitative information. A few kinematic models provide quantitative information. Buchholz developed a kinematic

model using ellipsoids to evaluate prehensile capabilities (Buchholz and Armstrong 1992). The model was developed to simulate and predict the prehensile posture of the hand for power grasp of objects that can be described as ellipsoids or elliptical cylinders. Lee suggested a model to predict hand posture using optimization under the premise that the hand configuration in a power prehension best conforms to the shape of the object (Lee and Zhang 2005). These models explained how the grip posture varies in power grip, but were not sufficient to explain other types of postures (e.g., lateral pinch, pulp pinch). Also, they cannot be applied to other object shapes that cannot be represented mathematically. Using a contact algorithm to find a posture is effective for complicated object shapes, because the object geometry can be easily imported to the model in the form of array of points. Recently, some researchers and commercial softwares have used a contact algorithm to predict hand posture (Endo and Kanai 2006; Miyata, Kouchi et al. 2006); however, posture predictions using these models have not been evaluated. Also, it is not clear how hand movement is modeled, which affects posture prediction (Armstrong, Choi et al. 2008). Humans control the hand, a complex system with more than 20 degrees of freedom, using synergies (Santello, Flanders et al. 1998). Finger movement patterns differ according to the size and shapes of object to be grasped and also by the grip types (e.g., power grip, pinch grip) that humans choose. Predictions of posture should include consideration of such patterns to be realistic and avoid awkward postures predictions. In summary, a few models can predict hand posture for varied hand sizes, object sizes, object shapes in quantitative manners, but existing models are limited in their applications.

The objective of this study was to develop a 3-D kinematic model of the hand to predict hand posture, based on inputs such as human properties, object properties, and task properties. We hypothesize that (1) posture prediction using a contact algorithm

matches well with observed posture, (2) posture prediction using a “variable rotation algorithm” – observation-based joint rotation – improves prediction accuracy, and (3) hand postures are affected by object size, object location, object orientation, hand size, and skin deformation level. The first two hypotheses were tested through model development and experiment and the third hypothesis was tested by performing a sensitivity study.

2.2 MODEL DEVELOPMENT

2.2.1 KINEMATICS OF THE HAND

Twenty-five degrees of freedom (DOF's) were used to characterize the joints of the five fingers and wrist, and all the joints were mathematically approximated by ideal joints in which joint centers were located in the center of adjacent segments. The origin of the root coordinate system is the center of the wrist and Y-axis is the unit vector connecting the wrist and the middle finger MCP joint in distal direction. The Z-axis is the unit vector in the dorsal direction and perpendicular to the palm plane. The X-axis is in the ulnar direction and defined by right hand rule. The wrist joint was modeled with three degrees of freedom (F/E: flexion-extension, radial-ulnar deviation, P/S: pronation-supination) and was regarded as the origin. The proximal (PIP) and distal (DIP) interphalangeal joints of the four fingers were modeled as hinge joints with one DOF (F/E) for each joint. Metacarpophalangeal (MCP) joints of the four fingers were modeled with two DOF's (F/E, ABD/ADD: abduction-adduction). The IP joint of thumb was modeled as a hinge joint with one DOF (F/E), whereas the MCP joint of thumb was modeled with two DOF's (F/E, ABD/ADD). The carpometacarpal (CMC) joint of the thumb was described as having three DOF's (Buchholz and Armstrong 1992; Savescu and Cheze 2005; Li and Tang 2007) to facilitate the comparison with experimental data, even though some studies described the trapezium as saddle-shaped with two DOF's (Giurintano, Hollister et al. 1995; Abdel-Malek, Yang et al. 2006). All the angles were represented by Eulerian angles, and homogeneous transformation matrices were used to represent angular transformation of joints. Figure 2.1 shows the coordinate system defined in the hand.

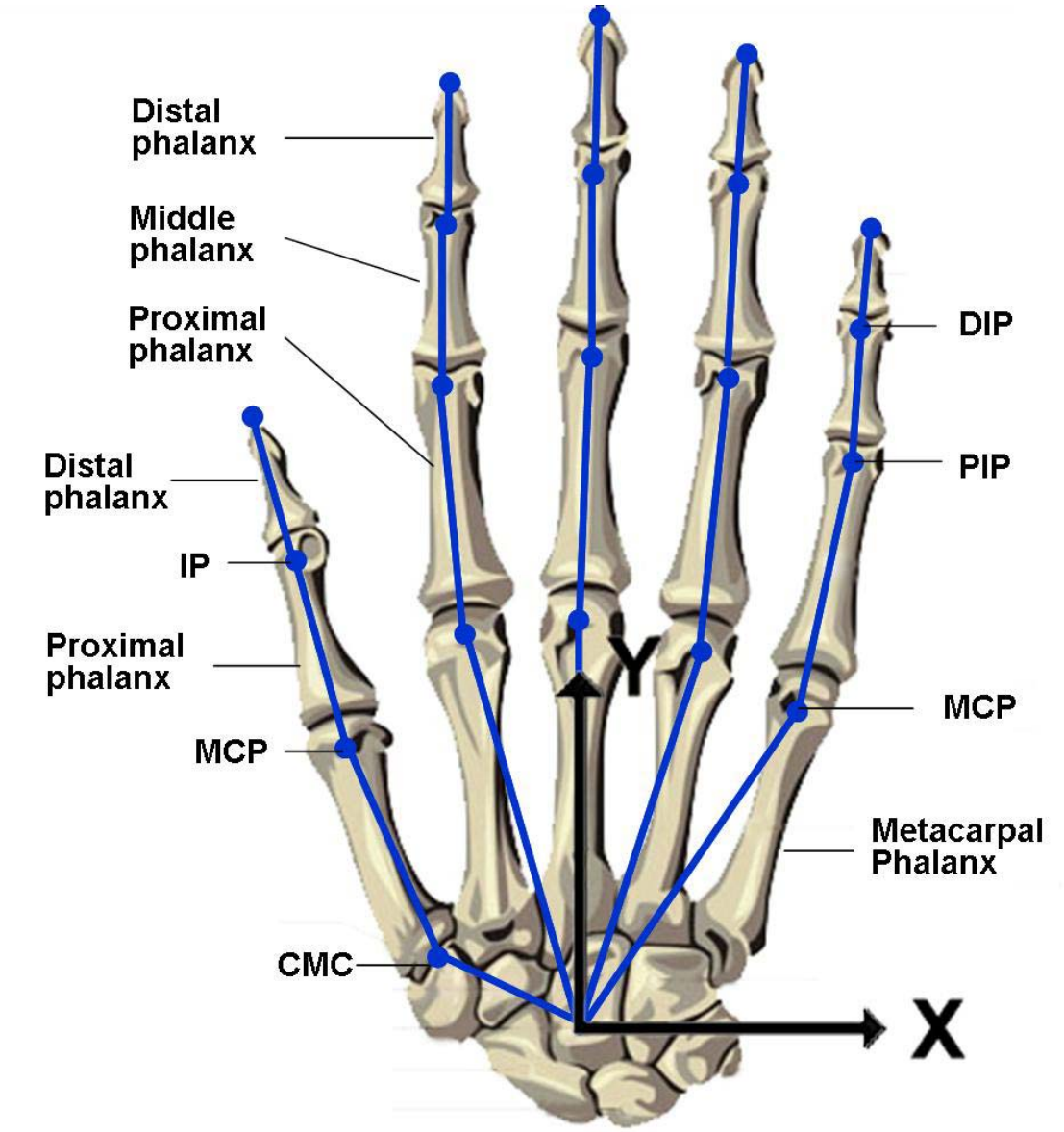

Figure 2.1 Definition of coordinate system in the hand. Twelve-five degrees of freedom were used to characterize the joints of the fingers and wrist. The root coordinate system of the hand has an origin at the center of the wrist, with the Y-axis pointing to the third MCP joint, the Z-axis pointing to dorsal direction to the palm plane. The wrist has three DOF's (F/E, A/A, P/S). The thumb has six DOF's – IP (1 DOF), MCP (2 DOF's : F/E, A/A), CMC (3 DOF's : F/E, A/A, P/S). The MCP joints of four fingers have 2 DOF's each (F/E, A/A), and PIP and DIP joints of four fingers have one DOF each (F/E).

2.2.2 Model Implementation

The computational model was developed in a Visual C++ environment (Microsoft Visual C++ ® 6.0). OpenGL graphic functions were used to display the hand and object. The hand was modeled as open chains of rigid body segments, which were described as truncated cones, the simplest reasonable representation of hand segments. The length of hand segments was calculated based on work by Buchholz, which models the hand anthropometry as a function of external hand measurements such as a hand length and a hand breadth (Buchholz, Armstrong et al. 1992).

Contact algorithm

A collision detection algorithm was used to determine when contact occurred between hand and object. The collision detection is a computationally intensive process; many methods for detecting collision have been developed, such as the use of minimum distance, the use of bounding regions, and the use of special data structures (Lin and Gottschalk 1998; Hui and Wong 2002). To enhance accuracy, the minimum distance method was used in this model. Quadratic surface meshes were created for the surfaces of both hand and object. The distances between the meshes on the hand and those on the object were calculated while the joint angles of each joint rotated according to the specific joint rotation algorithm – variable rotation algorithm (Choi and Armstrong 2007). When the minimum distance between the hand and object was smaller than a preset threshold value, it was regarded as a collision. When distal segments of all four fingers contacted the object, the simulation terminated.

Joint rotation algorithm

It can be shown that the final posture prediction using a contact algorithm is affected by the rotation rate of finger joints. The modeled hand is actuated by rotating 15 joints with 18 degrees of freedom – 3 DOF's for each finger and 6 DOF's for the thumb. Abduction-adduction angles of MCP joints were not varied, because they were observed to be small during cylinder grasping. We used two joint angle rotation algorithms and compared the predicted postures. The first algorithm, "constant rotation algorithm," describes the rotations of all joints of the fingers at the constant rate. In this method, the thumb cannot be modeled because the motion pattern of thumb joints during grasping is not yet known. The second algorithm, "variable rotation algorithm," describes rotations of all joints at observation-based rates (Choi and Armstrong 2007).

2.3 VALIDATION OF THE MODEL

2.3.1 EXPERIMENTS

Experimental Design

Sixteen healthy subjects with no history of musculoskeletal disorders in upper extremities participated in the experiment. Demographic information for the study population is shown in Table 2.1. Their hand lengths ranged from 2% female to 83% male according to Garret's data (Garrett 1971). All subjects gave their written consent to participate in the study. The experimental design was reviewed and approved by the University of Michigan Institutional Review Board.

Table 2.1 Hand length summary of study participants. Percentiles are listed in parenthesis (Garrett, 1970).

Gender	Age	Hand Length (cm)	Range (cm)
Female (n=5)	21.0± 1.0	17.4± 1.3 (25 %ile)	16.3– 19.5
Male (n=11)	23.7± 4.3	19.6± 0.9 (43 %ile)	17.8– 20.6
Pooled	23.0± 3.9	18.9± 1.4	16.3– 20.6

Three sizes (cylinder diameter: 26.2 mm, 60.0 mm, 114.3 mm) of cylindrical objects were used. The object was placed 40 cm in front and at elbow height of the subject so that the subject's elbow angles when grasping the object were approximately 90º. To measure the position of markers on the hand and the object, the OptoTrak® Certus™ motion tracking system (Northern Digital Inc.), whose RMS positional accuracy is 0.1 mm, was utilized. Four markers per each finger were secured at the tip, and at the DIP, PIP, and MCP joints on the dorsal side of the hand. For six of the subjects, seven

markers were attached to the thumb. Four markers were at the tip, and at the IP, MCP and CMC joints of the thumb. An additional three markers in a plate were attached to the proximal phalanx of the thumb. Three markers were on the dorsal side of the center of the wrist and the distal ends of the dorsal tubercle of the radius and the ulnar styloid process. Four markers were attached to the cylindrical object to identify the position and orientation of the cylinder with respect to the hand (Figure 2.2 (a)). Two position sensors (three position sensors for six subjects with thumb markers) simultaneously tracked the positions of markers during the task (Figure 2.2 (b)). The subjects were asked to start with their elbows flexed 90º and no abduction in the shoulder, and to grasp the object with their power and pulp pinch grip (for six subjects with thumb markers). The task was repeated three times for each condition.

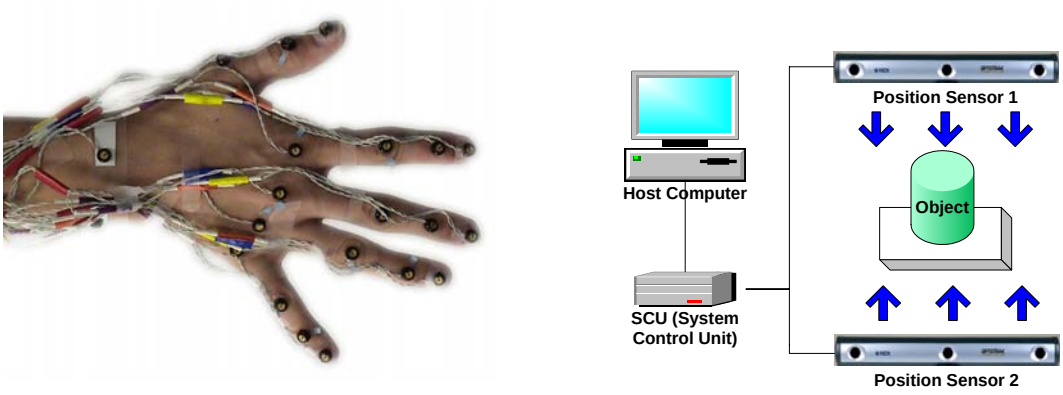

(a) OptoTrak marker locations (b) Experimental Setup

Figure 2.2 Experimental Setup. (a) Twenty-six markers were attached to the dorsal side of the hand. (b) Two OptoTrak position sensors were used to track the positions of markers

Data analysis

The data obtained were processed with Matlab® software. The DIP, PIP, and MCP joint angles of four fingers were calculated from the 3D marker position data, using dot products of the adjacent vectors, each of which represents each segment. The IP joint angle of the thumb was calculated in the same way. The thumb MCP joint has two degrees of freedom – F/E and ABD/ADD. The plane containing tip, IP, and MCP markers was defined and the vector between MCP and CMC joint marker was projected onto the plane. The F/E angle was calculated using dot products of the IP-MCP vector and the projected vector. The AA angle was calculated using dot products of MCP-CMC vector and the projected vector. Thumb CMC joint angles were calculated using Euler angles of flexion-extension, abduction-adduction, and pronation-supination rotation sequence. Therefore, all the joint angles used in this study are marker-defined joint angles. The object's positions and orientations with respect to the wrist were obtained from the experiments and used as inputs to the program.

2.3.2 COMPARISON WITH EXPERIMENTAL DATA

The effect of joint rotation methods

To investigate the effect of joint rotation methods, root-mean-square (RMS) values of differences in joint angles between prediction and measurement during the power grip were compared for two joint rotation algorithms -constant rate rotation vs. observed rate rotation in Table 2.2. When comparing all joints of four fingers, the magnitude of RMS prediction difference ranged from 5.1º to 20.4º with the "variable rotation algorithm," and that of RMS prediction difference ranged from 6.8º to 30.5º with

the “constant rotation algorithm.” These RMS values for prediction difference are comparable to those in the previous study by Lee et al (Lee and Zhang 2005).

Table 2.2 RMS prediction difference (left – variable rotation algorithm vs. right – constant rotation algorithm)

		Variable Rotation			Constant Rotation		
Digit	Joint	Large (114mm)	Medium (60mm)	Small (26mm)	Large (114mm)	Medium (60mm)	Small (26mm)
1	IP	8.81	14.63	19.18	8.81	14.63	19.18
	MCPFE	15.80	19.04	17.44	15.80	19.04	17.44
	MCPAA	9.85	7.95	10.19	9.85	7.95	10.19
	CMCFE	18.46	7.50	5.82	18.46	7.50	5.82
	CMCAA	12.24	12.06	9.69	12.24	12.06	9.69
	CMCPS	19.47	15.57	5.67	19.47	15.57	5.67
2	MCP	10.97	11.02	9.25	12.60	15.98	14.86
	PIP	14.45	17.02	7.44	7.44	10.59	10.71
	DIP	19.23	12.31	15.38	10.93	13.45	9.82
3	MCP	7.81	6.31	5.41	17.33	23.40	15.89
	PIP	11.06	13.50	6.45	8.61	10.10	12.76
	DIP	13.27	10.70	9.05	14.27	13.92	16.09
4	MCP	7.75	11.88	5.08	9.16	13.40	30.50
	PIP	10.66	11.34	6.34	15.73	19.69	29.95
	DIP	11.52	9.51	8.73	11.41	9.53	8.98
5	MCP	10.32	20.41	6.68	18.32	6.80	11.41
	PIP	16.74	9.91	13.10	13.54	13.17	9.03
	DIP	13.87	12.17	12.69	19.71	11.73	8.99

Model accuracy

To estimate the accuracy of the model, the hand postures predicted by the kinematic model were compared with the hand postures observed through the experiment based on the location of markers on the back of each joint. The prediction difference was defined as

$$\text{Prediction difference} = \text{predicted joint angle} - \text{measured joint angle} \qquad (2.1)$$

Therefore, positive value of prediction difference means that the model overestimates the joint angles, whereas negative value means that the model underestimates the joint angles.

- **Power grip**

Table 2.3 shows the prediction difference between measured and predicted joint angles for three differently sized objects with sixteen subjects in power grip. Over all cylinder sizes, the range of average prediction differences was from -10.0º (PIP joint of index finger) to 9.1º (MCPFE of the thumb). Among four fingers, the average of absolute differences was smallest in the middle finger (2.0º) and largest in the index finger (7.6º). The differences for the MCP joint angle ranged from -6.7º to 14.3º, those of the PIP joint angle ranged from -13.0º to 11.8º, and those of the DIP joint angle ranged from -10.5º to 10.7º. On average, the model underestimated joint angles in the index finger, whereas overestimated joint angles in the ring and little fingers. The prediction differences were not significantly affected by the object size. For the small object, differences ranged

from -10.5º to 11.2º. In the medium-sized object, the differences ranged from -11.9º to 14.3º. In the large object, differences ranged from -13.0º to 12.7º. These differences are comparable to those in the previous studies by Buchholz and Lee who reported the differences between predicted and observed joint angles separately (Buchholz and Armstrong 1992; Lee and Zhang 2005).

Table 2.3 Prediction differences between predicted and measured joint angles in power grip

Digit	Joint	Large (114mm)	Medium (60mm)	Small (26mm)	All
1	IP	1.86±8.96	10.00 ± 11.09	8.32 ± 18.05	6.77 ± 13.21
	MCPFE	8.58±13.81	11.93 ± 15.41	6.36 ± 16.97	9.09 ± 15.17
	MCPAA	-4.58±9.08	-3.13 ± 7.59	-5.70 ± 8.83	-4.40 ± 8.33
	CMCFE	12.66±14.00	-3.24 ± 7.02	-2.29 ± 5.60	2.36 ± 11.93
	CMCAA	1.49±12.66	5.68 ± 11.05	8.62 ± 4.63	5.18 ± 10.34
	CMCPS	-1.16±20.24	-8.91 ± 13.26	-0.91 ± 5.86	-3.86 ± 14.63
2	MCP	-6.23±9.15	-6.67 ± 8.89	-1.35 ± 9.28	-4.85 ± 9.33
	PIP	-12.99±6.43	-11.9 ± 12.32	-4.80 ± 5.78	-10.02 ± 9.46
	DIP	8.24±17.61	4.98 ± 11.40	10.66 ± 11.24	7.84 ± 13.81
3	MCP	5.18±5.93	-3.13 ± 5.56	0.34 ± 5.48	0.71 ± 6.58
	PIP	-0.56±11.19	10.12 ± 9.05	4.34 ± 4.84	4.77 ± 9.81
	DIP	-2.1±13.27	2.44 ± 10.55	-2.24 ± 8.89	-0.53 ± 11.2
4	MCP	3.07±7.21	6.81 ± 9.85	1.87 ± 4.80	4.02 ± 7.90
	PIP	7.72±7.46	7.81 ± 8.34	2.34 ± 5.98	6.06 ± 7.73
	DIP	4.99±10.52	1.90 ± 9.43	-3.89 ± 7.93	1.10 ± 9.98
5	MCP	5.60±8.79	14.3 ± 14.75	-2.53 ± 6.27	6.14 ± 12.68
	PIP	11.77±12.07	-0.11 ± 10.03	11.19 ± 6.92	7.36 ± 11.32
	DIP	-2.84±13.76	7.10 ± 10.01	-10.49 ± 7.26	-1.71 ± 12.86

Figure 2.3 shows overall plots of predicted joint angles vs. measured joint angles. The model gave reasonable predictions of joint angles for different object sizes. The coefficient of determinants (R^2) between predicted and measured joint angles was 0.76.

To investigate the model accuracy at each joint, coefficients of determinants (R^2) between predicted and measured joint angles were calculated and displayed for each finger and joint as shown in Table 2.4. Regardless of digits, R^2 values were largest (from 0.69 to 0.93) in MCP joint angles, and they were smallest in DIP joint angles (from 0.29 to 0.56).

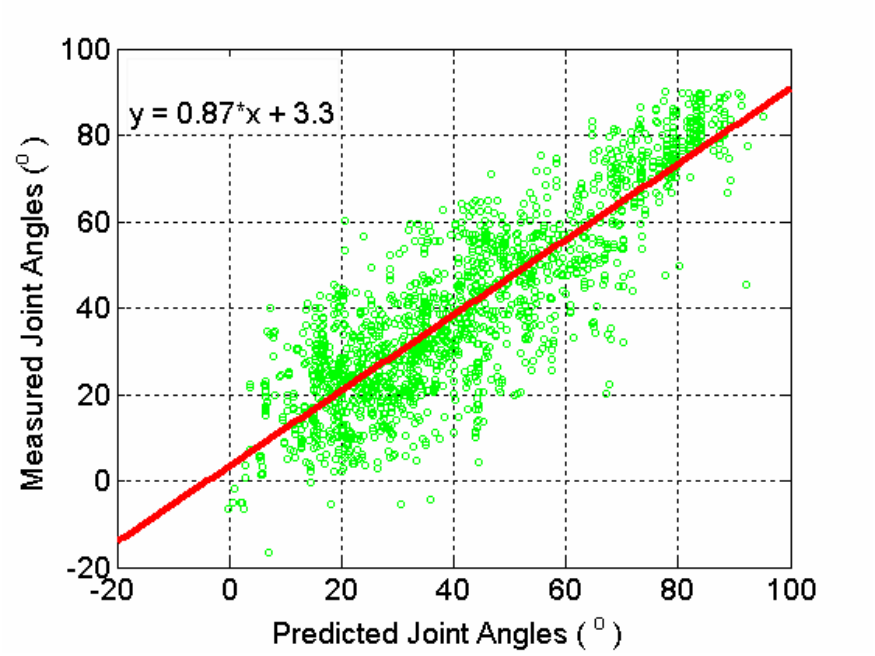

Figure 2.3 Plot of predicted joint angles vs. measured joint angles in power grip (N = 1,692).

Table 2.4 Coefficients of determinant between predicted and measured joint angles

Digit	IP	MCPFE	MCPAA
1	0.57	0.30	0.30
	CMCFE	CMCAA	CMCPS
	0.75	0.32	0.31
Digit	MCP	PIP	DIP
2	0.83	0.87	0.29
3	0.93	0.84	0.44
4	0.88	0.90	0.56
5	0.69	0.75	0.35

- **Pinch grip**

Prediction differences between predicted and measured joint angles in pinch grip are shown in Table 2.5. The differences ranged from -9.4º to 15.6º for the large object, from -6.5º to 12.9º for the medium object, and from -12.0º to 20.6º for the small object. The thumb showed larger errors (from -12.0º to 20.6º) than the other four fingers (from -16.4º to 7.6º).

Figure 2.4 displays overall plots of measured and predicted joint angles. The coefficient of determinants (R^2) between predicted and measured joint angles in pinch grip was 0.88.

Table 2.5 Prediction differences between predicted and measured joint angles in pinch grip

Digit	Joint	Large (D=114 mm)	Medium (D=60 mm)	Small (D=26 mm)	All
1	IP	-1.72±7.34	-3.03±5.67	-9.50±5.85	-4.07±7.02
	MCPFE	-0.09±11.19	2.60±9.35	8.32±14.52	2.90±11.65
	MCPAA	2.90±9.91	12.90±13.9	0.90±14.37	5.92±13.27
	CMCFE	15.59±13.96	3.43±18.00	4.81±9.00	8.70±15.35
	CMCAA	4.35±10.29	-2.95±10.39	-11.96±9.63	-2.18±11.82
	CMCPS	-3.95±8.82	1.40±9.04	20.55±12.7	3.89±13.81
2	MCP	-1.43±6.66	-5.41±12.24	1.11±13.03	-2.21±10.57
	PIP	-9.43±7.07	-6.45±11.21	-16.35±10.75	-10.07±10.09
	DIP	0.18±8.92	0.46±16.25	2.96±8.31	0.96±11.65
3	MCP	2.74±7.41	-1.20±12.17	6.52±13.89	2.28±11.07
	PIP	-3.30±9.26	2.79±8.95	-10.23±16.91	-2.85±12.19
	DIP	-2.59±12.63	-0.81±10.14	1.40±7.45	-0.99±10.54
4	MCP	1.29±7.92	0.29±7.09	7.75±9.07	2.51±8.29
	PIP	-1.74±9.19	5.04±6.97	-6.79±13.32	-0.59±10.49
	DIP	0.55±9.32	3.31±7.08	0.38±1.14	1.48±7.26
5	MCP	-4.77±4.73	2.91±5.82	5.64±3.78	0.46±6.59
	PIP	7.64±11.62	3.88±4.38	-3.34±6.39	3.65±9.32
	DIP	-2.92±10.79	3.86±6.69	1.03±14.89	0.42±10.89

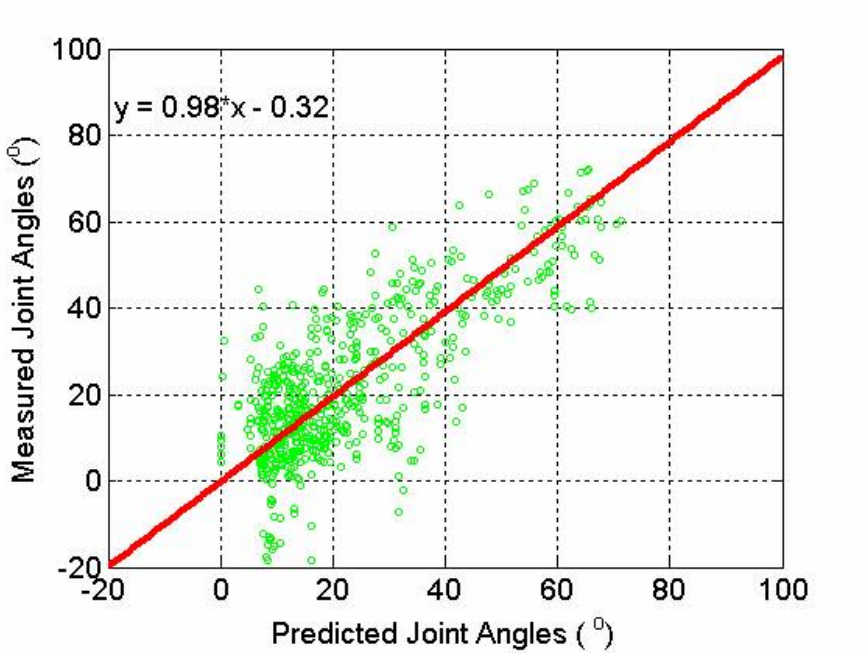

Figure 2.4 Plot of predicted joint angles vs. measured joint angles in power grip (N = 684).

2.4 SENSITIVITY STUDY

2.4.1 Design of sensitivity study

To validate the model and examine the effects of various input variables, a sensitivity study was performed for all joints of four fingers with respect to six input parameters: hand length, hand breadth, object size (cylinder diameter), object location, object orientation, and skin deformation. Six hand lengths and hand breadths were selected for the simulation based on those of the participants. Hand lengths ranged from 163 mm (2% female) to 206 mm (82% male) and the hand breadth ranged from 73 mm (14% female) to 90.5 mm (63% male). In the simulation, the results from four differently sized cylindrical objects, whose diameters were 26.2 mm, 60 mm, and 114.3 mm, were selected for comparison with experimental results. Object location was defined as a distance from the wrist joint to the object along the axis of the forearm (Figure 2.5 (a)). The center position of the object varied from -10 mm to +10 mm by 5-mm intervals with respect to the positions decided from the experiment. The object's orientation was defined as the slip angle in the palmar plane and was manipulated from 10º to 40º by 5º intervals, because it was observed that slip angles changed within the range of 10º to 40º in the experiment (Figure 2.5 (b)). Skin deformation was simulated by modifying the thickness of the finger segments when calculating the distance between the hand and the object; reducing the thickness 1 mm corresponded to 1 mm of skin deformation. Three levels of deformation were investigated: no deformation, 10% deformation, and 20% deformation.

Sensitivity testing methods were applied by predicting joint angles for all possible combinations of the above parameters. The total number of simulations was 1,980. All the simulations were done by the batch setup of the model.

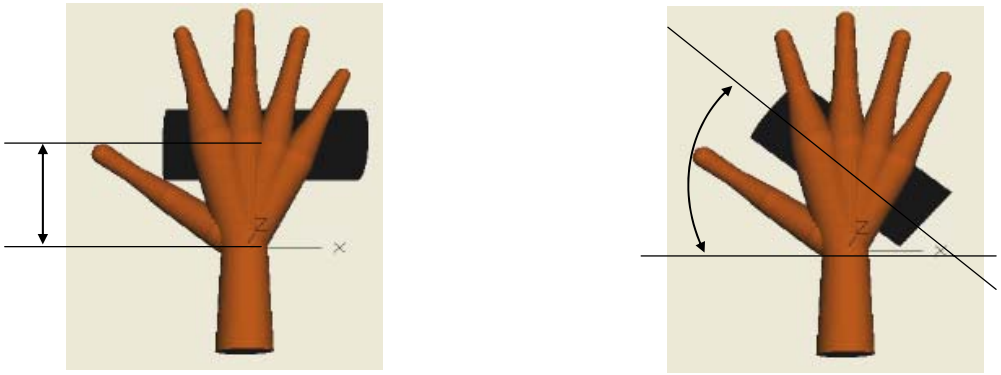

(a) Object location (b) Object orientation

Figure 2.5 Definition of object location and object orientation in sensitivity study

2.4.2 Sensitivity Measure

Regression analysis was performed to investigate the sensitivity of joint angles to variation of hand length, skin deformation, object size, object orientation and object location. For each joint of each finger, regression analysis was done separately. Linear regression equations were tested as follows.

$$y_{ij} = a_{ij}x_1 + b_{ij}x_2 + c_{ij}x_3 + d_{ij}x_4 + e_{ij}x_5 \pm \varepsilon_{ij} \quad , \qquad (2.2)$$

where y : joint angle

x_1 : hand length

x_2 : object size

x_3 : object orientation

x_4 : object location

x_5 : skin deformation

ε : error

i : 2,3,4,5 (digit)

j : 1,2,3 (MCP:1, PIP:2, DIP:3)

Based on the set of linear regression Eqs. (2), the following measure was used to quantify the sensitivity of the joint angles with respect to each parameter.

$$Sensitivity = \sigma_{parameter} \times \frac{\partial(Joint \quad Angle)}{\partial(parameter)} \quad , \qquad (2.3)$$

where σ: range of parameters.

2.4.3 Sensitivity analysis

Linear regression Eqs. (2.2) closely account for most of the joints' variability. For all joints of four fingers, R^2 ranged from 0.60 to 0.95. For MCP joint angles, R^2 ranged from 0.80 to 0.90, from 0.85 to 0.95 for PIP joint angles, and from 0.60 to 0.77 for DIP joint angles.

Figure 2.6 - Figure 2.10 display the results of the sensitivity study. Increase of hand length resulted in increase in the joint angle predicted even though local decreases were observed in all joints. Sensitivity to this parameter seemed to be relatively low (Figure 2.6).

The model predicted that increasing the object's size (diameter of cylindrical object) would lead to a decrease in the joint angle (Figure 2.7). On average, the MCP joint angle (-6.3º/cm) and the PIP joint angle (-6.1º/cm) decreased more than the DIP joint angle (- 2.0º/cm).

The increase of object orientation angle decreased all MCP joint angles of the index and middle finger, while it increased MCP joint angles of digits 4 and 5 (Figure 2.8). The MCP joint angle of the index finger showed the largest decrease (-0.77º/º) and the MCP joint of the little finger showed the largest increase (0.59º/º). The DIP joint angles of the middle and ring fingers showed the smallest change (-0.06º/º and 0.03º/º , respectively).

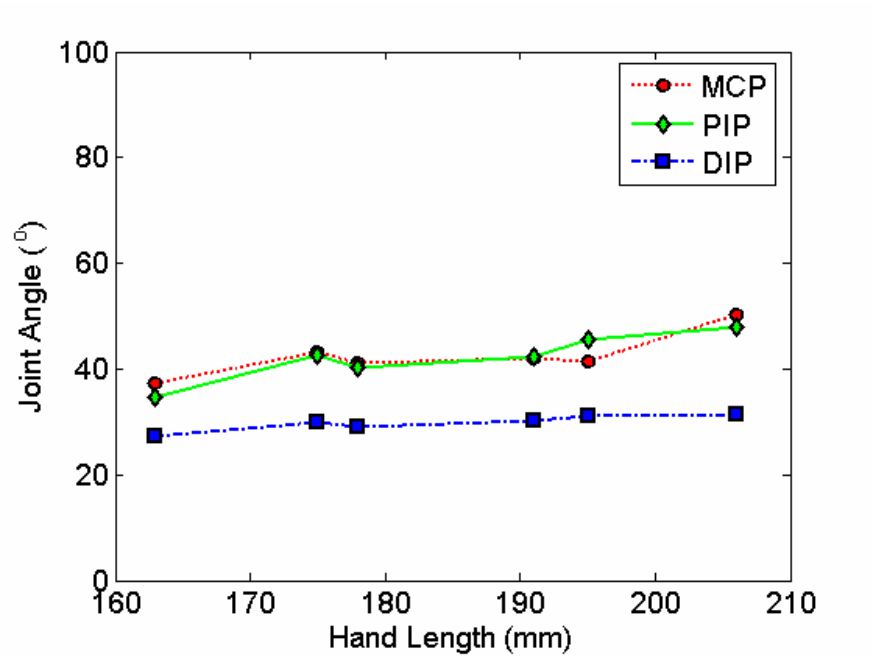

Figure 2.6 Effect of hand length on joint angle prediction

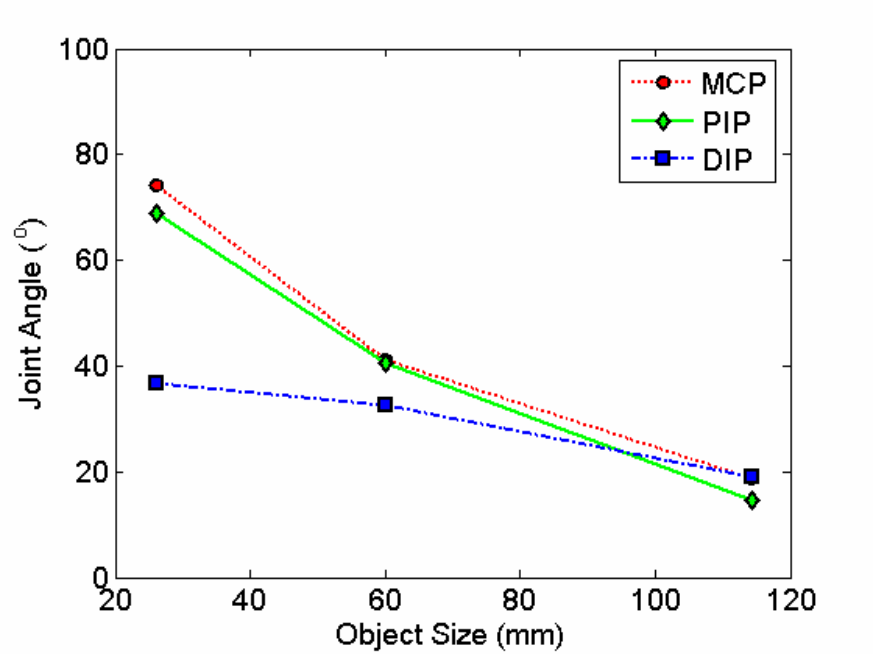

Figure 2.7 Effect of object size on joint angle prediction

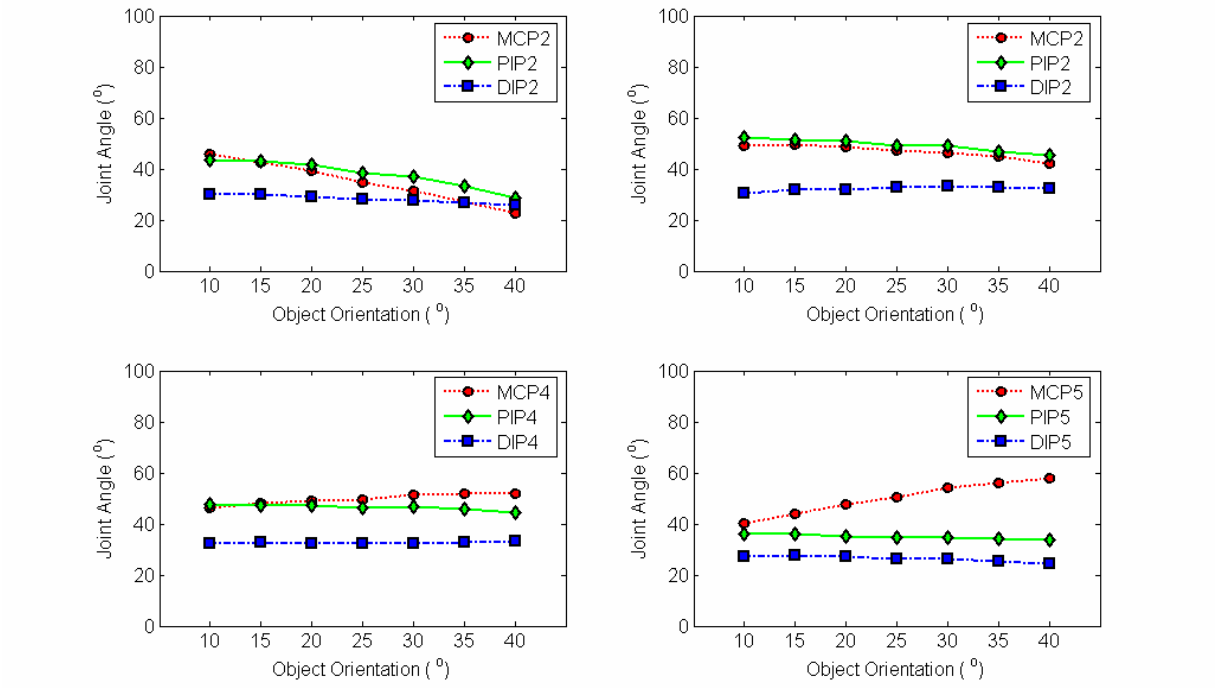

Figure 2.8 Effect of orientation on joint angle prediction for each finger joint. (a) index, (b) middle, (c) ring, and (d) little

The object location seems to have a relatively large effect on hand posture (Figure 2.9). The MCP joint angle changed -10.2º/cm. The PIP and DIP joint angle changes were much smaller (0.2º/cm and -0.1º/cm, respectively) than the MCP joint angle change. The sensitivities of the predicted joint angles and those of the observed joint angles were similar for the above parameters such as hand length, object size, object orientation, and object location.

The skin deformation showed little effect on predicted joint angle over the range examined (Figure 2.10). MCP joint angles increased 1.31º per 10% deformation. PIP joint angles decreased 1.47º per 10% deformation and DIP joint angles increased 1.67º for 10% deformation

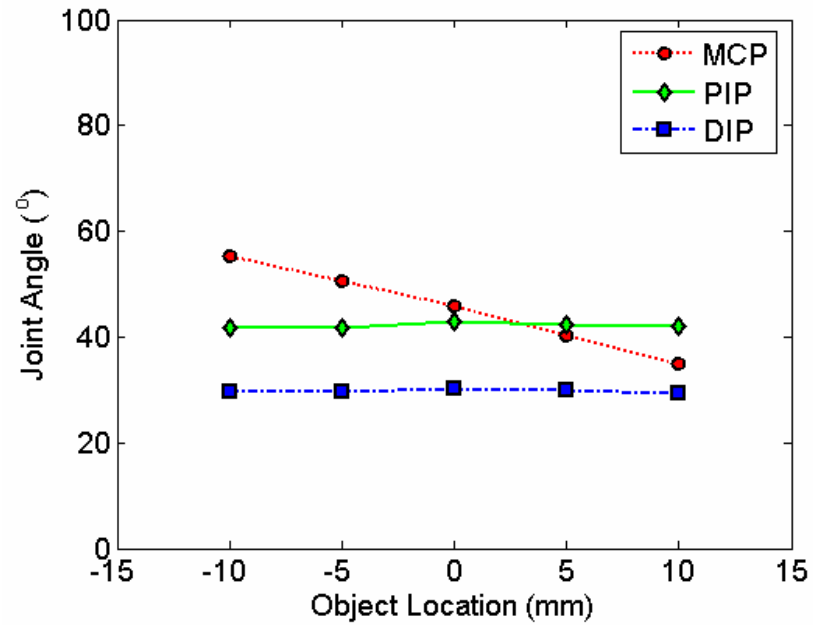

Figure 2.9 Effect of object location on joint angle prediction

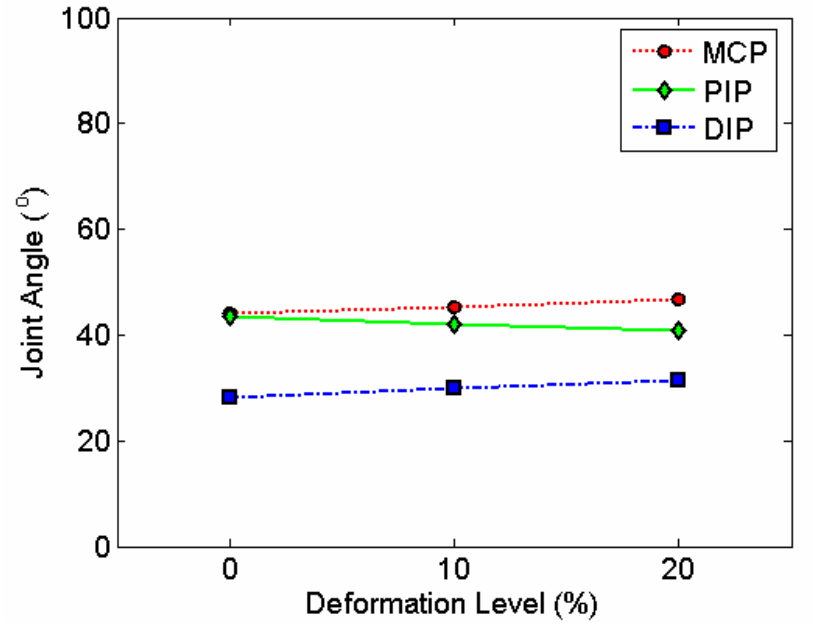

Figure 2.10 Effect of skin deformation on joint angle prediction

The sensitivity measures obtained by Eqs. (3) are listed in Table 2.6 and Table 2.7. These measures were higher in OS (object size), OO (object orientation), and OL (object location) than HL (hand length) and SD (skin deformation).

Table 2.6 Sensitivity measures [Eqs. (3)] for each joint with respect to HL(hand length), OS(object size), OL(object location) and SD(skin deformation)

Var / Joint	OS	OL	HL	SD
MCP	-61.81	-20.04	4.58	1.35
PIP	-61.02	0.74	5.63	-2.25
DIP	-20.67	0.02	3.79	1.59

Table 2.7 Sensitivity measures [Eqs. (3)] for each joint with respect to object orientation

Digit / Joint	2	3	4	5
MCP	22.86	6.78	-6.18	-18.36
PIP	14.37	6.48	2.43	2.20
DIP	4.50	-2.00	-0.61	2.60

2.5 OBJECT PROPERTIES (LOCATION AND ORIENTATION)

In grasping an object, object properties such as object's location and orientation influence the hand posture significantly as shown in the sensitivity study. We developed empirical model to describe object's location and orientation based on our experimental database.

- **Object Location**

The distance from the wrist to the center of the cylinder was determined from the experimental data. Y-location was defined as the distance between the center of the wrist and the point where the axis vector of the cylindrical object and wrist-third metacarpophalangeal joint vector cross each other, when the two vectors were projected onto the palm plane (Figure 2.5). The empirically derived equation was derived using linear regression analysis to estimate Y-location in power grasping of the cylindrical object. In power grip, only the cylinder's diameter showed significant effects on the Y-location ($p=0.000$). External hand sizes such as hand length ($p=0.288$) and did not show significant effects on determination of Y-location. Therefore, Y-location for power grip is determined by the following equation:

$$\text{Y-location} = 0.386X \text{ Cylinder Diameter} + 38.5 \text{ (mm)} \quad (2.4)$$

Coefficient of determination (R^2) for this equation was 0.60.

In pinch grip, the cylinder's diameter significantly affect Y-location (p = 0.000), but the hand length did not affect the Y-location significantly (p = 0.386). Y-location for pinch grip is:

Y-location = 0.424 X Cylinder Diameter + 79.7 (mm) (2.5)

Coefficient of determination (R^2) for this equation was 0.37.

Z-location (distance from palmar plane to object center) is also one of the most important determinant of pinch grip posture. Both hand length (p=0.000) and cylinder diameter (p=0.000) significantly affected the Z-location. Coefficient of determination (R^2) for this equation was 0.47.

Z-location = -0.314 X Cylinder Diameter – 0.548 X Hand Length + 29.2 (mm)

(2.6)

- **Object Orientation**

Object orientation was obtained from the experimental data. 'Cylinder angle' was determined by the angle between the long axis of the cylindrical object and the unit vector of x-axis (Figure 2.5). In both power grip and pinch grip, only the cylinder's diameter significantly affects cylinder angle (p = 0.000 and p = 0.025 for power and pinch grip, respectively). In power grip, cylinder angle is:

Cylinder Angle =0.113XCylinder Diameter +13.9 (º) (2.7)

Coefficient of determination (R^2) for this equation was 0.22.

In pinch grip, the cylinder angle can be determined by the following equation:

Cylinder Angle = -0.108 X cylinder Diameter + 30.9 (º) (2.8)

Coefficient of determination (R^2) for this equation was 0.12.

2.6 DISCUSSION

The predictive model of hand posture was developed by other researchers (Buchholz and Armstrong 1992; Lee and Zhang 2005). In Buchholz's study, ellipsoidal representation of the hand segment and object made it possible to use ellipsoidal contact equations, but the model was limited to the application for ellipsoidal or similarly shaped objects only. Lee suggested a hand posture prediction model based on the premise that the hand configuration in the power grip posture best conforms to the object's shape. This model requires mathematical representation of the object's shape and size, which makes it difficult to apply to variously shaped objects. Among the most important factors determining hand posture are the object properties such as shape, size, and location, as was shown in the sensitivity study. The irregular shapes of objects, which are hard to approximate by mathematical equations, can be easily used in this model by importing surface mesh data. Also, the proposed model can represent the hand segment in other shapes in addition to truncated cones by using 3-D arrays of points, while the previous models could use only ellipsoids or empirically obtained segment thickness at contact.

In none of the above models is the thumb fully implemented. In Buchholz's model, only flexion/extension angles of IP and MCP joints were modeled, and thus abduction/adduction joint angle of MCP joint and all joint angles of CMC joint must be specified. Lee's model does not have the data for the thumb. The thumb is the most important finger on the hand, accounting for at least 40% of hand function. The complex structure of the thumb – at least 5 DOF's with non-orthogonal axes of rotation (Hollister et al. 1995) – makes its movements complicated and hard to predict (Li and Tang 2007).

In this model, observation-based finger motion was applied to the thumb, so that the final posture of the thumb could be obtained using the contact algorithm.

The model gave reasonable predictions with R^2=0.76 for power grip and R^2 = 0.88 for pulp pinch grip. In power grip, R^2 values for individual joints revealed that the model predicted MCP and PIP joint angles better than DIP joint angles. The DIP joint may have been more sensitive to hand force than other joints because the distal segment end was unconstrained. Even though all finger segments were modeled as rigid body segments, all segments experienced deformation of soft tissue under loading. The proximal and middle segments were constrained by the MCP, PIP, and DIP joints, while the distal segment was not.

The prediction accuracy was affected by the rotation methods of finger joints. Average RMS errors between predicted and measured joint angles of four fingers were 11.1º with "variable rotation methods" and 13.9º with "constant rotation methods." More importantly than this improvement of model accuracy, prediction of thumb joint angles or pinch grip posture cannot be accomplished without knowledge about the relative rotation of finger joints. Even though hand posture in power grip can be partly approximated by contacting all finger segments with the object surface, hand posture using other grip types cannot be predicted similarly. Application of the "variable rotation method" can be a solution to predict hand postures of various grip types such as pulp pinch grip or tip pinch grip.

The sensitivity study results showed how much each parameter affected hand posture. The joint angles were the most sensitive to object size. The influence of object location was relatively high in MCP joint angles but low in PIP and DIP joint angle. Object orientation had a relatively large effect on MCP joint angles of the index and little fingers, but less effect on those of the middle and index fingers. Overall, the hand

posture was more sensitive to object attributes such as object size, location, and orientation than human attributes such as hand length and skin deformation.

The kinematic structure of the hand in this model is not perfectly congruent with the anatomic structure of the hand. First, four metacarpals in the palm are placed in parallel, but they were modeled as four bones spreading from the wrist. Many kinematic models (Buchholz and Armstrong 1992; Lee and Zhang 2005; Abdel-Malek, Yang et al. 2006) used the same kinematic structure as this model. Such kinematic structure enables the model to have scalability based on the external hand size such as hand length and hand breath, because the model used anthropometric data by Buchholz (1992) who modeled hand anthropometry as a function of external hand measurement. Second, the CMC joints of the second and fourth digits were not modeled in this study. Those joints enable the hand to change its shape to make the transverse arch during tip pinch posture or in grasping spherical objects. Savescu et al.(2005) added two more degrees of freedom in their hand model to represent the transverse arch of the hand. This can lead to better prediction of hand posture during tip pinch or grasping a spherical shaped object, but doesn't seem to have much effect on the hand posture during grasping cylindrical objects.

Another product of the experiment is the information of object properties (object's location and orientation). The regression Eqs. (4) -(8) can be used to simulate hand postures in power grip and pinch grip. Hand size did not significantly change Y-location and cylinder angle, whereas object size showed significant effect on those parameters. This result could be caused by the constraints on the object and variability in grip strategies between subjects. As the object was fixed in space, some subjects seem to be unable to contact their palms completely to the object. It seems obvious that two

different strategies – one with complete palm contact and the other with partial palm contact – make the Y-location and cylinder angle considerably different.

2.7 LIMITATIONS AND FUTURE RESEARCH

Even though the model's predictions of hand posture were reasonably accurate, there were some limitations. This model used the anthropometric data from Buchholz (Buchholz, Armstrong et al. 1992); however, there could have been discrepancies between actual and predicted segment dimensions. Skin deformation could also be another reason for differences of the experiments and the predictions, even though its effect was small as shown in the sensitivity study. Another possible source of prediction differences is from a center of rotation. We used marker-defined joint angles when comparing measured joint angles. On the other hand, the model assumed the ideal joints in the process of constructing the skeleton linkage. Therefore, the comparison was made between marker-defined joint angles and ideally modeled joint angles. It has been reported that coefficients of multiple determination between marker-defined joint angles and rotation-center based joint angles were 0.96, 0.98, and 0.94 for MCP, PIP, and DIP joint flexion-extension motion, respectively. But the thumb joints have not only flexion-extension movements but also pronation-supination and abduction-adduction movements, which could have increased errors when comparing measured and predicted joint angles. Lee and Zhang reported the optimization-based method to determine a center of rotation from the data collected by a 3-D motion capture system, which assumed that the markers were attached to the skin completely and moved with skin movements (Zhang, Lee et al. 2003). The method could not be applied to our data, because of the characteristics of our data collection system (OptoTrak® Certus™). In

using an active marker system which has wires, it is important to route wires so that the wires do not block markers during the data collection. The small tapes we used to route wires seem to have restrained the movements of markers when the skin moved. Therefore, the markers did not move together with skin movements through the joint rotation, which made the method inapplicable to our data.

It should be noted that all the solutions in this model were based only on kinematics with rigid body modeling of hand segments. This approach is appropriate when the location of the hand and the object are fixed in space. If they are not fixed in space, the biomechanical aspects and force equilibrium should be considered while simulating the grasp. Grasping a non-constrained object can also change the object location and orientation with respect to the hand, which ultimately influence the grip posture.

This model can be expanded to biomechanical models that predict hand strengths and muscle forces during the grasping of objects. It can also give useful information to hand tool designers and can be extended to clinical applications.

2.8 CONCLUSIONS

- A 3-dimensional kinematic model of the hand to predict hand posture was developed in Visual C++ environment using a contact algorithm.
- The kinematic model using a contact algorithm was validated through the experiment. The model gave a reasonable prediction of hand posture for both power grip (R^2 = 0.76) and pulp pinch grip (R^2 = 0.88).
- Application of the “variable rotation algorithm” in rotating joint angles improved the accuracy of the model.
- Application of the “variable rotation algorithm” in rotating joint angles enabled the prediction of thumb joint angles and pinch grip posture.
- The results of sensitivity study showed that hand posture is more sensitive to object size, orientation, and location than hand size and skin deformation.

2.9 REFERENCES

Abdel-Malek, K., J. Yang, T. Marler, et al. (2006). "Towards a new generation of virtual humans." Int. J. Human Factors Modelling and Simulation **1**(1): 2-39.

Armstrong, T. J., J. Choi and V. Ahuja (2008). Development of kinematic and biomechanical hand models for ergonomic applications. Handbook of Digital human Modeling. V. G. Duffy, CRC Press.

Blackwell, J. R., K. W. Kornatz and E. M. Heath (1999). "Effect of grip span on maximal grip force and fatigue of flexor digitorum superficialis." Appl Ergon **30**(5): 401-5.

Buchholz, B. and T. J. Armstrong (1992). "A kinematic model of the human hand to evaluate its prehensile capabilities." J Biomech **25**(2): 149-62.

Buchholz, B., T. J. Armstrong and S. A. Goldstein (1992). "Anthropometric data for describing the kinematics of the human hand." Ergonomics **35**(3): 261-73.

Choi, J. and T. J. Armstrong (2007). Quantitative analysis of finger movements during reaching and grasping tasks. ASB annual meeting, Stanford, CA.

Choi, J., C. D. Grieshaber and T. J. Armstrong (2007). Estimation of grasp envelope using a 3-dimensional kinematic model of the hand. Human Factors and Ergonomics Society Annual Meeting, Baltimore, MD.

Crosby, C. A., M. A. Wehbe and B. Mawr (1994). "Hand strength: normative values." J Hand Surg [Am] **19**(4): 665-70.

Cutkosky, M. R. (1989). "On grasp choice, grasp models and the design of hands for manufacturing tasks." IEEE Transactions on Robotics and Automation **5**(3): 269-279.

Endo, Y. and S. Kanai (2006). An Application of a Digital Hand to Ergonomic Assessment of Handheld Information Appliances. Digital Human Modeling for Design and Engineering Conference, Lyon, France.

Garrett, J. W. (1971). "The adult human hand: some anthropometric and biomechanical considerations." Hum Factors **13**(2): 117-31.

Giurintano, D. J., A. M. Hollister, W. L. Buford, et al. (1995). "A virtual five-link model of the thumb." Med Eng Phys **17**(4): 297-303.

Grieshaber, C. D. (2007). Factors affecting hand posture and one-handed push force during flexible rubber hose insertions tasks. Industrial and Operations Engineering. Ann Arbor, University of Michigan.

Hui, K. C. and N. N. Wong (2002). "Hands on a virtually elastic object." The Visual Computer **18**(3): 150-163.

Imrhan, S. N. and C. H. Loo (1989). "Trends in finger pinch strength in children, adults, and the elderly." Hum Factors **31**(6): 689-701.

Josty, I. C., M. P. Tyler, P. C. Shewell, et al. (1997). "Grip and pinch strength variations in different types of workers." J Hand Surg [Br] **22**(2): 266-9.

Landsmeer, J. M. (1962). "Power grip and precision handling." Ann Rheum Dis **21**: 164-70.

Lee, S. W. and X. Zhang (2005). "Development and evaluation of an optimization-based model for power-grip posture prediction." J Biomech **38**(8): 1591-7.

Li, Z. M. and J. Tang (2007). "Coordination of thumb joints during opposition." J Biomech **40**(3): 502-10.

Lin, M. C. and S. Gottschalk (1998). Collision detection between geometric models: a survey. Proc. of IMA Conference on Mathematics of Surfaces, Loughborough, UK.

Mathiowetz, V., N. Kashman, G. Volland, et al. (1985). "Grip and pinch strength: normative data for adults." Arch Phys Med Rehabil **66**(2): 69-74.

Miyata, N., M. Kouchi and M. Mochimaru (2006). Posture Estimation for Design Alternative Screening by DhaibaHand - Cell Phone Operation. Digital Human Modeling for Design and Engineering Conference, Lyon, France.

Napier, J. R. (1956). "The prehensile movements of the human hand." J Bone Joint Surg Br **38-B**(4): 902-13.

Santello, M., M. Flanders and J. F. Soechting (1998). "Postural hand synergies for tool use." J Neurosci **18**(23): 10105-15.

Savescu, A. and L. Cheze (2005). Numerical model of the thumb. Digital Human Modeling for Design and Engineering Conference, Iowa city, IA.

Yan, J. H. and J. H. Downing (2001). "Effects of aging, grip span, and grip style on hand strength." Res Q Exerc Sport **72**(1): 71-7.

Zhang, X., S. W. Lee and P. Braido (2003). "Determining finger segmental centers of rotation in flexion-extension based on surface marker measurement." J Biomech **36**(8): 1097-102.

CHAPTER 3

ESTIMATION OF HAND SPACE ENVELOPES USING A 3-D KINEMATIC HAND MODEL

Abstract

Obstructions often interfere with workers' ability to perform manual tasks that involve joining parts or using tools. The objective of this study was to investigate the use of a 3-D kinematic hand model to predict the hand space envelope in a hose placement task. Twelve subjects (7 males and 5 females) participated in the experiments and were asked to push the hose onto the flange using two different methods – the 'straight' method and the 'rotation' method. The hand space envelope was defined as a series of rectangles perpendicular to the long axis of the hose. The 3-D kinematic model was used to estimate hand space envelopes based on prediction of hand posture. The simulation results showed good agreement with measured data with an average 17% underestimation of sectional areas of rectangles which defined hand space envelopes. The effects of the grip type, method, and hand size on hand space envelope were investigated by simulation. Pinch grip required an average of 72% larger sectional area than power grip, but smaller values in horizontal direction of the hose. The rotation method needs an average of 26% larger sectional area than the straight method. A 95% male hand size required an average of 44% larger sectional area than 5% female

hand size. The hand space envelope can give useful information to designers and engineers who design work space and parts to avoid problems of obstruction.

3.1 INTRODUCTION

Obstructions that penetrate the hand space envelope often interfere with workers' ability to perform hand tasks such as joining parts or using tools. It has been observed that workers are often forced to perform hose installation tasks in spite of varying levels of obstructions (Ebersole 2005). An obstruction may cause workers to choose awkward hand or wrist postures, which may lead to reduction of hand strength capabilities. Awkward hand postures are positively associated with cumulative trauma disorders of the hand and wrist (Armstrong and Chaffin 1979; Kuorinka and Koskinen 1979; Luopajarvi, Kuorinka et al. 1979; Moore and Garg 1994; English, Maclaren et al. 1995; Tanaka, Wild et al. 1995).

Not much attention has been paid to the role of hand space in limiting manual work. Baker et al. measured hand space envelopes while using common hand tools such as screwdrivers and wrenches by utilizing photographic methods (Baker, McKendry et al. 1960). They collected data from six subjects whose hand sizes (hand length and breath) were at or above the 95th percentile of the male population. They approximated the space envelope using dimensions in horizontal and vertical directions along the distance from fingers' ends. This study suggested a good concept for the space envelope, but the accuracy and reliability of the photographic method remain questionable. Recently, Grieshaber measured hand space envelopes in hose insertion tasks by using a motion capture system (Grieshaber 2007). He attached 23 markers to the hand and wrist and let the subjects insert rubber coolant hoses into a stationary flange using four different insertion methods. The trajectories of markers were used to determine the lateral and vertical extreme locations of the hand along the length of the hose.

These studies provided useful information about the space envelope; however, such direct measurements of the envelope are time-consuming and cannot be easily generalized to other object shapes, object sizes, grip types, or hand sizes. The hand space envelope is determined by both hand posture and the task's dynamic characteristics. Hand posture is a function of object properties and hand anthropometry (Choi and Armstrong 2006). Dynamic characteristics of a specific task represent the methods that the workers choose. Considering the existence of a number of hand postures and dynamic characteristics in various manual works, simulation can be a solution to approximate hand space envelopes for a specific task.

This study explored the use of a kinematic model of the hand to predict hand space envelopes. By using a kinematic model, we could accommodate varying job conditions - object size, object shapes, hand size, and grip types. For this purpose, we selected a hose insertion task encountering many obstructions in an automotive assembly plant.

3.2 METHODS

3.2.1 Kinematic model description

The kinematic model of the hand and wrist was developed using Visual C++ with OpenGL graphic functions (Choi and Armstrong 2005). The hand was modeled as open chains of rigid body segments, which were represented as truncated cones, the simplest and most reasonable depiction of hand segments. The model used twenty-five degrees of freedom (DOF) to represent the main joints of the hand and wrist. The proximal (PIP) and distal (DIP) interphalangeal joints of four fingers and interphalangeal (IP) joint of the thumb were modeled with one DOF (F/E: flexion-extension). The metacarpophalangeal (MCP) joints of the thumb and four fingers were described with two DOFs (F/E and ABD/ADD: abduction-adduction). The carpometacarpal (CMC) joint of the thumb and the wrist joints were modeled as three DOFs (F/E, ABD/ADD, and P/S: pronation-supination). All joints were assumed to be ideal joints. The finger segment lengths and breadths were calculated from the dimension of hand length and breadth, based on Buchholz's data (Buchholz and Armstrong 1992).

The model can be used to predict a hand posture for given object properties such as object size, shape, location, and orientation, using a collision detection algorithm. Each joint of the fingers is rotated according to an observation-based rotation algorithm (Choi and Armstrong 2007) until each segment detects a contact with the object surface. Prediction and measured postures were highly correlated that R^2 between predicted and observed joint angles was 0.76 for power grip and 0.88 for pinch grip.

3.2.2 Experiments

Twelve participants (7 males and 5 females) with no history of upper extremity disorders volunteered for the experiment. The hand sizes of study participants are summarized in Table 3.1. A 19-mm rubber coolant hose (25-mm outer diameter) was placed onto a flange located at elbow height. Twenty-three markers were attached to the dorsal side of the hand and wrist. Four markers per each finger were secured at the tip, and at the DIP, PIP, and MCP joints on the dorsal side of the hand. For the thumb, four markers were located at the tip, and at the IP, MCP, and CMC joints. Three markers were located on the dorsal side of the center of the wrist and on the distal ends of the dorsal tubercle of the radius and the ulnar styloid process. An OptoTrak® Certus™ motion-tracking system (whose RMS positional accuracy is 0.1 mm) was used to collect posture data during the placement of the hose. Two position sensors, placed left and right side of the subject, tracked positions of markers at 30 Hz of sampling rate. Subjects were asked to push the hose using the straight method and the rotation method. The straight method is to push the hose directly onto the flange along the insertion axis without any movement to other directions. The rotation method is to push the hose with rotation about the insertion axis. These experiments were performed in the previous study (Grieshaber 2007) and their results were compared with the simulation results of this study.

Table 3.1 Hand length summary of study participants. Percentiles are listed in parenthesis (Garrett 1971).

Gender	Age (years)	Hand Length (cm)	Range (cm)
Female (n=5)	21.5 ± 2.6	18.3 ±0.8 (67 %ile)	17.3 – 19.4
Male (n=7)	25.7 ± 4.2	19.2 ± 1.3 (27 %ile)	17.6 – 21.1
Pooled	23.6 ± 4.0	18.8 ± 1.1	17.3 – 21.1

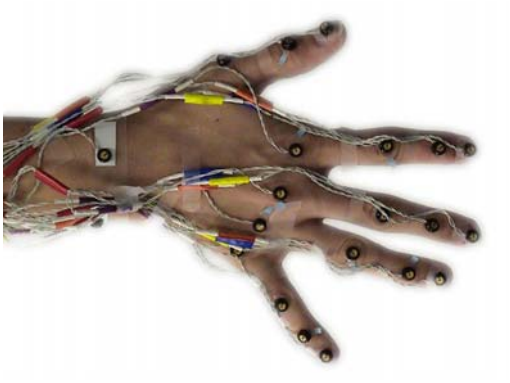

(a) OptoTrak marker locations

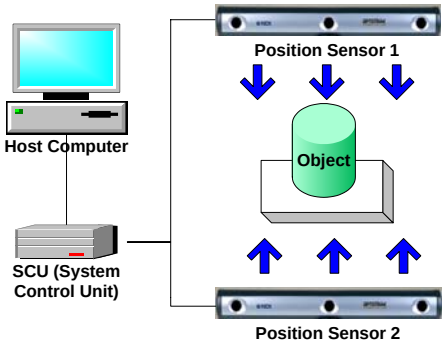

(b) Experimental Setup

Figure 3.1 Experimental Setup. (a) Twenty-six markers were attached to the dorsal side of the hand. (b) Two OptoTrak position sensors were used to track the positions of markers

3.2.3 Simulation

Hand posture was predicted by the model for a given hose shape (cylindrical), size (25 mm outer diameter), orientation (36º between long axis of hose and the vector between ulnar and radial styloid process), and location (6.98 mm between center of the hose and the center of the wrist). In the model, the joint angle of each joint increased at its observation-based rate until the corresponding segment contacted the hose (Choi and Armstrong 2007). Once the posture was predicted, we calculated positions of 23 markers which were attached to the dorsal side of the hand and the wrist in the experiment. Using homogeneous transformation, these marker positions were expressed with respect to the newly defined local coordinate system. The origin of this system is the center of the flange in the plane of the front end. Its x-axis is the unit vector to dorsal direction, its y-axis is the unit vector to superior direction, and its z-axis is the unit vector to the body (Figure 3.2).

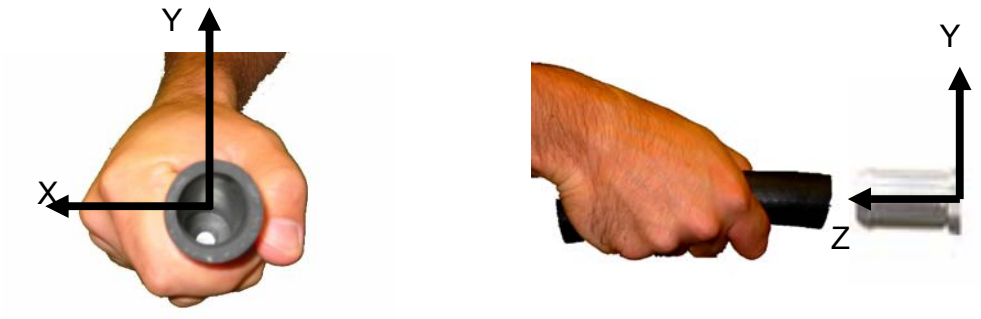

Figure 3.2 Definition of the new local coordinate system attached on the flange. The origin of this system is the center of the flange in the plane of the front end. Its x-axis is the unit vector to dorsal direction, its y-axis is the unit vector to superior direction, and its z-axis is the unit vector to the body.

Two insertion methods – a straight method and a rotation method - were simulated. Figure 3.3 illustrates these two methods. As the hose is rotated while it is pushed forward, the relationship between rotation angle (θ) and the distance (d) from the end of the flange was assumed as the following equation:

$$\theta = \theta_0 \cdot \sin(\omega \cdot t)$$
$$d = v \cdot t \qquad (3.1)$$

where θ_0: maximum amplitude of rotation angle

θ: rotation angle

d: distance from the end of the flange

v: velocity in axial direction

ω: angular frequency of rotation

t : time

(a) straight method (b) rotation method

Figure 3.3 Hose insertion methods. The 'straight' method is to insert the hose directly onto the flange along the insertion axis without any movement in other directions. The 'rotation' method is to insert the hose with rotation about the insertion axis.

For Eq.(3.1), values of parameters were assumed based on the observation (Grieshaber 2007) the angular frequency was assumed to be 1.75 Hz because it was observed that subjects changed direction of rotation 3.5 times during insertion. The maximum amplitude of the rotation angle was 73º for the rotation method and 10º for the

straight method based on our observations. The axial velocity was constant (35 mm/s), and the distance from the end of the flange changed from 35 to 0 mm, because the length of the flange used in the experiment was 35 mm. We assumed 10º amplitude of rotation angle in the straight method because we observed that subjects rotated the hose a little during the insertion even when they were instructed to push the hose forward using the straight method.

To compare the simulation results with measurement, the use of power grip with the rotation method was assumed. The simulation was performed for 25% of male hand size in order to represent the average hand size of subjects who participated in the experiments. To investigate the effect of grip types on the hand space envelope, two grip types – a power grip and a pinch grip – with the rotation method and 25% male hand size were simulated. To examine the effect of hose insertion method, straight and rotation methods with 25% male hand size and power grip were simulated. Finally, hand size effect was investigated by simulating the hose insertion task with the power grip and the rotation method using 5% female and 95% male hand size.

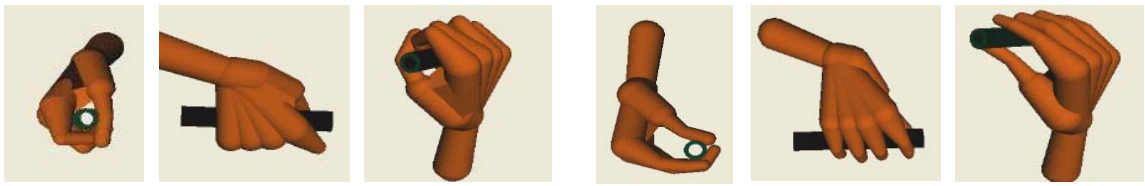

(a) power grip **(b) pinch grip**

Figure 3.4 Different views of predicted hand posture grasping a 25 mm diameter hose.

3.3 RESULTS

3.3.1 Comparison of results of simulation and measurement

To compare the simulation results with the data derived from measurements, four critical dimensions were defined as illustrated in Figure 3.5. X_1 and X_2 are the distances from the center to the palmar side and dorsal side of the x-axis, respectively. Y_1 and Y_2 are defined as the distances from the center to the inferior part and superior part of the y-axis. The envelopes were calculated for six ranges which were divided by the distance from the end of the hand: 0~25 mm, 25~50 mm, 50~75 mm, 75~100 mm, 100~125 mm, and 125~150 mm.

Table 3.2 shows critical dimensions defined in Figure 3.5 and areas calculated by these critical dimensions when subjects were using a rotation insertion method with a power grip. Simulation underestimated most of the horizontal directional dimensions (simulation – measurement : X_1 = -4 mm, X_2 = -7 mm, on average) , but the patterns of those values along six different distance ranges were similar to the patterns of the measured values. The differences of horizontal dimensions (X_1 and X_2) between measurement and simulation ranged from -11 mm (at 125~150 mm) to 4 mm (at 25 ~ 50 mm). For vertical directional dimensions, the differences between measurement and simulation ranged from -12 mm (at 75~100 mm) to 33 m (at 125~150 mm). Over all ranges, the simulation results show good agreement with measured data with an average 17% underestimation of sectional areas(Figure 3.6). The difference in space envelope areas between measurement and simulation was largest in the 125~150 mm range (2210 mm^2) and smallest in the 50~75 mm range (454 mm^2).

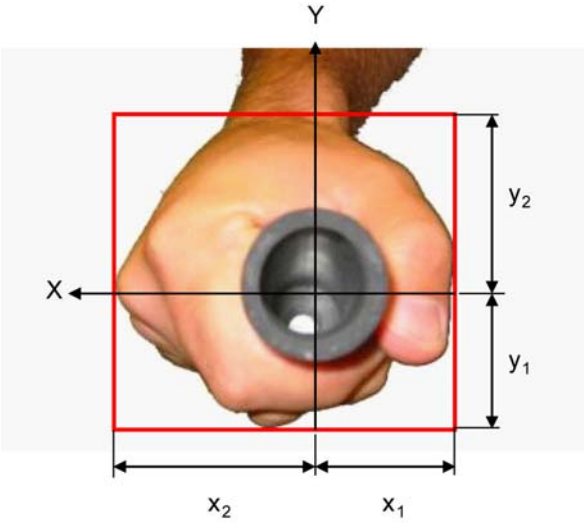

Figure 3.5 Definition of critical dimensions. X_1 and X_2 are the distances from the center to the palmar side and dorsal side of x-axis, respectively. Y_1 and Y_2 are defined as the distances from the center to superior part and inferior part of y-axis.

Table 3.2 Comparison of critical dimensions and areas for different ranges from the front end of the hand.

Distance from the end of the hand (mm)	Method	Horizontal Axis		Vertical Axis		Area
		X_1 (mm)	X_2 (mm)	Y_1 (mm)	Y_2 (mm)	(mm^2)
25	Simulation	-22	28	-32	13	2229
	Measurement	-24	38	-36	26	3844
50	Simulation	-32	48	-37	37	5893
	Measurement	-36	48	-45	40	7140
75	Simulation	-48	49	-42	51	8986
	Measurement	-41	57	-53	47	9800
100	Simulation	-48	53	-46	52	9847
	Measurement	-41	60	-53	40	9393
125	Simulation	-40	53	-49	26	7000
	Measurement	-37	62	-43	50	9207
150	Simulation	-25	53	-41	21	4859
	Measurement	-14	59	-22	54	5586

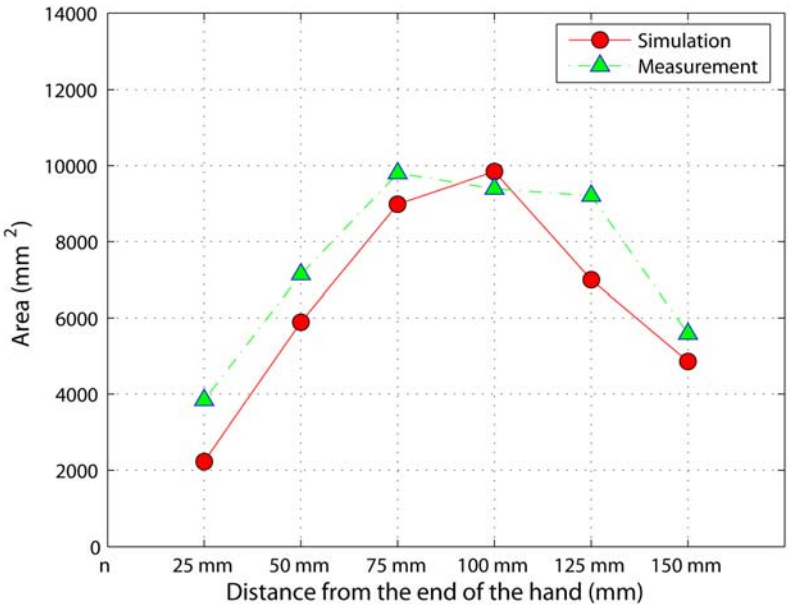

(a) Comparison of sectional areas along the distance from the end of the hand between simulation and measurement

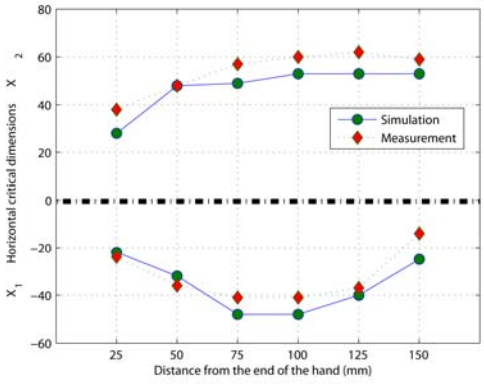

(b) Horizontal dimensions

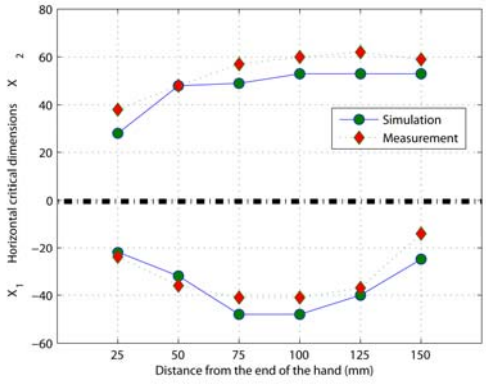

(c) Vertical dimensions

Figure 3.6 Comparison between simulation and measurement. (a) Comparison of sectional areas along the distance from the end of the hand; (b) Comparison of horizontal dimensions along the distance from the end of the hand; and (c) Comparison of vertical dimensions along the distance from the end of the hand. On average, the areas from simulation were 17% less than those from measurement.

3.3.2 Effect of grip type, insertion method, and hand size

Figure 3.7 shows the effect of grip type on hand space envelope (25% male hand size, rotation method). As all the MCP joints of fingers, thumb CMC and MCP joints, and wrist joints were located much further from the center of the hose, the pinch grip required much more sectional areas than the power grip. From the simulation result, pinch grip required 72% more sectional areas than power grip on average. However, the required space in horizontal direction from the hose was much smaller in the pinch grip than in the power grip. X_1 values were 47% smaller in pinch grip than in power grip.

Figure 3.8 shows the space envelopes when using straight method and rotation method during hose insertion tasks (power grip, 25% male hand size). On average, the rotation method required 26% larger sectional areas than the straight method.

Figure 3.9 shows the effect of hand size on the space envelope when using rotation method with a power grip. On average, the 95% male hand size required 44% larger sectional areas than the 5% female hand size. In particular, the 95% male hand size required much more space at 100~150 mm ranges, because the 95% male hand size had a bigger hand breadth (9.6 mm) than that of 5% female hand size (7.1 mm).

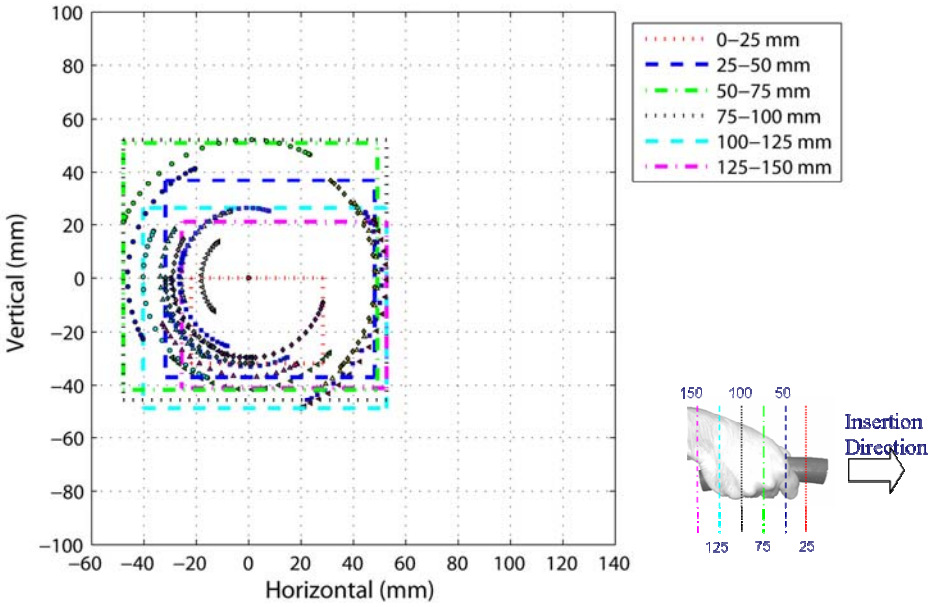

(a) Power grip

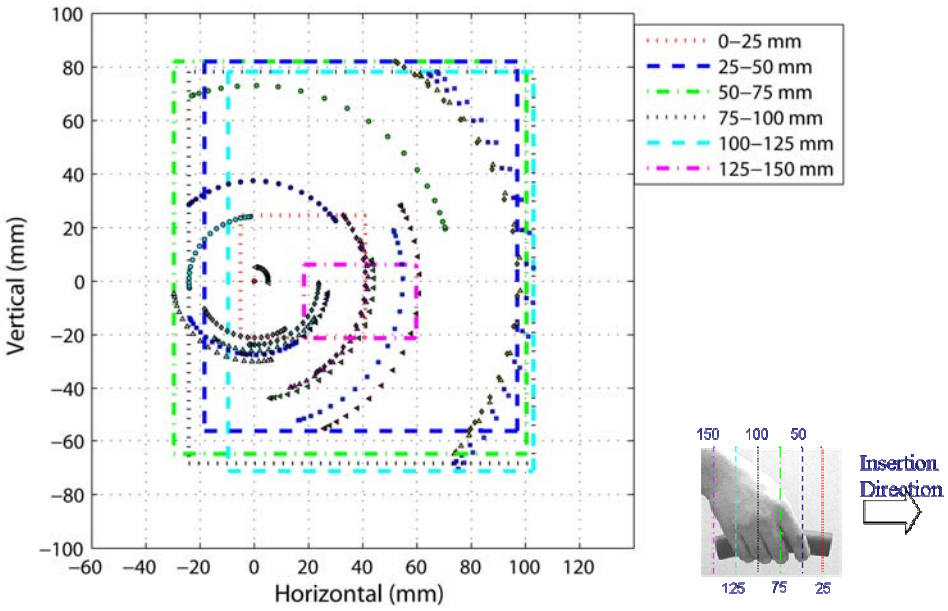

(b) Pinch grip

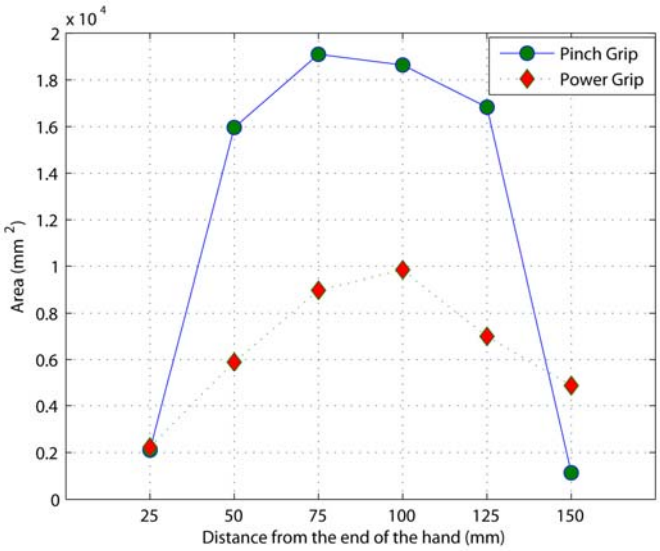

(c) Area comparison between power and pinch grip

Figure 3.7 Comparison of space envelopes in power grip and pinch grip (25% male hand size, rotation method)

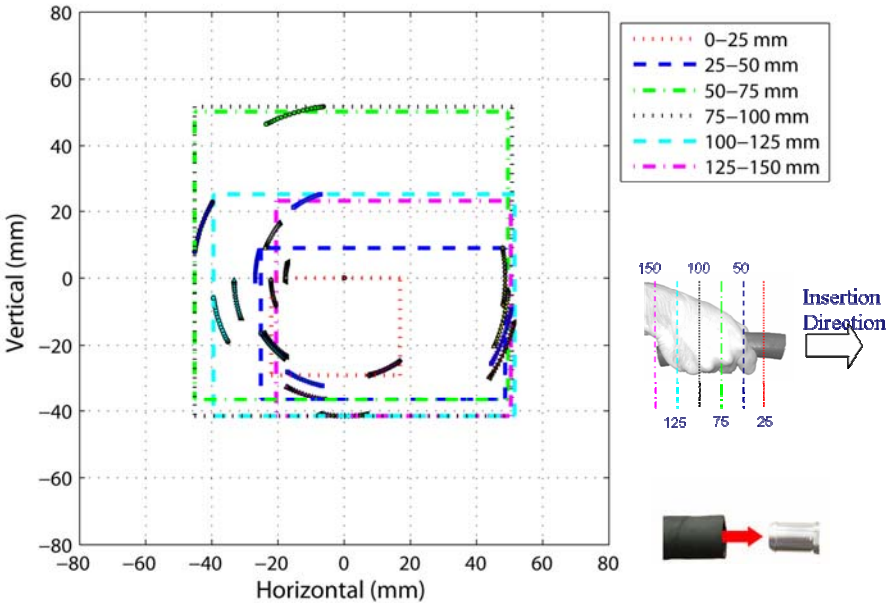

(a) straight method

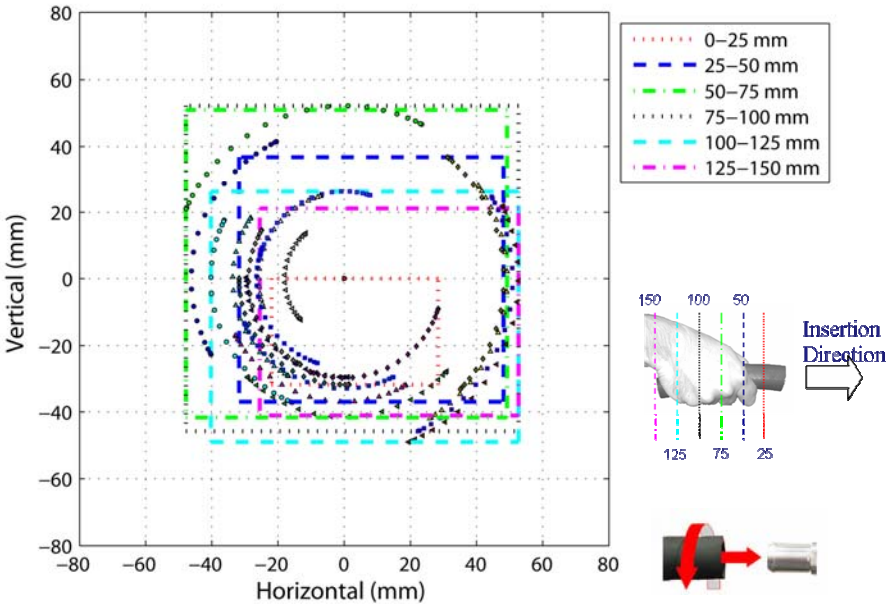

(b) rotation method

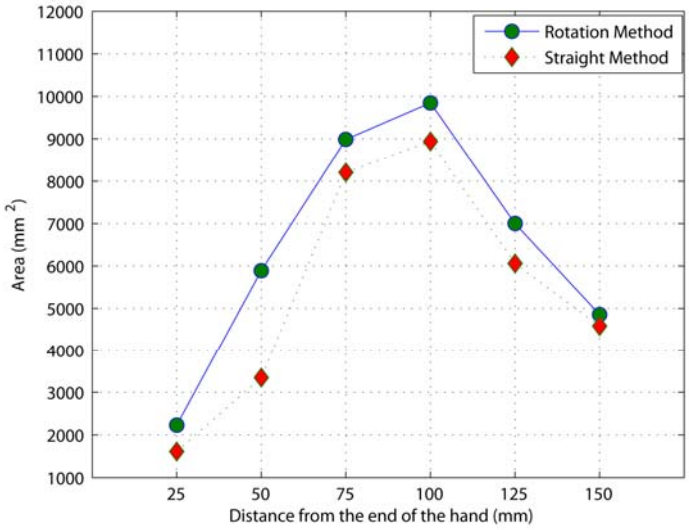

(c) Area comparison between rotation and straight methods

Figure 3.8 Comparison of space envelopes for straight and rotation hose insertion methods (power grip, 25% male hand size).

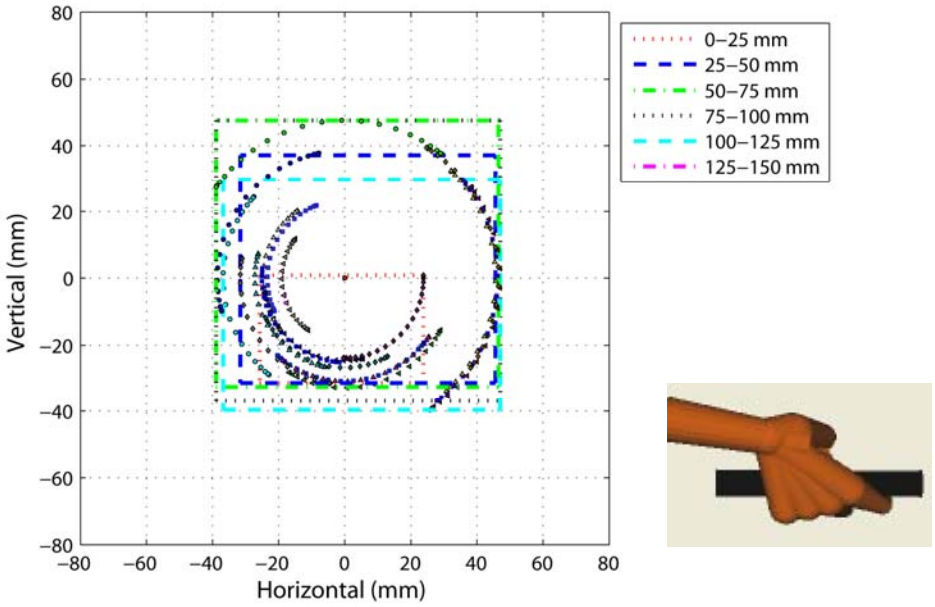

(a) 5% Female

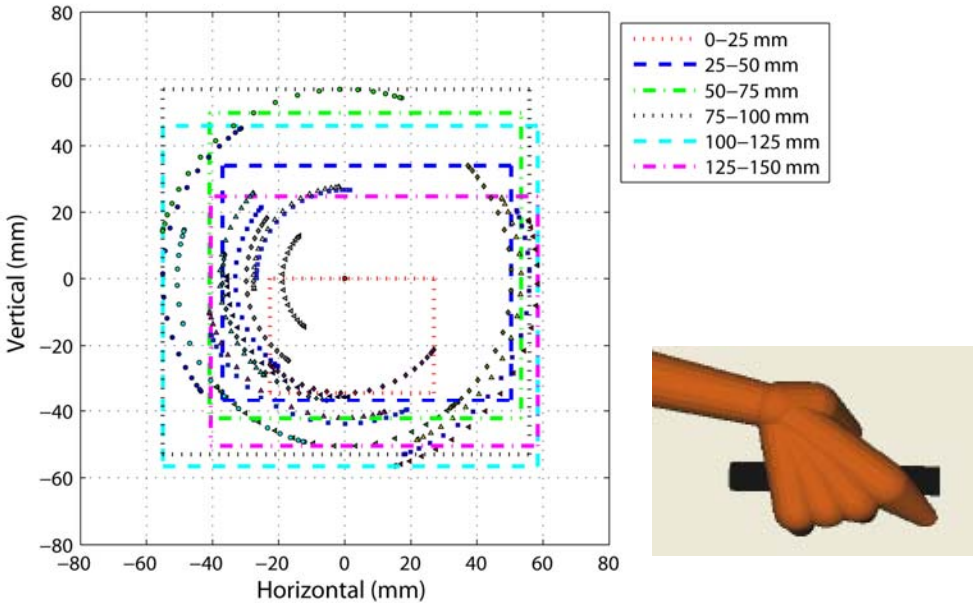

(b) 95% male

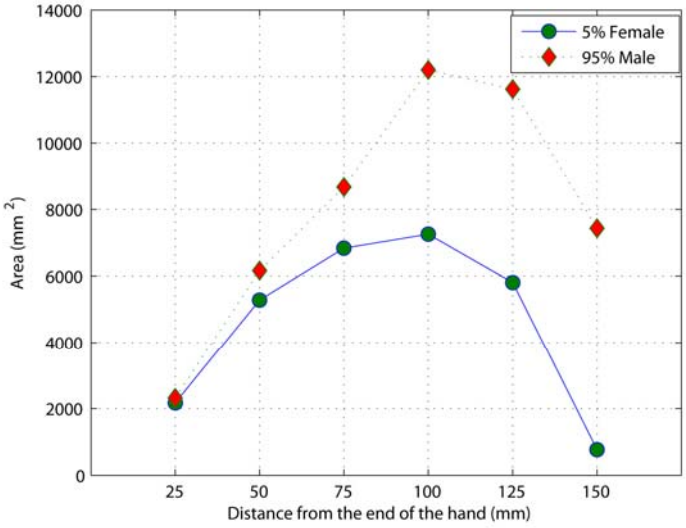

(c) Area comparison between 5% female and 95% male hand size

Figure 3.9 Comparison of space envelopes for 5% female and 95% male hand sizes (power grip, rotation method)

3.4 DISCUSSION

Hand space envelopes were characterized using a series of rectangles perpendicular to the long axis of a cylindrical hose after Baker et al. (1960). Baker's study was the first attempt to measure the space requirement during common tools use such as wrenches and screwdrivers (Baker, McKendry et al. 1960). The photographic method they used includes potential errors, because the method is based on 2-D images. The development of technology, such as a 3-D motion capture system, enabled us to measure space requirement directly and more accurately. Grieshaber used this technology to measure hand space envelope in hose insertion jobs with different methods and provided more accurate results (Grieshaber 2007). As mentioned earlier, these direct measurements have innate limitations for application, because many factors affect the space envelope. Empirical models based on an object of a given shape and size and a given task cannot be always generalized to another object and task. Use of complete simulations using a 3-D kinematic model can help to overcome the limitations of empirical models.

The space envelope is affected by various factors such as hand size, grip type, and dynamic characteristics of a task. The effect of hand size comes not only from the length and breadth but also from the different posture. It has been reported that larger hand size causes smaller joint angles when grasping objects of same size (Buchholz and Armstrong 1992; Choi and Armstrong 2006). Accurate prediction of hand posture is essential to predict the hand space envelope. Dynamic (behavioral) characteristics is another important factor for prediction of the hand space envelope. We used a simple sinusoidal function to model the behavioral characteristics during hose insertion, but some dynamic motion might not have been described with the function.

Underestimation of horizontal critical dimensions and larger differences of vertical critical dimensions at 100~150 mm seem to be caused by the difference of dynamic characteristics in the simulation and the measurement. The simulation results were shifted to medial direction for most of ranges, which means that subjects exerted the force in the lateral direction during insertion. It is natural to push the hose in the lateral direction while rotating the hose. All of these subjects were right-handed and finally rotated their hands in clockwise direction. This is consistent with finding of Seo et al. (2007) who showed that twisting a cylindrical handle in the direction that the fingers tighten the grip improved maximum torque by 45% for a person with given strength. The flexibility of the hose seems to be a causative factor explaining larger differences at 100~150 mm, which could not be captured by our simple dynamic model.

The force required for certain tasks can change dynamic (behavioral) characteristics significantly. It has been reported that hand space envelopes are affected by the insertion method and the force required for hose insertion tasks (Grieshaber 2007). The required force can change the number of direction changes and the amplitude of rotation angles, both of which can change the modeling of dynamic characteristics in this study. We used the data with high interference between flange and hose, but low interference data will decrease the space envelope, because the amplitude of rotation angle and the number of direction changes decrease.

Comparison of hand space envelopes in power grip and pinch grip demonstrates the largest difference. Interestingly, the pinch grip requires smaller space than the power grip over the range of 0 ~ 25 mm, and all amplitudes of X_1 values were smaller in the pinch grip. Generally, the hand posture has been known to be decided by many factors – force requirements, hand size, object size, object location, and object orientation, task requirement (Armstrong, Keyserling et al. 2003; Choi and Armstrong

2006). Grieshaber observed that workers are more likely to select the pinch grip for the job where the object size is small or the force requirement is low, than to select a power grip posture (2007). Workers tend to use a power grip for forceful exertion and large grip objects, but this may not be possible if there is not sufficient space. The hand pace envelope data (power and pinch grip) predicted by the 3-D model can be used to predict the selection of grip type.

Hand space envelopes were calculated as a series of rectangles perpendicular to the long axis of the hose. The rectangles circumscribed the minimum and maximum values of horizontal and vertical dimensions. This approach enables us to simplify interpretation of data and to compare the results with the previous measurement data by Grieshaber (2007). The cross-sectional areas can be described in four critical dimensions using the 3-D kinematic model. This makes it possible to superimpose the envelope on 3-D renderings of work spaces so that we can identify whether intrusions into the hand space force the workers to use a pinch grip or prevent them from gripping the object.

3.5 LIMITATIONS AND FUTURE RESEARCH

The prediction of space envelope was performed by calculating positions of markers corresponding to experimental settings, because our first goal was to determine whether simulation results can match measured results. This approach can capture most of the hand space requirements, but some part of the hand might not have been captured, especially the thumb. Also, the prediction was based on a kinematic model in which the hand segments were modeled with truncated cones, which cannot accurately

represent the skin of the hand. More accurate prediction can be performed by importing real hand surface data and calculating of all arrays of points representing hand shape.

One of the potential extensions of this study is the prediction of the dynamic space envelope, which means the required space during reaching and grasping. The modeling of dynamic characteristics such as joint angle profile as a function of object size, and grip types will be essential to estimate the dynamic space envelope accurately.

The inter-subject grip variability can also affect space envelope, because they can affect hand posture. We simulated only two grip types (power grip and pulp pinch grips), but there are a lot of variability in grip types. We observed that subjects used two different grip types depending on the thumb position while they were using power grip - transverse volar grasp with the thumb abducted for added power, and diagonal volar grasp with the thumb adducted for an element of precision. The change of thumb position will definitely affect the hand space, especially the inferior directional dimension in hose placement task. Observation of more subjects will enable us to examine the effect of inter-subject grip variability.

Object shape, object orientation, and constraints of object (fixed or free to move) also should be considered in estimating hand space envelope, because they affect hand posture and wrist posture. Our study investigated the use of a cylindrical object (hose), but the use of different object shape such as a connector can change the hand space envelope.

3.6 CONCLUSIONS

- Hand space envelopes during the hose placement task were estimated using the kinematic model of the hand. The simulation results show good agreement with measured data with an average 17% underestimation of sectional areas
- On average, the use of pinch grip required 72% larger sectional areas than the use of power grip during the hose insertion task. But the pinch grip required 50% smaller values in the medial direction than the power grip.
- The rotation method requires an average of 26% greater sectional area than the straight method.
- A 95% male hand size requires 44% larger sectional areas than a 5% female hand size.

3.7 REFERENCES

Armstrong, T. J. and D. B. Chaffin (1979). "Carpal tunnel syndrome and selected personal attributes." J Occup Med 21(7): 481-6.

Armstrong, T. J., W. M. Keyserling, D. C. Grieshaber, et al. (2003). Time based job analysis for control of work related musculoskeletal disorders. 15th Congress of the Internatinal Ergonomics Association, Seoul, Korea.

Baker, P. T., J. M. McKendry and G. Grant (1960). "Volumetric requirements for hand tool usage." Human Factors 2: 156-162.

Buchholz, B. and T. J. Armstrong (1992). "A kinematic model of the human hand to evaluate its prehensile capabilities." J Biomech 25(2): 149-62.

Choi, J. and T. J. Armstrong (2005). 3-dimensional kinematic model for predicting hand posture during certain gripping tasks. International Society of Biomechanics Meeting, Cleveland, OH, USA.

Choi, J. and T. J. Armstrong (2006). Sensitivity study of hand posture using a 3-dimensional kinematic hand model. 16th International Ergonomics Association Meeting, Maastricht, Netherlands.

Choi, J. and T. J. Armstrong (2007). Quantitative analysis of finger movements during reaching and grasping tasks. ASB annual meeting, Stanford, CA.

Ebersole, M. L. (2005). An investigation of exposure assessment methods for selected physical demands in hand-intensive work. Industrial and Operations Engineering. Ann Arbor, MI, University of Michigan.

English, C. J., W. M. Maclaren, C. Court-Brown, et al. (1995). "Relations between upper limb soft tissue disorders and repetitive movements at work." Am J Ind Med 27(1): 75-90.

Garrett, J. W. (1971). "The adult human hand: some anthropometric and biomechanical considerations." Hum Factors 13(2): 117-31.

Grieshaber, C. D. (2007). Factors affecting hand posture and one-handed push force during flexible rubber hose insertions tasks. Industrial and Operations Engineering. Ann Arbor, University of Michigan.

Kuorinka, I. and P. Koskinen (1979). "Occupational rheumatic diseases and upper limb strain in manual jobs in a light mechanical industry." Scand J Work Environ Health 5 suppl 3: 39-47.

Luopajarvi, T., I. Kuorinka, M. Virolainen, et al. (1979). "Prevalence of tenosynovitis and other injuries of the upper extremities in repetitive work." Scand J Work Environ Health 5 suppl 3: 48-55.

Moore, J. S. and A. Garg (1994). "Upper extremity disorders in a pork processing plant: relationships between job risk factors and morbidity." Am Ind Hyg Assoc J 55(8): 703-15.

Seo, N. J., T. J. Armstrong, J. A. Ashton-Miller, et al. (2007). "The effect of torque direction and cylindrical handle diameter on the coupling between the hand and a cylindrical handle." J Biomech 40(14): 3236-43.

Tanaka, S., D. K. Wild, P. J. Seligman, et al. (1995). "Prevalence and work-relatedness of self-reported carpal tunnel syndrome among U.S. workers: analysis of the Occupational Health Supplement data of 1988 National Health Interview Survey." Am J Ind Med 27(4): 451-70.

CHAPTER 4

QUANTITATIVE ANALYSIS OF FINGER MOVEMENTS DURING REACH AND GRASP TASKS

Abstract

Finger movement affects final hand posture. Previous studies have investigated the use of contact algorithm to predict hand posture, but they have not considered relative rotation of finger joints explicitly. Many studies on finger movements were limited for flexion movement only or for a limited set of joints, which cannot fully describe hand motion. The objective of this study was to investigate the coordination of hand movement during reaching and grasping (power grasping and pinch grasping) including all the joints of four fingers and thumb so that it can be used for modeling purpose. We defined spatial and temporal variables characterizing hand movement and examined how these variables were affected by object size. Maximum aperture increased as object size increased both in power and pinch grasping, but time to reach maximum aperture was dependent on object size only in pinch grasping. We found that all the joints of the four fingers flexion-extension of MCP and CMC joints of the thumb were used in power grasping, whereas all the MCP joints of the four fingers and the thumb CMC joint were used in pinch grasping in order to adjust hand to differently sized object. Subjects changed the angular velocities of their finger joints as the object size changed, which reduced the time difference to complete grasping objectsof varying size.

4.1 INTRODUCTION

Ergonomic analyses of hand function remain a challenge for engineers and designers. The hand strength is closely related to hand posture (Mathiowetz, Kashman et al. 1985; Imrhan and Loo 1989; Crosby, Wehbe et al. 1994; Josty, Tyler et al. 1997; Blackwell, Kornatz et al. 1999; Yan and Downing 2001). The space taken up by the hand is also determined by the hand posture which is affected by the geometric and material properties of grip object and hand size (Choi, Grieshaber et al. 2007; Grieshaber 2007). The hand posture is imperative for tendon excursion to be predicted, because tendon displacement is determined by the joint angles of finger (Landsmeer 1961; Landsmeer 1961; Armstrong and Chaffin 1978).

Finger movement affects the final hand posture (Armstrong, Choi et al. 2008). Previous studies have investigated the use of contact algorithms to predict hand postures (Buchholz and Armstrong 1992; Pollard and Zordan 2005; Endo and Kanai 2006; Miyata, Kouchi et al. 2006; UGS 2006). Contact algorithms used in these studies entailed rotating the finger joints until contact occurred between hand and grip object, and thus the predicted posture was affected by the relative rate of finger joint rotation. However, previous studies have not considered relative rotations of finger joints explicitly. The movement pattern also enables us to predict hand posture not only in power grip but also in other grips such as pulp pinch and tip pinch, because selection of different grip type changes movement pattern significantly. Therefore, it is necessary to understand finger movements to evaluate the final hand posture in a specific task.

The coordination of the finger movements has been investigated to find the dominant pattern during grasping. Some researchers have suggested that the hands are controlled by kinematic synergies which reduced the possible movement patterns

significantly (Santello, Flanders et al. 1998; Santello and Soechting 1998; Mason, Gomez et al. 2001; Santello, Flanders et al. 2002; Braido and Zhang 2004). They analyzed the movement data using PCA (principal component analysis) and found that a few eigenpostures can describe the reaching and grasping motion sufficiently. But these analyses were performed for either flexion movement only or for a limited set of joints excluding some degrees of freedom (especially the thumb) which are necessary to fully describe hand motion.

The effects of characteristics of interacting objects should be considered in describing grasp movements. It was observed that the aperture (distance between the thumb tip and the index finger tip) changed as the object size changed in grasping movement (Jeannerod 1981; Jeannerod 1984; Paulignan, Frak et al. 1997). However, the effects of object characteristics on the individual DOFs have not been well investigated. Both temporal and spatial data associated with object characteristics are also important in describing human hand movements.

The purpose of this study was to investigate the hand movement pattern including all fingers and thumb quantitatively during reaching and grasping tasks, so that the results of this study can be applied to the prediction of hand posture during manual work tasks. The effect of object size on the hand movement pattern was tested through direct measurement and analysis. We hypothesized that spatial and temporal variables are significantly affected by object size and that there are dominant movement patterns of grasping movement owing to the synergy effect of motor control. Eighteen DOFs of all finger and thumb joints were analyzed to sufficiently describe the hand movements. Information about the finger movements provides knowledge about the required space for the hand during grasping an object. As the finger movement is accomplished by the movement of muscles and connected tendons, tendon excursions – one of the main risk

factors for WRMSDs (work-related musculoskeletal disorders) – can be estimated by modeling finger movement. The results also can be used for the rehabilitation purpose such as clinical diagnosis of hand-related disorders.

4.2 METHODS

4.2.1 Experiments

Experimental Design

Sixteen healthy subjects with no history of musculoskeletal disorders in upper extremities participated in the experiment. Demographic information for the study population is shown in Table 4.1. Their hand lengths ranged from 2% female to 83% male according to Garret's data (Garrett 1971). All subjects gave their written consent to participate in the study. The experimental design was reviewed and approved by the University of Michigan Institutional Review Board. The detailed methods are described in Chapter 2.

Table 4.1 Hand length summary of study participants. Percentiles are listed in parenthesis (Garrett, 1970).

Gender	Age	Hand Length (cm)	Range (cm)
Female (n=5)	21.0± 1.0	17.4± 1.3 (25 %ile)	16.3– 19.5
Male (n=11)	23.7± 4.3	19.6± 0.9 (43 %ile)	17.8– 20.6
Pooled	23.0± 3.9	18.9± 1.4	16.3– 20.6

4.2.2 Data analysis

The data obtained were processed with Matlab® software. The DIP, PIP, and MCP joint angles of four fingers were calculated from the 3D marker position data, using the dot products of the adjacent vectors, each of which represents each segment. The IP joint angle of the thumb was calculated in the same way. The thumb MCP joint has two degrees of freedom – F/E (flexion/extension) and ABD/ADD (abduction/adductio.

The plane containing tip, IP, and MCP markers was defined and the vector between MCP and CMC joint marker was projected onto the plane. The F/E angle was calculated using dot products of the IP-MCP vector and the projected vector. The AA angle was calculated using dot products of MCP-CMC vector and the projected vector. Thumb CMC joint angles were calculated using Euler angles of flexion-extension, abduction-adduction, and pronation-supination rotation sequence. Flexion was positive for flexion-extension angles, abduction was positive for abduction-adduction angle, and supination was positive for pronation-supination angle. Therefore, all the joint angles used in this study are marker-defined joint angles.

A representative plot of joint angle profile during reach and grasp movement is shown in Figure 4.1. We defined five temporal and five spatial variables which characterize the movement pattern. "Initial angle" was defined as the average joint angles for the first 50 ms, because the subjects started moving their arms at least 0.5 seconds after beginning of data recording. "Final angle" was calculated as the angle when the joint angle became steady – when the velocity is less than a preset threshold. "Open angle" was then obtained by finding the minimum angle for flexion-extension (the maximum angle for abduction-adduction, pronation-supination). From the velocity profile, the minimum velocity and the maximum velocity were found, and the joint angles when joint angular velocity reached the minimum or maximum velocity were found. Those angles were defined as "minimum velocity angle" and "maximum velocity angle," respectively. A "start open" time was defined as a time when the joint angle reached 5% of the difference between initial and open angle. An "opening time (T_{open})" was defined as a time taken for the joint angle to reach the open angle from "start open" time. "Closing time (T_{close})" was a time taken for the joint angle to travel from the open angle to the final angle. "Minimum velocity time" and "maximum velocity time" were defined as

times during which the joint angular velocity reached the minimum and maximum velocity from “start open” time and “end open” time, respectively. All time variables were normalized by the duration of hand movement, i.e., the time for the hand to reach the handle located 30 cm in front of the subject, because each subject moved the hand at different speed. Therefore, the time when the hand reaches the object is 1. We used normalized time for the analysis of temporal variables hereafter.

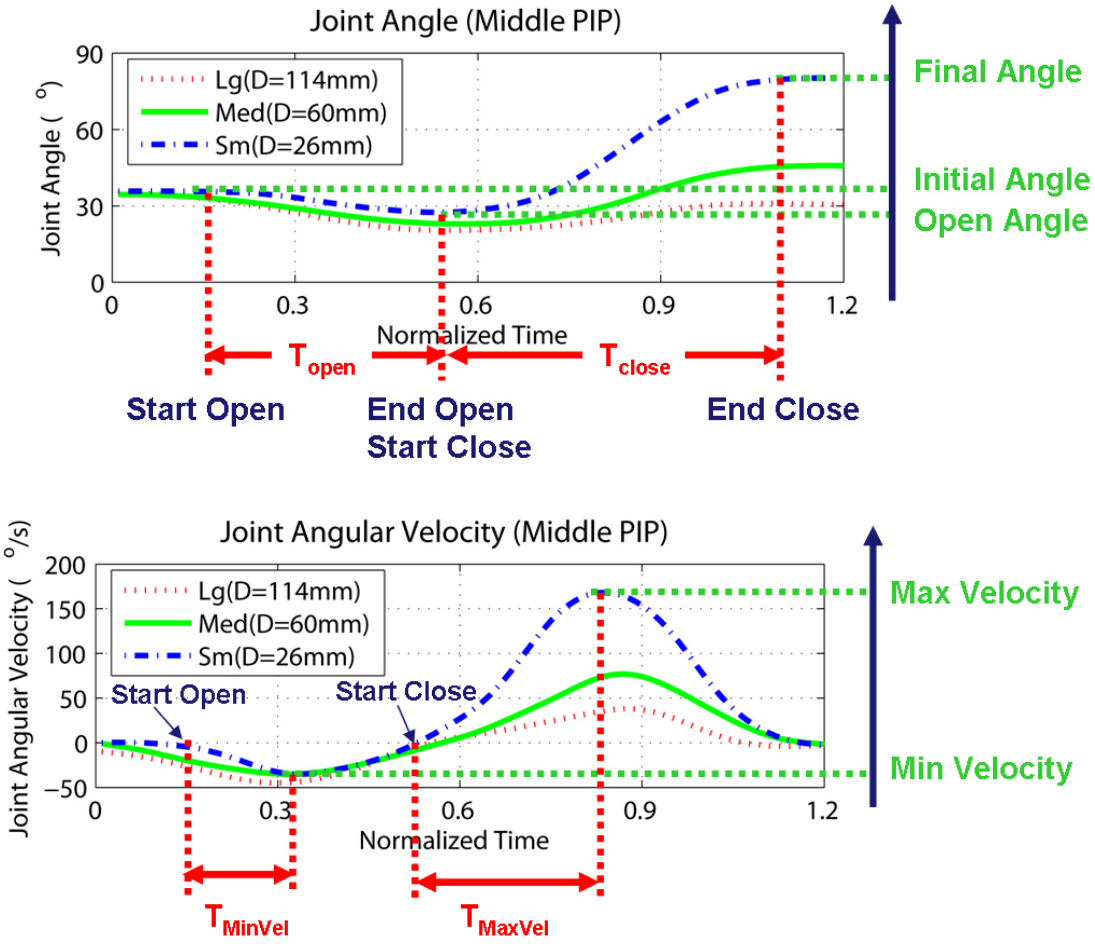

Figure 4.1 Representative plot of joint angle profile during a reach and grasp movement. Five temporal and spatial variables were defined to characterize the movement. (Lg: Large, Med: Medium, Sm: Small, D: Diameter)

4.3 RESULTS

4.3.1 Maximum aperture and maximum aperture time

Movement time – time for the hand to travel to the object – was 1.05 ± 0.28 seconds for power grasping and 1.06 ± 0.19 seconds for pinch grasping and showed no significant difference ($p>0.05$). Table 4.2 shows the maximum apertures and the maximum aperture times (time to reach the maximum aperture) of four fingers during power and pinch grasping. All maximum apertures were significantly affected by the object size ($p<0.05$) for both power and pinch grasping. The ratio of maximum aperture to object size (diameter) decreased as the object size increased. The ratio (maximum aperture/object size) was 3.9 - 4.6 (3.0 - 3.3) in small object, 2.1 - 2.3 (1.8-2.0) in medium object, and 1.4 - 1.6 (1.3 – 1.4) in large object during power (pinch) grasping. The time to reach maximum aperture for power grasping did not correspond to the object size, even though the maximum apertures were affected by the object size. In particular, no significant difference in the maximum aperture times between the large object (D=114 mm) and the medium object (D=60 mm) was observed. However, the maximum aperture times for pinch grasping showed significant differences ($p < 0.05$) across the object size and also corresponded to the object size. On average, the maximum aperture time was 37% larger in pinch grasping (0.59 seconds) than in power grasping (0.43 seconds).

Table 4.2 Maximum apertures (mm) and maximum aperture times (s) of four fingers during power and pinch grasping

	Object Size	POWER GRIP (mm)			
		Index	Middle	Ring	Little
Max Aperture	Lg(D:114mm)	156.1±19.1	177±19.7	180.4±20.4	178.2±12.7
	Med(D:60mm)	124.6±22.7	132.7±21.9	137.7±26.5	140.7±25.6
	Sm(D:26mm)	101.4±13.7	110±14.3	114.9±15	120.8±15.1
Max Aperture Time	Lg(D:114mm)	0.38±0.12	0.45±0.12	0.48±0.10	0.49±0.13
	Med(D:60mm)	0.46±0.10	0.45±0.06	0.48±0.08	0.49±0.08
	Sm(D:26mm)	0.37±0.07	0.37±0.08	0.38±0.08	0.4±0.10
	Object Size	PINCH GRIP (mm)			
		Index	Middle	Ring	Little
Max Aperture	Lg(D:114mm)	146.5±8.9	155.0±10.1	156.4±11.2	153.7±10.4
	Med(D:60mm)	109.7±9.1	115.7±9.7	118.2±12.7	118.1±11.5
	Sm(D:26mm)	77.1±5.7	81.7±6.7	85.6±9.8	86.5±9.6
Max Aperture Time	Lg(D:114mm)	0.66±0.15	0.64±0.14	0.65±0.16	0.67±0.16
	Med(D:60mm)	0.60±0.13	0.56±0.12	0.56±0.12	0.57±0.13
	Sm(D:26mm)	0.51±0.06	0.50±0.06	0.51±0.04	0.51±0.05

4.3.2 Spatial variables

Figure 4.2 -Figure 4.5 display spatial variables for all joints and different object sizes during power and pinch grasping. The final angle variables during power grasping (Figure 4.3), except that of CMCAA, were significantly different for object size ($p<0.05$). Open angles were affected by the object size except in index MCP, little DIP, thumb IP, thumb MCPAA, thumb CMCAA, and thumb CMCPS joint angles. The minimum and maximum velocities during power grasping were also affected by the object size. The minimum velocities were significantly different across object size in all joint angular velocities except middle DIP, little DIP, thumb IP, and thumb CMCAA joint angular

velocities. The maximum velocities were significantly affected by the object in all joint angular velocities except thumb CMCAA joint. Minimum velocities became smaller (larger in thumb MCPAA and CMCPS) as the object size decreased, while maximum velocities became larger (smaller in thumb MCPAA and CMCPS) as the object size decreased. To summarize, as the object size decreased, the difference between initial and open angle decreased and the magnitude of minimum velocity also decreased. As the object size increased, the difference between open and final angle increased, as did the maximum velocity.

During pinch grasping, open angles significantly affected ($p<0.05$) all MCP joint angles of four fingers, ring PIP joint angle, little PIP joint angle, and thumb CMCPS joint angles. Final angles were significantly different ($p<0.05$) for all MCP joint angles of four fingers, ring PIP joint angle, thumb CMCFE and CMCPS joint angles. The minimum velocities were not affected by the object size except the thumb CMCPS joint angular velocity. The maximum velocities were significantly affected by object size ($p<0.05$) only in all MCP joints of four fingers and thumb CMCPS joints.

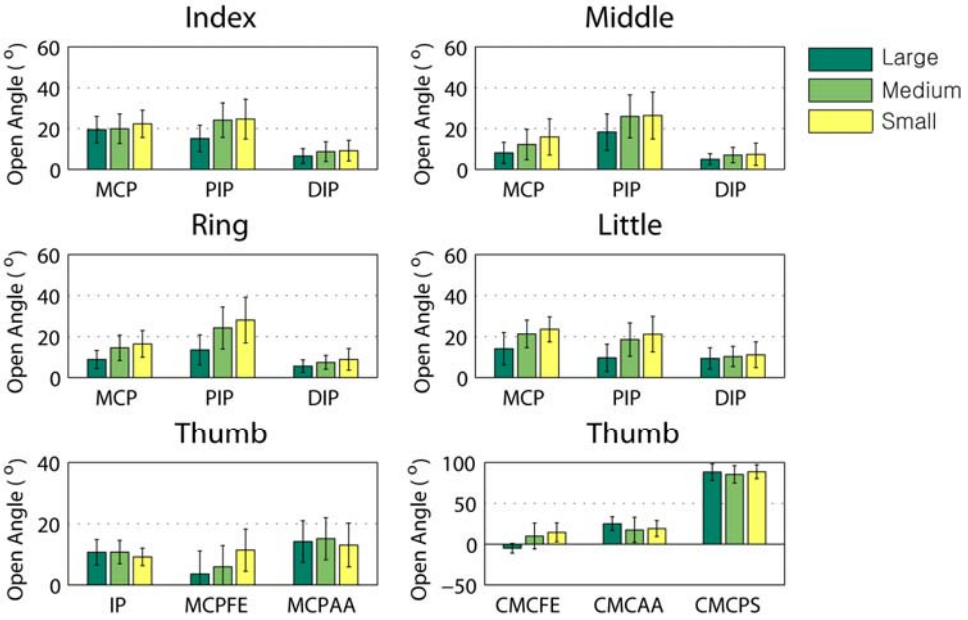

(a)

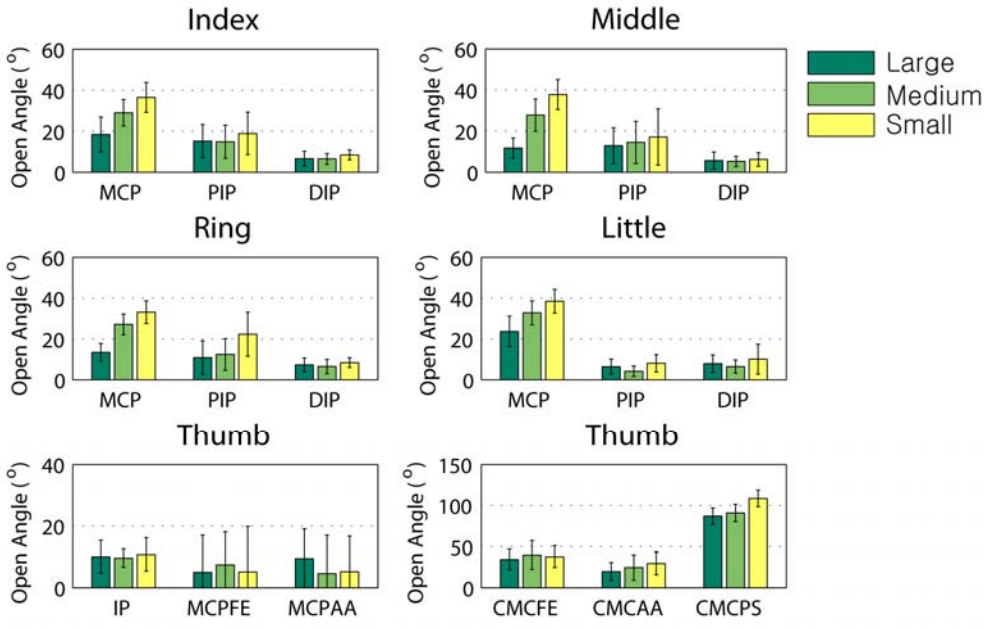

(b)

Figure 4.2 Open angles for (a) power grasping and (b) pinch grasping

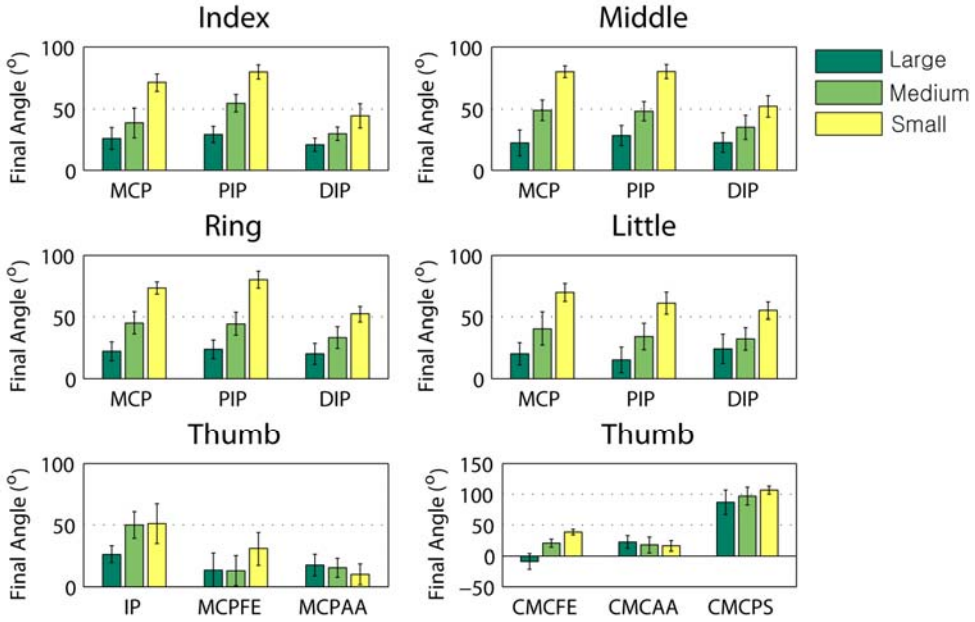

(a)

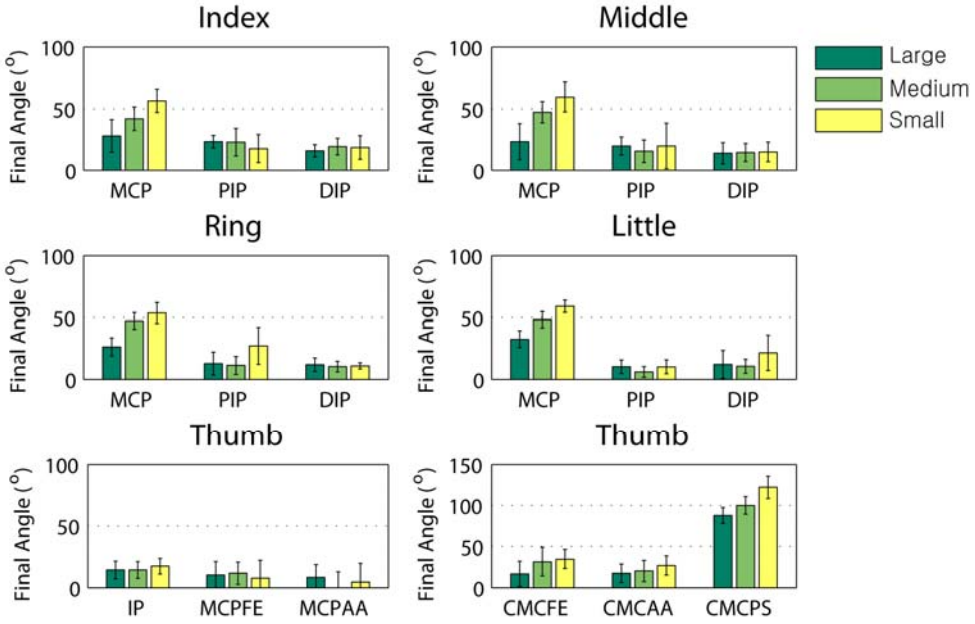

(b)

Figure 4.3 Final angle for (a) power grasping and (b) pinch grasping

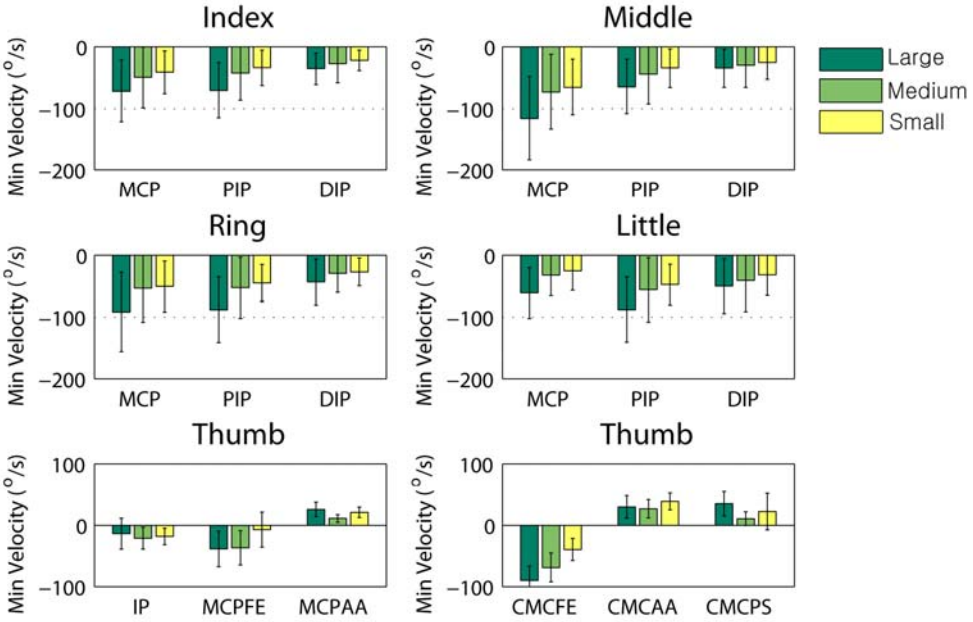

(a)

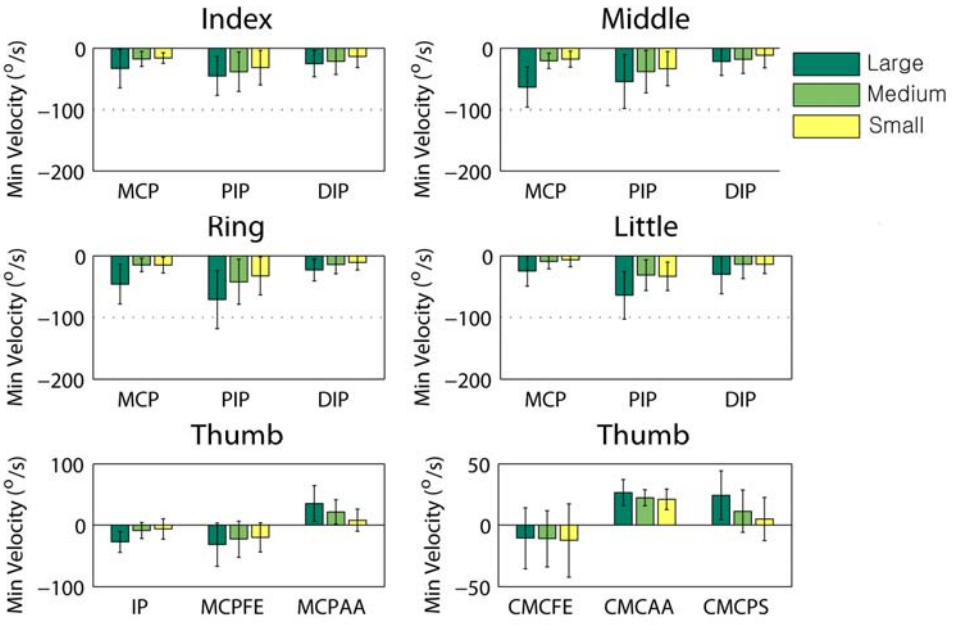

(b)

Figure 4.4 Minimum velocity for (a) power grasping and (b) pinch grasping

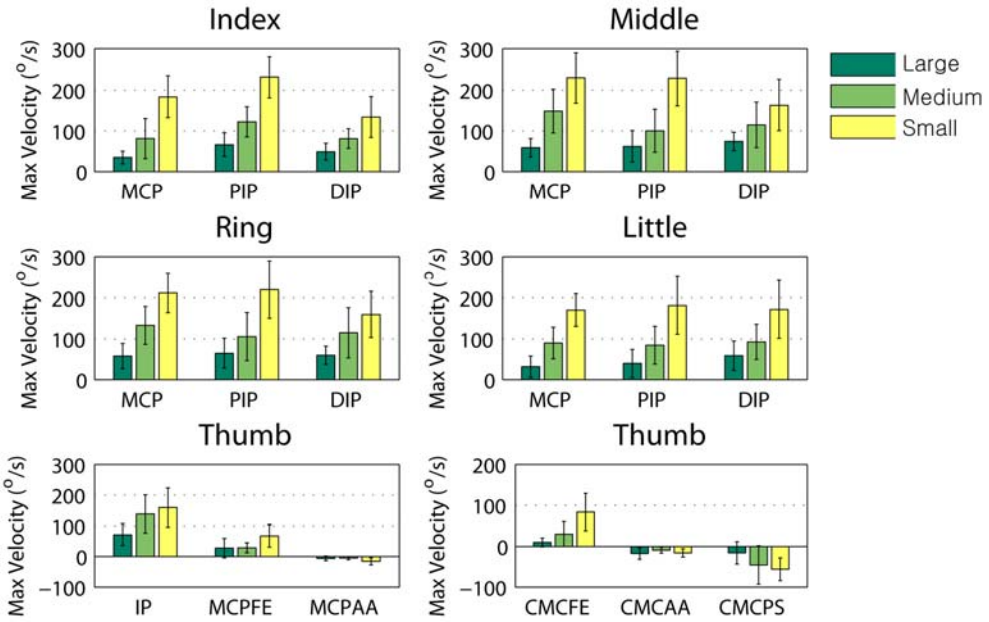

(a)

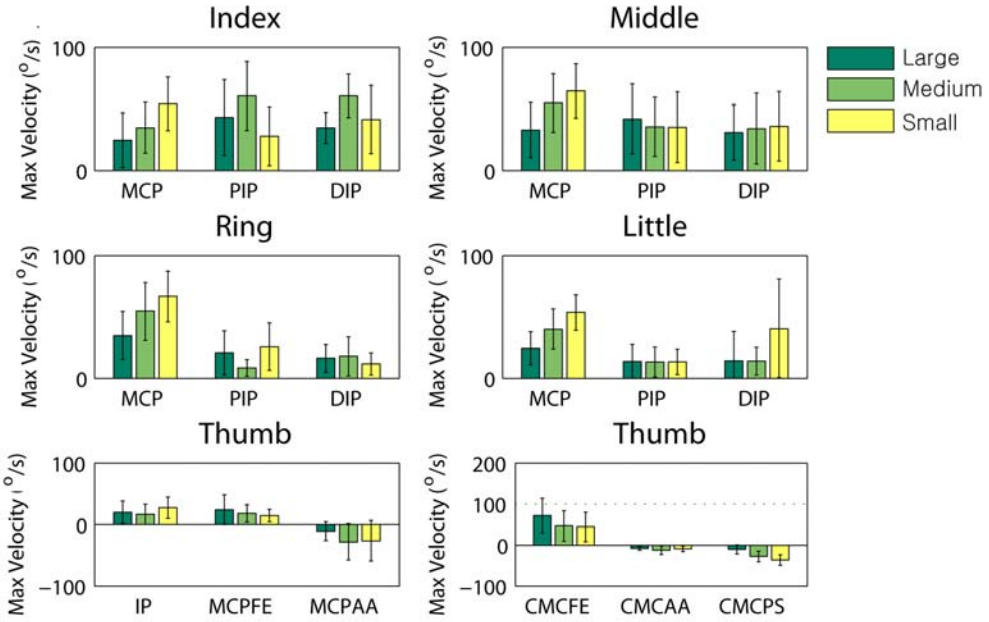

(b)

Figure 4.5 Maximum velocity for (a) power grasping and (b) pinch grasping

A multiple regression model was developed to predict open angle from object sizes and hand lengths as the Eq. (4.1).

$$Open \quad Angle = a \times CD + b \times HL + c \tag{4.1}$$

,where CD : Cylinder Diameter (cm)

HL : Hand Length (cm)

c : constants

The coefficients (a, b), constants, and coefficients of determination between prediction and measurement are shown in Table 4.3 (power grasping) and Table 4.4 (pinch grasping). Coefficients of determination ranged from 0.20 to 0.57 in power grasping. In pinch grasping, coefficients of determination were large in all MCP joints, but those values of other joints ranged from 0.13 to 0.58. For all flexion-extension angles, object size and joint angle showed negative relationship.

Table 4.3 Coefficients and constants of multiple regression model predicting open angles in power grasping

Joint	MCP2	PIP2	DIP2	MCP3	PIP3	DIP3
a (°/cm)	-0.32	-1.15	-0.30	-0.92	-0.98	-0.30
b (°/cm)	0.61	0.26	-0.25	2.30	0.38	0.42
c (°)	11.07	24.08	14.88	-25.17	22.99	0.57
R^2	0.20	0.44	0.25	0.56	0.32	0.28
Joint	MCP4	PIP4	DIP4	MCP5	PIP5	DIP5
a (°/cm)	-0.88	-1.69	-0.38	-1.10	-1.34	-0.18
b (°/cm)	0.12	0.11	0.33	0.34	-0.20	-0.59
c (°)	16.87	31.02	3.58	20.53	29.20	22.55
R^2	0.48	0.53	0.34	0.50	0.52	0.20
Joint	IP	MCPFE	MCPAA	CMCFE	CMCAA	CMCPS
a (°/cm)	0.19	-0.64	0.17	-2.21	0.61	0.11
b (°/cm)	-0.65	2.50	-1.85	-0.54	2.88	-3.03
c (°)	21.30	-36.06	47.95	31.35	-38.12	-30.82
R^2	0.25	0.43	0.29	0.57	0.34	0.33

Table 4.4 Coefficients and constants of multiple regression model predicting open angles in pinch grasping

Joint	MCP2	PIP2	DIP2	MCP3	PIP3	DIP3
a (°/cm)	-2.08	-0.23	-0.16	-2.99	-0.30	-0.04
b (°/cm)	0.03	-0.08	0.00	0.02	-0.08	0.00
c (°)	41.02	19.41	8.29	45.22	18.62	5.87
R^2	0.71	0.28	0.20	0.85	0.24	0.04
Joint	MCP4	PIP4	DIP4	MCP5	PIP5	DIP5
a (°/cm)	-2.37	-0.97	-0.06	-1.76	-0.31	-0.13
b (°/cm)	0.06	-0.04	-0.01	0.05	-0.02	-0.02
c (°)	39.15	22.94	7.98	42.11	9.96	9.32
R^2	0.88	0.39	0.13	0.71	0.30	0.15
Joint	IP	MCPFE	MCPAA	CMCFE	CMCAA	CMCPS
a (°/cm)	0.00	0.03	0.66	0.55	-1.09	2.14
b (°/cm)	-0.04	-0.09	-0.11	-0.05	0.01	0.00
c (°)	11.00	7.71	4.34	-40.14	31.76	-109.17
R^2	0.24	0.20	0.32	0.15	0.29	0.58

4.3.3 Temporal variables

Figure 4.6-Figure 4.7 show time variables – start time, minimum velocity time, open time, and maximum velocity time – of four finger joints in power grasping and pinch

grasping, respectively. Among time variables, only opening times were significantly affected by the object size at all joints of four fingers except index DIP joint($p<0.05$). Other time variables were not affected by object size in most joints.

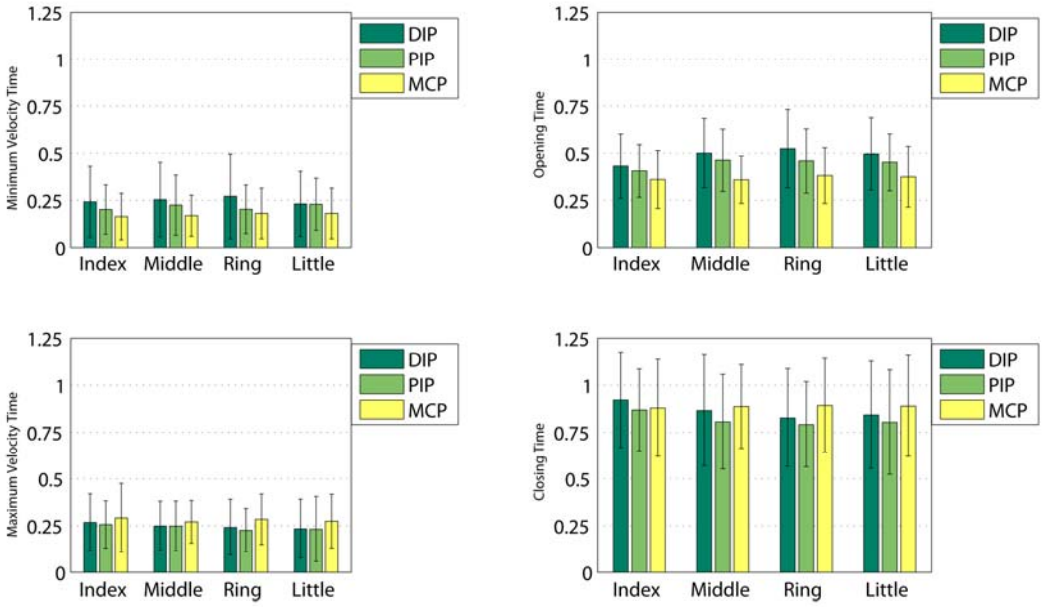

Figure 4.6 Normalized time variables for four finger joints in power grasping

In power grasping, MCP joints showed the smallest time variables and DIP joints showed the largest time variables during opening process at all four fingers. Average minimum velocity time was 0.17 ± 0.13 for MCP joints, 0.21 ± 0.14 for PIP joints, and 0.25 ± 0.20 for DIP joints. Opening time was 0.37 ± 0.15 for MCP joints, 0.44 ± 0.16 for Pip joints, and 0.49 ± 0.19 for DIP joints. Both time variables of the same joint types (MCP, PIP, and DIP) showed no significant difference for different fingers ($p<0.05$).

During flexion period of power grasping, no significant difference between joints within a digit was observed in maximum velocity time and closing time ($p<0.05$). The same joint types showed similar values of time variables at all fingers except PIP and

DIP joints of the index finger. On average, maximum velocity time was 0.28 ± 0.15 for MCP joints, 0.24 ± 0.14 for PIP joints, and 0.25 ± 0.15 for DIP joints. Average closing time was 0.89 ± 0.25 for MCP, 0.82 ± 0.25 for PIP, and 0.86 ± 0.28 for DIP joints.

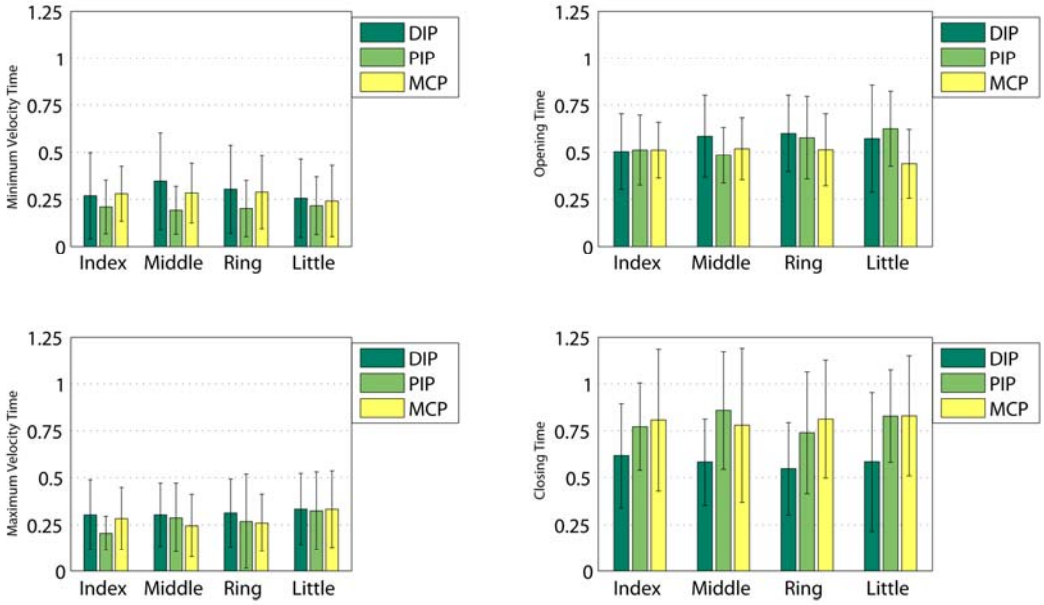

Figure 4.7 Normalized time variables for four finger joints in pinch grasping

In pinch grasping, it was hard to observe any consistent pattern among joint types within a digit. But through all time variables, MCP joints always showed similar time variables for different fingers. Average minimum velocity time was 0.27 ± 0.17 for MCP, 0.21 ± 0.14 for PIP, and 0.29 ± 0.23 for DIP joints. Average opening time was 0.50 ± 0.17 for MCP, 0.55 ± 0.20 for PIP, and 0.56 ± 0.23 for DIP joints. Both time variables (minimum velocity time and opening time) was greater in pinch grasping than in power grasping at all joints.

During flexion period of pinch grasping, most maximum velocity times and closing times showed larger values in power grasping than in pinch grasping. Average

maximum velocity time was 0.28 ± 0.17 for MCP, 0.27 ± 0.20 for PIP, and 0.31 ± 0.18 for DIP joints. Closing time was largest in MCP joints (0.81 ± 0.36) and PIP (0.80 ± 0.28) and DIP (0.58 ± 0.28) joints followed. As the extension period, time variables in MCP joints showed similar values across fingers.

4.3.4 Application to the model

The primary goal of this study is to apply actual finger movement patterns to the model that predicts hand posture, presented in Chapter 2. The model predicts the posture by detecting contacts between hand segments and the object while driving finger joint at some specific rates. Each finger joints rotates at different rates depending on the size of the grip object and grip types. Figure 4.8 displays average joint angular velocity of the middle finger over time during reaching for and grasping three differently sized objects. Each joint has different minimum and maximum velocities as shown in Figure 4.4 and Figure 4.5. Using spatial and temporal variables obtained from the experiments, linear curve fitting was conducted for each joint. The shape of actual velocity curve is sigmoidal in the flexion movement and inverse-sigmoidal shape in the extension movement, but linear curve fitting was found to explain 86% - 93% of variability of velocities on average.

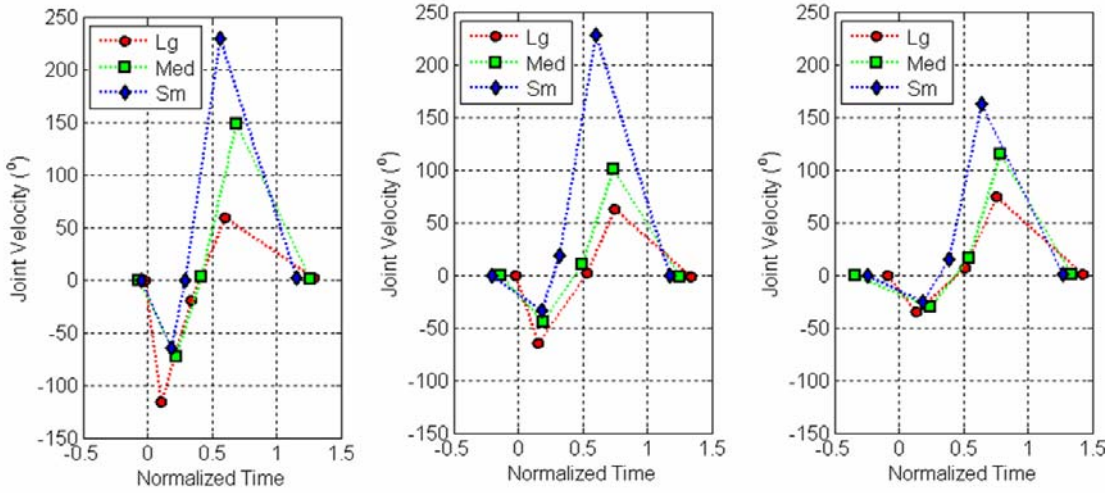

(a) Power grip

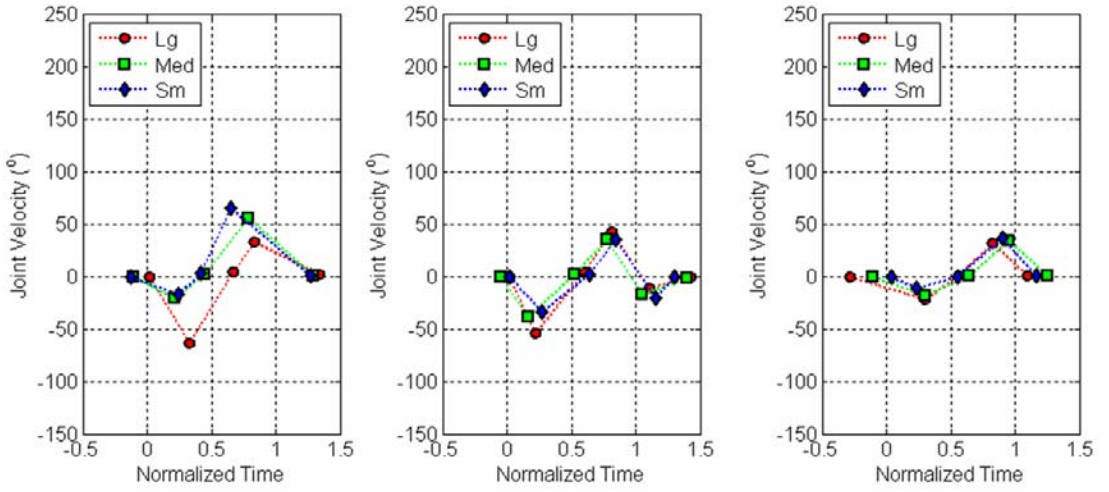

(b) pinch grip

Figure 4.8 Average normalized joint angular velocity vs. time plots of the middle finger during reaching for and grasping different sized objects. (a) Power grasp for 16 subjects. (b) pinch grasp for 6 subjects

4.4 DISCUSSION

The objective of this study was to quantify the finger movements during power and pinch grasping. Spatial and temporal variables used in this study characterized the movement pattern during power and pinch grasping.

In both power and pinch grasping, open angles decreased as the object size increased to make larger grip apertures (Figure 4.2). The effect of object size on grip aperture during two-finger pinch grasping has been observed by many researchers (Jeannerod 1984; Bootsma, Marteniuk et al. 1994; Brenner and Smeets 1996; Paulignan, Frak et al. 1997), but quantitative information for finger joint angle changes in other grip types such as power grip and pulp pinch grip was lacking. Our results showed how open angles are quantitatively affected by object size so that they can be applied to modeling of human grasping movements. Open angles are the determinant of grip aperture. The object size affected open angles of most joints in power grasping, whereas it affected open angles of all MCP joints in pinch grasping, which explains why grip aperture is larger in power grip than pinch grip.

The ratio of maximum aperture to object size was affected by the object size. Smaller objects resulted in a larger ratio, which gave a larger safety margin. This result agrees with previous studies reporting the maximum aperture to vary linearly with object size with a slope less than 1 (approximately 0.8). It would seem that the anatomic structure of the hand caused the difference. The passive moments of finger joints play a significant role during free finger movements (Sancho-Bru, Perez-Gonzalez et al. 2001; Kamper, George Hornby et al. 2002). When object size is large, finger joints need to use a larger range of motion to open the hand, which increase the passive moments at the joints. Increased passive moments might have decelerated finger joint rotation

more. When the object size is small, finger joints do not need to use a large range of motion, and thus the role of passive moments is not as great as when grasping large objects. Reduction of passive moments might have decreased the braking force to deccelerate the joint rotation. The result that power grasp showed a lower slope (0.62) than pinch grasp (0.78) supports this assumption because power grasp uses all finger joints while pinch grasp uses mainly MCP joints of four fingers to open the hand.

The effects of object size on maximum aperture time was apparent in pinch grip, but not in power grip. It has been reported that the maximum aperture occurred at approximately 60-80% of total movement time (Jeannerod 1984; Castiello 1996) (Wallace and Weeks 1988), but our data showed a faster occurrence of the maximum aperture in pinch grasping especially when grasping a small object (Table 4.2). These data may reflect the different definition of movement time. We defined onset time of movement as a time when the distance decreased by 5% of total distance, which is usually later than actual onset time. This might have underestimated the maximum aperture time. The dependence of timing on object size corroborates the previous studies (Marteniuk, Leavitt et al. 1990; Gentilucci, Castiello et al. 1991; Churchill, Hopkins et al. 2000). However, the maximum aperture time in power grasping was independent of the object's size. The larger magnitude of minimum velocity in larger object size supports this independency (Figure 4.4). The time to reach maximum aperture was much smaller in power grasping than in pinch grasping even though the maximum apertures were larger in power grasping than in pinch grasping. Comparing the minimum velocities between power grasping and pinch grasping, the magnitudes of minimum velocities were much larger in power grasping than in pinch grasping. It seems that subjects used pure extension of all joints of four fingers in power grasping, whereas they tried to control mainly the MCP joint angles in pinch grasping - PIP and

DIP joint angles of four fingers were not affected by the object size (Figure 4.2 - Figure 4.3).

Object size affected all spatial variables significantly. Final angles were most sensitive to the object size, which agrees with the result of study by Choi and Armstrong (2006). The regression model for the open angle (Eq. 4.1) shows how open angle is affected by object size and hand size. For four finger joints, all coefficient of object size had negative values, which means that increasing object size decreases open angles. In particular, the open angles of MCP joints showed strong negative relationships with object size in pinch grasping, meaning that MCP joints played more important roles during grasping than PIP or DIP joints.

The thumb joint spatial variables yield insight into how the thumb joints move to adjust the hand to object size. In power grasping, open angles in MCPFE and CMCFE were significantly affected by the object size ($p<0.05$), which means that the flexion-extension movements of the MCP and CMC joints were used to open the hand differently for varying object sizes. The object size affected final angles of all thumb joints except CMCAA joint, meaning most joints of the thumb were used to fit the hand to different object size. The significant effect of object size on minimum and maximum velocity variables of thumb joints also support the finding which thumb joints were used to adjust the hand to object size. In pinch grasping, all time variables were significantly affected by the object size only at CMCPS joint. It seems that pronation-supination movement of the thumb plays an important role to adjust the hand to the object during pinch grasping.

It should be noted that all time variables were normalized with respect to movement time. The movement time was 1.05 ± 0.28 seconds for power grasping and 1.06 ± 0.19 seconds for pinch grasping. Normalized time variables were used to

investigate the relative finger joints' rotations excluding the effect of movement time, because movement time was different for every trial. Additional analysis is required to examine the effect of movement time on the finger joint rotation.

In power grasping, temporal variables during extension period were smallest in MCP and largest in DIP joints at four fingers, whereas temporal variables during flexion period were almost similar throughout all joints. Temporal variables were not significantly different across type of joints within each digit ($p<0.05$). More temporal synergies were observed among the same type of joints (MCP, PIP, and DIP) rather than among the joints within digit. These findings corroborate previous studies (Santello, Flanders et al. 1998; Santello and Soechting 1998; Mason, Gomez et al. 2001; Santello, Flanders et al. 2002; Braido and Zhang 2004) that humans use synergies during power grasping movement. In pinch grip, time variables at MCP, PIP, and DIP joints within a digit did not show a significant difference from one another at most digits, but the MCP joints of four fingers showed similar values for all temporal variables. Comparing temporal variables of power and pinch grasping, power grasp required less times than pinch grasp for extension, and both grasps required similar times during flexion period.

An interesting observation in this study was the dependence of minimum and maximum velocity on object size. Even though the object size changed the open and final angles, time to complete grasping was not affected by the object size due to the velocity dependence on object size. This finding can be one of the evidence that humans used velocity control strategy for motor control (Kelso, Fuchs et al. 1998; Zhang, Kuo et al. 1998).

Thumb movement is essential to model the grasping movement, but the data for describing full DOF's of thumb motion are lacking. Li and Tang reported the thumb movement pattern during opposition and circumduction movements (Li and Tang 2007).

In this study, we showed how the thumb joint angles vary when grasping differently sized objects, which can be useful to model grasping movement. CMCFE and MCPFE were found to be an important joint angles to adjust hand to different object size. The correlation of flexion-extension movements of CMC and thumb MCP joints was 0.906 ± 0.141 in power grasping. Anatomically, the flexor pollicis longus crosses CMC, MCP, and IP joints, and thus causes simultaneous rotations of these joints. It seems that the flexor longus plays an important role to adjust hand to varying object size.

The data displayed in Figure 4.8 are not congruent with constraints (Landsmeer 1963) on flexion of the interphalangeal joints ($\theta_{DIP} = 2/3*\theta_{PIP}$) which were used in the previous studies (Landsmeer 1963; Lee and Kunii 1995; Endo and Kanai 2006). For example, the average ratio of the maximum DIP angular velocity to the maximum PIP angular velocity was 1.02 during flexion period at the middle finger. This ratio was also affected by the object size: 1.20 for large (D:114 mm) object, 1.14 for medium (D:60 mm) object, and 0.71 for small (D:26 mm) object. During grasping small objects, it is very similar to free flexion of fingers, which was the experimental condition used in Landsmeer's study. But as the object size increased, the ratio ($\theta_{DIP}'/ \theta_{PIP}'$) increased, which means that more complicated coordination of muscles may be used during grasping.

4.5 LIMITATIONS AND FUTURE RESEARCH

One of the limitations in this study was consideration of a joint center of rotation. We used marker-defined joint angles for the analysis of movement data. It has been reported that coefficients of multiple determination between marker-defined joint angles and rotation-center based joint angles were 0.96, 0.98, and 0.94 for MCP, PIP, and DIP

joint flexion-extension motion, respectively. But the thumb joints do not only make flexion-extension movements but also pronation-supination and abduction-adduction movements, which could have increased errors when comparing measured and predicted joint angles.

It was unavoidable to use the computational algorithm to detect spatial and temporal variables for analyzing a large dataset, but some of the movements might have not been detected correctly by the algorithm. As finger movements normally include a lot of between-subject variability, the movements that did not follow the typical movement pattern (Figure 4.1) could not be included in this study.

4.6 CONCLUSIONS

- Finger movements during grasping differently sized objects, characterized quantitatively using spatial and temporal variables, can successfully be used to model a grasping movement.
- Object size changes both spatial and temporal variables during reaching and grasping movements.
- Power grasp uses all joints of four fingers and flexion-extension of MCP and CMC joints of the thumb to adjust the hand to different object sizes.
- Pinch grasp uses MCP joints of four fingers and thumb CMC joints to adjust the hand to different object sizes.
- During grasping movements, humans change the velocities of joints as the object size changes in such a way so as to reduce the difference of time to complete grasping.

4.7 REFERENCES

Armstrong, T. J. and D. B. Chaffin (1978). "An inverstigation of the relationship between displacements of the finger and wrist joints and the extrinsic finger flexor tendons." Journal of biomechanics 11: 119-128.

Armstrong, T. J., J. Choi and V. Ahuja (2008). Development of kinematic and biomechanical hand models for ergonomic applications. Handbook of Digital human Modeling. V. G. Duffy, CRC Press.

Blackwell, J. R., K. W. Kornatz and E. M. Heath (1999). "Effect of grip span on maximal grip force and fatigue of flexor digitorum superficialis." Appl Ergon 30(5): 401-5.

Bootsma, R. J., R. G. Marteniuk, C. L. MacKenzie, et al. (1994). "The speed-accuracy trade-off in manual prehension: effects of movement amplitude, object size and object width on kinematic characteristics." Exp Brain Res 98(3): 535-41.

Braido, P. and X. Zhang (2004). "Quantitative analysis of finger motion coordination in hand manipulative and gestic acts." Hum Mov Sci 22(6): 661-78.

Brenner, E. and J. B. Smeets (1996). "Size illusion influences how we lift but not how we grasp an object." Exp Brain Res 111(3): 473-6.

Buchholz, B. and T. J. Armstrong (1992). "A kinematic model of the human hand to evaluate its prehensile capabilities." J Biomech 25(2): 149-62.

Castiello, U. (1996). "Grasping a fruit: selection for action." J Exp Psychol Hum Percept Perform 22(3): 582-603.

Choi, J. and T. J. Armstrong (2006). Sensitivity study of hand posture using a 3-dimensional kinematic hand model. 16th International Ergonomics Association Meeting, Maastricht, Netherlands.

Choi, J., C. D. Grieshaber and T. J. Armstrong (2007). Estimation of grasp envelope using a 3-dimensional kinematic model of the hand. Human Factors and Ergonomics Society Annual Meeting, Baltimore, MD.

Churchill, A., B. Hopkins, L. Ronnqvist, et al. (2000). "Vision of the hand and environmental context in human prehension." Exp Brain Res 134(1): 81-9.

Crosby, C. A., M. A. Wehbe and B. Mawr (1994). "Hand strength: normative values." J Hand Surg [Am] 19(4): 665-70.

Endo, Y. and S. Kanai (2006). An Application of a Digital Hand to Ergonomic Assessment of Handheld Information Appliances. Digital Human Modeling for Design and Engineering Conference, Lyon, France.

Garrett, J. W. (1971). "The adult human hand: some anthropometric and biomechanical considerations." Hum Factors 13(2): 117-31.

Gentilucci, M., U. Castiello, M. L. Corradini, et al. (1991). "Influence of different types of grasping on the transport component of prehension movements." Neuropsychologia 29(5): 361-78.

Grieshaber, C. D. (2007). Factors affecting hand posture and one-handed push force during flexible rubber hose insertions tasks. Industrial and Operations Engineering. Ann Arbor, University of Michigan.

Imrhan, S. N. and C. H. Loo (1989). "Trends in finger pinch strength in children, adults, and the elderly." Hum Factors 31(6): 689-701.

Jeannerod, M. (1981). "Specialized channels for cognitive responses." Cognition 10(1-3): 135-7.

Jeannerod, M. (1984). "The timing of natural prehension movements." J Mot Behav 16(3): 235-54.

Josty, I. C., M. P. Tyler, P. C. Shewell, et al. (1997). "Grip and pinch strength variations in different types of workers." J Hand Surg [Br] 22(2): 266-9.

Kamper, D. G., T. George Hornby and W. Z. Rymer (2002). "Extrinsic flexor muscles generate concurrent flexion of all three finger joints." J Biomech 35(12): 1581-9.

Kelso, J. A., A. Fuchs, R. Lancaster, et al. (1998). "Dynamic cortical activity in the human brain reveals motor equivalence." Nature 392(6678): 814-8.

Landsmeer, J. M. (1961). "Studies in the anatomy of articulation. I. The equilibrium of the "intercalated" bone." Acta Morphol Neerl Scand 3: 287-303.

Landsmeer, J. M. (1961). "Studies in the anatomy of articulation. II. Patterns of movement of bi-muscular, bi-articular systems." Acta Morphol Neerl Scand 3: 304-21.

Landsmeer, J. M. (1963). "The Coordination of Finger-Joint Motions." J Bone Joint Surg Am 45: 1654-62.

Lee, J. W. and T. L. Kunii (1995). "Model-based analysis of hand posture." IEEE Computer Graphics and Applications 15(5): 77-86.

Li, Z. M. and J. Tang (2007). "Coordination of thumb joints during opposition." J Biomech 40(3): 502-10.

Marteniuk, R., J. Leavitt, C. MacKenzie, et al. (1990). "Functional relationships between grasp and transport components in a prehension task." Hum Mov Sci 9: 149-176.

Mason, C. R., J. E. Gomez and T. J. Ebner (2001). "Hand synergies during reach-to-grasp." J Neurophysiol 86(6): 2896-910.

Mathiowetz, V., N. Kashman, G. Volland, et al. (1985). "Grip and pinch strength: normative data for adults." Arch Phys Med Rehabil 66(2): 69-74.

Miyata, N., M. Kouchi and M. Mochimaru (2006). Posture Estimation for Design Alternative Screening by DhaibaHand - Cell Phone Operation. Digital Human Modeling for Design and Engineering Conference, Lyon, France.

Paulignan, Y., V. G. Frak, I. Toni, et al. (1997). "Influence of object position and size on human prehension movements." Exp Brain Res 114(2): 226-34.

Pollard, N. S. and V. B. Zordan (2005). Physically based grasping control from example. Eurographics/ACM SIGGRAPH Symposium on Computer Animation, Los Angeles.

Sancho-Bru, J. L., A. Perez-Gonzalez, M. Vergara-Monedero, et al. (2001). "A 3-D dynamic model of human finger for studying free movements." J Biomech 34(11): 1491-500.

Santello, M., M. Flanders and J. F. Soechting (1998). "Postural hand synergies for tool use." J Neurosci 18(23): 10105-15.

Santello, M., M. Flanders and J. F. Soechting (2002). "Patterns of hand motion during grasping and the influence of sensory guidance." J Neurosci 22(4): 1426-35.

Santello, M. and J. F. Soechting (1998). "Gradual molding of the hand to object contours." J Neurophysiol 79(3): 1307-20.

UGS (2006). UGS Tecnomatix Jack.

Wallace, S. A. and D. L. Weeks (1988). "Temporal constraints in the control of prehensile movement." J Mot Behav 20(2): 81-105.

Yan, J. H. and J. H. Downing (2001). "Effects of aging, grip span, and grip style on hand strength." Res Q Exerc Sport 72(1): 71-7.

Zhang, X., A. D. Kuo and D. B. Chaffin (1998). "Optimization-based differential kinematic modeling exhibits a velocity-control strategy for dynamic posture determination in seated reaching movements." J Biomech 31(11): 1035-42.

CHAPTER 5

A RETROSPECTIVE STUDY OF THE RISK OF HAND AND WRIST MSDS USING TIME-BASED VIDEO ANALYSIS

Abstract

The objective of this study was to test the hypothesis that wrist motion and tendon excursion are associated with the risk of upper extremity musculoskeletal disorders. A re-analysis of manual jobs from a cross-sectional study showing the relationship between repetitive work and the prevalence of upper limb musculoskeletal disorders by (Latko et al.) was performed. A time-based analysis was performed to determine wrist flexion/extension and radial/ulnar deviation angles from video recordings on 10 jobs ranging from low- to high- repetition jobs (4 high-risk jobs, 3 medium-risk jobs, and 3 low-risk jobs). Using one-way ANOVA, the average wrist velocity, average wrist acceleration, and normalized cumulative tendon excursions of FDP and FDS tendons were found to differentiate MSD risk levels significantly and correctly ($p<0.05$). The role of dynamic variables and tendon excursions was examined using a conceptual modeling of wrist motions and biomechanical factors.

5.1 INTRODUCTION

5.1.1 Background

Much epidemiological evidence shows that repeated exertion with the hand is one of the important risk factors for UEMSDs (upper extremity musculoskeletal disorders) of upper extremities such as carpal tunnel syndrome and tendinitis (Feldman, Travers et al. 1987; Silverstein, Fine et al. 1987; Chiang, Chen et al. 1990; McCormack, Inman et al. 1990; Barnhart, Demers et al. 1991; Hagberg, Morgenstern et al. 1992; Keyserling, Stetson et al. 1993; Osorio, Ames et al. 1994; Latko, Armstrong et al. 1999; Leclerc, Landre et al. 2001; Gell, Werner et al. 2005). Chiang et al. found that prevalence of carpal tunnel syndrome is five times larger in a high-repetition group than in a low-repetition group. Silverstein et al. combined repletion and force, and found that highly repetitive jobs increased the risk more than five times compared to low repetitive jobs, irrespective of force. Many researchers have proposed several models of pathogenesis of these UEMSDs, which postulated repeated exertions play a role to develop the disorders (Goldstein, Armstrong et al. 1987; Fuchs, Nathan et al. 1991; Rempel, Dahlin et al. 1999). The most commonly used model is the one based on the assumption that thickening of tendon sheaths causes intracarpal pressure and contact pressure on the median nerves. Exertions of the hand produce normal and friction forces on adjacent tendons and tissues (Armstrong and Chaffin, 1979). Armstrong et al. (1984) observed that the density of connective tissue in the flexor synovium is greater in the areas where the tendons press and rub on adjacent anatomical structures. Repetitive loading from forceful exertion changes the geometric and material properties of tendons and ligaments (Wren, Beaupre et al. 1998). Thickening of the connective tissue in the carpal tunnel can produce secondary pressure on tendons, synovium, and

nerve tissues, resulting in MSDs such as carpal tunnel syndrome (Phalen 1966; Moore 2002).

Tendon excursion and wrist motion have been used as one of the indicators of the risk of UEMSDs (Moore, Wells et al. 1991; Marras and Schoenmarklin 1993; Wells, Moore et al. 1994; Wells, Moore et al. 1994; Sommerich, Marras et al. 1996; Marklin and Monroe 1998; Serina, Tal et al. 1999). Moore et al. (1991) used a tendon excursion as a measure of repetitive and forceful task. They categorized the tasks using a quantitative guideline by Silverstein et al. (1986; 1987) and directly measured wrist and index finger joint angles for six subjects. Wells et al. (Wells, Moore et al. 1994) compared the tendon excursions of 88 industrial workers and one data entry clerk. Sommerich et al. (1996) measured wrist and finger joint angles and computed the tendon excursion for three different groups of typing tasks. The dynamics of the wrist motion was investigated by many researchers. Marras et al.(1993) used goniometric instrumentation for measuring wrist angles of workers to investigate the relationship between angular velocities and accelerations of the wrist and UEMSDs. They showed that angular wrist velocities were associated with cumulative trauma disorders based on OSHA (US occupational safety and health administration) 200 logs. Marklin and Monroe (1998) measured the wrist motions in the meat-packing industry and compared the results with those of Marras and Schoenmarklin (1993). Serina et al. (1999) measure wrist and forearm motions during typing tasks, and concluded that the mean angular velocity and acceleration in typing tasks were similar to those in industrial tasks. These studies provided a benchmark to determine what levels of tendon excursion or wrist dynamics are associated with the risk of UEMSDs, but the connection of the tendon excursions with occurrence of UEMSDs were not clear.

5.1.2 Hypothesis

Posture θ(t) can be represented as the sum of a series of periodic functions of peak angle, θoi, frequency, ωi, time, t, and phase, ϕi:

$$\theta(t) = \sum_{i=1}^{\infty} \theta_{0i} \sin(\omega_i t + \phi_i) \tag{5.1}$$

Then the velocity and acceleration components can be obtained as the first and second derivatives of θ(t).

$$\dot{\theta}(t) = \sum_{i=1}^{\infty} \theta_{0i}\omega_i \cos(\omega_i t + \phi_i) \tag{5.2}$$

$$\ddot{\theta}(t) = -\sum_{i=1}^{\infty} \theta_{0i}\omega_i^{\,2} \sin(\omega_i t + \phi_i) = -\omega_i^{\,2} \cdot \theta(t) \tag{5.3}$$

Comparing Eqs. (5.1), (5.2), and (5.3), the frequency (ω) plays an important role to amplify or to lessen the magnitudes of velocity and acceleration components. If the frequency is high, it augments the magnitude of angular velocity more than the magnitude of angle, and it augments the magnitude of angular acceleration the most. Conversely, if the frequency is low, it diminishes the magnitude of velocity more and the magnitude of acceleration the most. The above equation also implies that the contribution of frequency to velocity and acceleration is larger than that of magnitude of the wrist angle. Frequency of the job augments or lessens each term of velocity or acceleration by multiplying ω or ω^2, while the magnitude affects angle, velocity, and acceleration by the same amount. Therefore, the dynamic variables, i.e., velocity and acceleration, are more effective than the angle variable in assessing the repetitive jobs.

Tendon excursions of flexor tendons can be used as an index to assess the risk of MSDs. Using Eq. (5.2), cumulative tendon excursion can be computed as the integral of absolute product of the radius of curvature in the wrist, r , and angular velocity, θ'(t) , over work duration, T.

$$Cumulative \quad Tendon \quad Excursion = \int_0^T \left| r\,\dot{\theta}(t) \right| dt = \int_0^T \left| \sum r\,\theta_{o_i}\,\omega_i \cos(\omega_i t + \phi_i) \right| dt \tag{5.4}$$

This equation shows the relationship between tendon excursion and angular velocity components. As the tendon excursion is closely related to angular velocity, cumulative tendon excursion can be used as an index of estimating MSD risk levels just as velocity components can. It also captures not only the peak wrist angle and frequency but also the duration of the job, which should be considered when assessing a job. The cumulative tendon excursion gives more physically meaningful values than velocity or acceleration component alone, because it is related to friction and wear that may contribute to MSDs.

5.1.3 Objective

The objective of this study was to test the hypothesis that wrist motion and tendon movements are associated with the risk of UEMSDs. For this purpose, a time-based analysis was performed for video recordings of selected jobs from the previous study of hand activity level and MSDs by Latko et al. (1999).

5.2 METHODS

5.2.1 Job Selection

Latko et al. (1999) classified the jobs from three manufacturing facilities (office furniture, industrial container, spark plug manufacturers) as high-risk, medium-risk, and low-risk, based on experts' repetition ratings. The repetition rating ranged from 6.7 to 10 for high-risk jobs, from 3.4 to 6.6 for medium-risk jobs, and from 0 to 3.3 for low-risk jobs. Prospective jobs were videotaped so that they could be viewed and rated by a team of experts. We selected ten jobs among them for re-analysis. Four high-risk jobs, three medium-risk jobs, and three low-risk jobs were selected from three manufacturing sites (Table 5.1). The average rating for high-risk, medium-risk, and low-risk jobs were 8.6, 5.8, and 2.1, respectively. Table 5.1 summarizes the brief descriptions and repetition ratings of the jobs analyzed in this study.

Table 5.1. Jobs included in study, categorized by repetition levels.

Repetition	Plant and job	Repetition Rating
Low	**Office furniture manufacturing**	
	Machine loading	**1.9**
	NC machine operation	**2.9**
	Industrial container manufacturing	
	Injection molding machine operator	**1.6**
Medium	**Office furniture manufacturing**	
	Office cubicle panel upholstery	**6.4**
	Industrial container manufacturing	
	Small drum cover glue	**5.3**
	Spark plug manufacturing	
	Spark plug transfer	**5.8**
High	**Industrial container manufacturing**	
	Band welding	**8.5**
	Handle assembly	**8.8**
	Spark plug manufacturing	
	Platinum spark plug weld	**7.9**
	Spark plug transfer B	**8.1**

5.2.2 Time-based analysis

Time-based analysis was used to estimate and record wrist postures at 0.25 second intervals as described by Armstrong et al. (2003). Analysis of digital job video was facilitated by a computer program in Microsoft Excel VBA that enabled the user to advance the video at predetermined steps and provided a menu for estimating job actions, hand and wrist postures and hand forces (Armstrong, Keyserling et al. 2003). Estimates were automatically stored in a spread sheet for further analysis

The flexion-extension and radial-ulnar deviation angles of the right wrist were observed, because the workers usually used the right hand more frequently than, or as often as, the left hand in our selected jobs. Selected job videos were analyzed at the time step of 0.25-second intervals. The entire job videos were observed first, and then representative job cycles were selected for further analysis. All the high-risk jobs have short job cycles (mean: 8.25 seconds), while all the low-risk jobs have long job cycles (mean: 89.5 seconds). Job cycles of mid-risk jobs (mean: 70.75 seconds) were between those of high-risk jobs and low-risk jobs. Two or three cycles of the jobs were observed for high-risk jobs. One representative cycle of the jobs was analyzed for medium-risk jobs and low-risk jobs.

5.2.3 Data analysis

In the original study, three groups of jobs were initially selected on the basis of repetition ratings – low, medium and high; subsequent health examinations showed that repetition was associated with elevated risk of WMSDs of the hand and wrist (Latko et al. 1999). These three job categories were independent variable studying this study.

The dependent variables in this study were angle, angular velocity, and angular acceleration of the wrist, and the tendon excursions of FDS (flexor digitorum superficialis) and FDP (flexor digitorum profundus) tendons. To investigate the distribution of the wrist angle, velocity, and acceleration over the entire job period, a probability histogram was built based on the observation data. Tendon excursions were calculated by using the regression equations suggested by (Armstrong and Chaffin 1978). Normalized tendon excursion was defined as cumulative tendon excursion for one hour. The cumulative tendon excursions were computed by adding the absolute difference of tendon excursions during each time intervals. The calculated cumulative tendon excursions were normalized as meters per hour so that tendon excursions of different jobs can be compared. The cumulative tendon excursion can be obtained using eq. (5.4). Since wrist angles, θi, were estimated at equal intervals, tendon excursion was computed:

$$Cumulative \quad Tendon \quad Excursion = \int_0^T \left| r\,\dot{\theta}(t) \right| dt = r \sum_{i=1}^{N} \left| \Delta \theta_i \right| \tag{5.5}$$

Once we calculated all dependent variables, one-way ANOVA was performed to test the effects of risk levels of MSDs on the dependent variables.

5.3 RESULTS

Histograms of the wrist angles, angular velocities, and angular accelerations for high, medium, and low risk jobs are shown in Figure 5.1 - Figure 5.3. The low-risk job shows a significantly larger mode at neutral posture (0º) than do the medium- and high-risk jobs; however, probability of F/E (flexion-extension) angle at neutral posture was higher in the high risk job than in the medium risk job. The probability of neutral F/E posture (0º) was 34%, 5% and 16% for low, medium, and high risk jobs, respectively. The Probability of neutral R/U (radial/ulnar deviation) posture angle was 53%, 26%, and 16% for low-, medium-, and high-risk jobs. For both F/E and R/U angles, the probability at neutral posture was not significantly different over the risk levels (p=0.114 for F/E, p=0.115 for R/U).

The probabilities in zero velocity and zero acceleration for both F/E and R/U increased significantly as the risk level decreased. For the angular velocity, the probability at the neutral velocity was highest in the low-risk job and lowest in the high-risk job (p=0.002). The same results could be found for R/U angular velocity (p=0.012), F/E angular acceleration (p=0.010), and R/U angular acceleration (p=0.017).

Averages and standard deviations of dependent variables (mean of wrist angle, wrist angular velocity, and wrist angular acceleration and normalized tendon excursions of FDP and FDS) are shown in Table 5.2. Comparisons of mean wrist angles, velocities, and accelerations for three different risk jobs are shown in Figure 5.4. The mean wrist angular velocities and accelerations in F/E movements were the highest in high-risk jobs (velocity: 51.4 ± 20.0º/s, acceleration: 338.0 ± 157.8º/s^2) and the lowest in low-risk jobs (velocity: 7.9 ± 3.5º/s, acceleration: 60.4 ± 29.1º/s^2) (p=0.014, 0.029 for velocity and acceleration, respectively), which corresponded to the risk of MSDs. Mean F/E angles (high-risk:19.2 ± 8.9º/s, mid-risk: 25.9 ± 4.6º/s, low-risk: 8.9 ± 4.0º/s) were significantly

different (p=0.025) across risk groups, but the difference did not correspond to the risk of MSDs. The mean wrist angles (high-risk: 12.3 ± 1.8º, mid-risk: 8.3 ± 1.4º, low-risk: 3.9 ± 3.1º), mean wrist angular velocities(high-risk: 19.1 ± 7.9º/s, mid-risk: 12.7 ± 3.3º/s, low-risk: 2.5 ± 1.4º/s), and mean wrist angular accelerations (high-risk: 118.4 ± 49.6º/s^2, med-risk: 87.0 ± 19.7º/s^2, low-risk: 18.7 ± 11.5º/s^2) in radial-ulnar movements were significantly different (p=0.005, 0.016, 0.020 for angle, velocity, and acceleration, respectively) for three risk groups, and these values corresponded to the risk of MSDs. None of maximums, minimums, 95%ile values, 5%ile values, and medians significantly differentiated the risk level (p>0.05), regardless of the type of variables (angle, velocity, and acceleration).

Tendon excursions of both FDP (high-risk: 42.9 ± 19.3 m/hr, mid-risk: 18.9 ± 8.9 m/hr, low-risk: 5.7 ± 2.7 m/hr) and FDS (high-risk: 49.7 ± 21.9 m/hr, mid-risk: 22.3 ± 10.1 m/hr, low-risk: 6.7 ± 3.2 m/hr) were significantly different across three risk groups (p=0.023 and 0.021 for FDP and FDS tendon excursions respectively) and corresponded well to the risk of MSDs as shown in Figure 5.5.

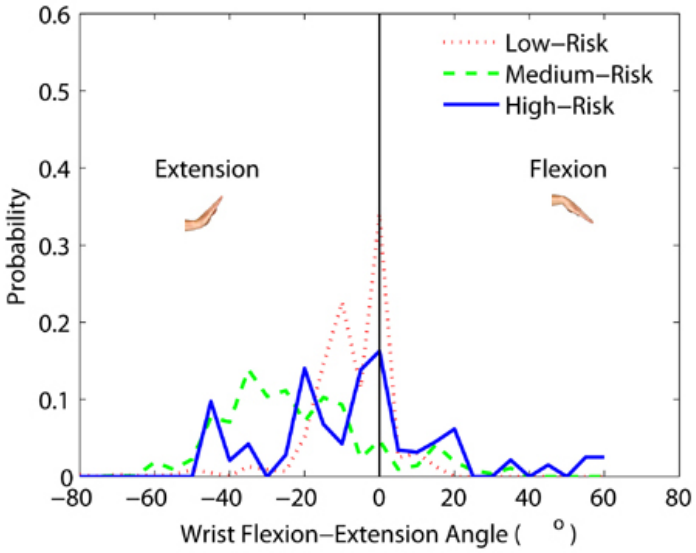

(a) Wrist flexion-extension angle

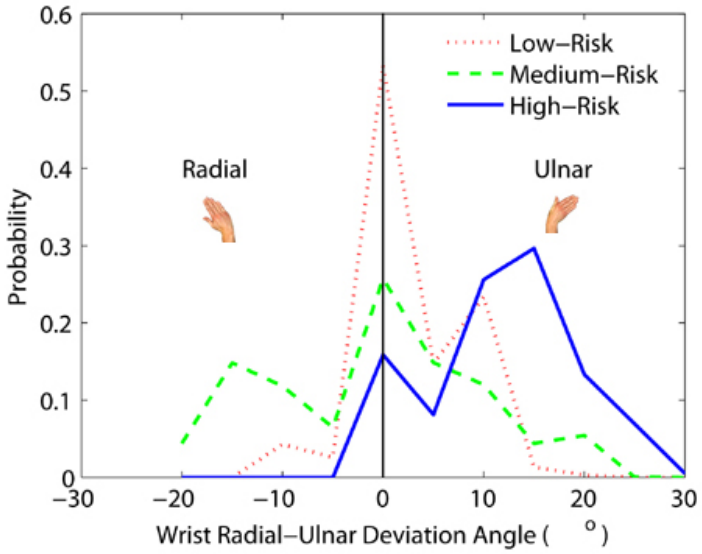

(b) Wrist radial-ulnar deviation angle

Figure 5.1 Histograms of F/E (flexion/extension) and R/U (radial/ulnar) deviation wrist angles for high-, medium-, and low-risk job.

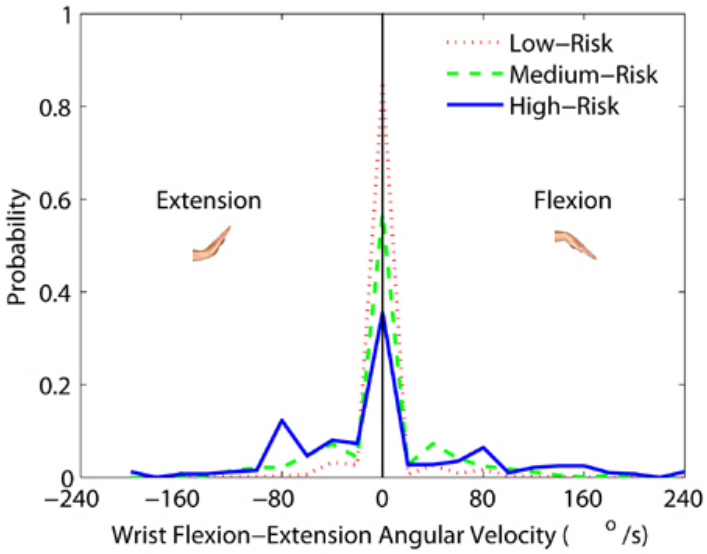

(a) Wrist flexion-extension angular velocity

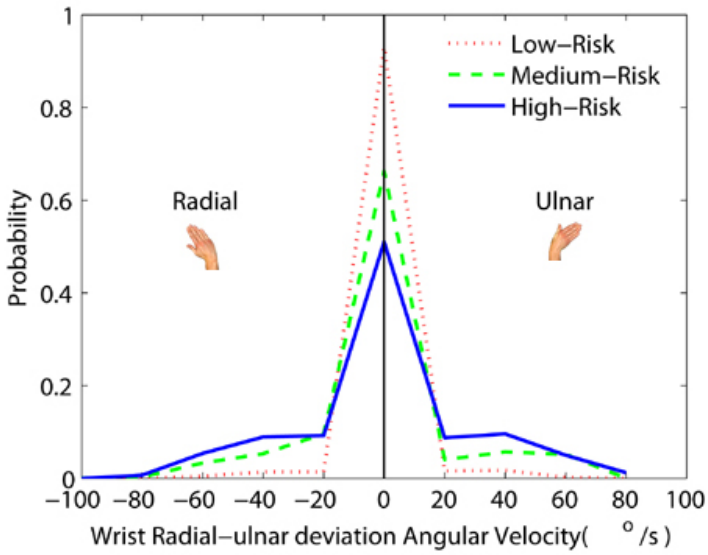

(b) Wrist radial-ulnar deviation angular velocity

Figure 5.2 Histograms of F/E (flexion/extension) and R/U (radial/ulnar) deviation wrist angular velocities for high-, medium-, and low-risk job.

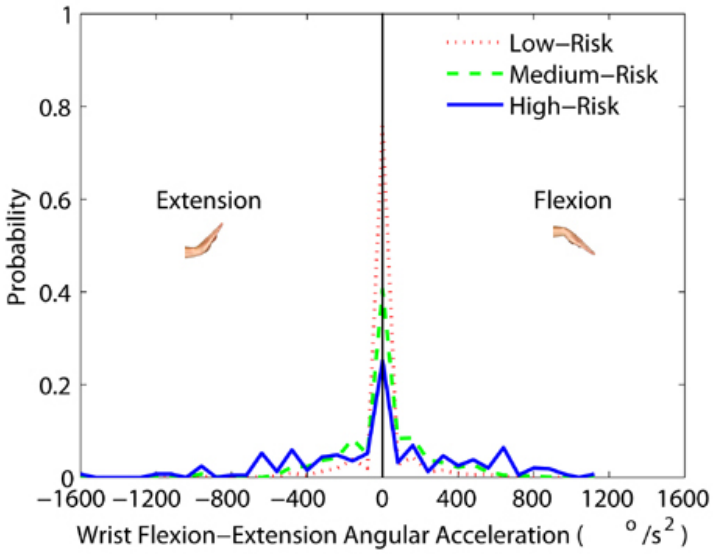

(a) Wrist flexion-extension angular acceleration

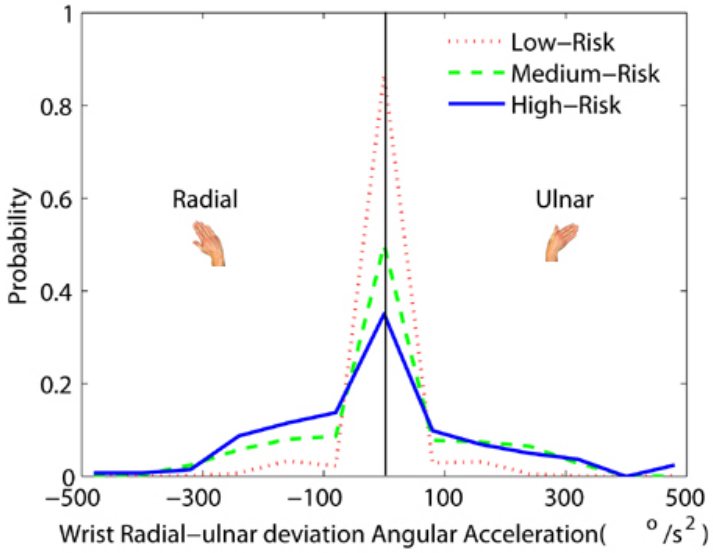

(b) Wrist radial-ulnar deviation angular acceleration

Figure 5.3 Histograms of F/E (flexion/extension) and R/U (radial/ulnar) deviation wrist angular accelerations for high-, medium-, and low-risk job.

Table 5.2 Averages and standard deviations of dependent variables (mean, probability at neutral value of wrist angle, angular velocity and angular acceleration, and normalized tendon excursion)

MSD risk level	Flexion/Extension			Radial/Ulnar Deviation		
	Angle	Velocity	Acceleration	Angle	Velocity	Acceleration
Mean	(º)	(º/s)	(º/s^2)	(º)	(º/s)	(º/s^2)
High risk job	19.2±8.9	51.4±20.0*	338.0±157.8*	12.3±1.8*	19.1±7.9*	118.4±49.6*
Mid risk job	25.9±4.6	25.5±9.3*	155.5±44.8*	8.3±1.4*	12.7±3.3*	87.0±19.7*
Low risk job	8.9±4.0	7.9±3.5*	60.4±29.1*	3.9±3.1*	2.5±1.4*	18.7±11.5*
Probability at	θ = 0º	θ' = 0º/s	θ" = 0º/s^2	θ = 0º	θ' = 0º/s	θ" = 0º/s2
High risk job	16.3±15.8	35.5±10.5*	25.1±17.2*	15.8±12.8*	51.3±18.0*	35.0±24.3*
Mid risk job	5.0±3.6	57.0±14.2*	40.3±16.4*	26.0±6.0*	66.3±10.2*	49.7±12.4*
Low risk job	34.3±19.6	85.3±5.5*	75.7±10.0*	53.3±34.3*	93.3±2.1*	86.7±5.1*
Normalized Tendon Excursion (m/hr)						
	FDP	FDS				
High risk job	42.9±19.3*	49.7±21.9*	-	-	-	-
Mid risk job	18.9±8.9*	22.3±10.1*	-	-	-	-
Low risk job	5.7±2.7*	6.7±3.2*	-	-	-	-

* significantly different ($p<0.05$)

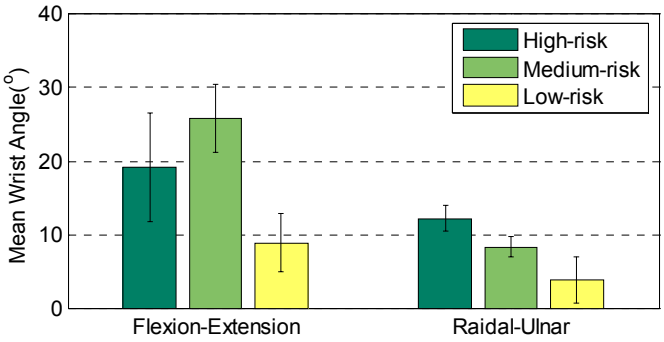

(a) Mean wrist angles of F/E and radial-ulnar movements.

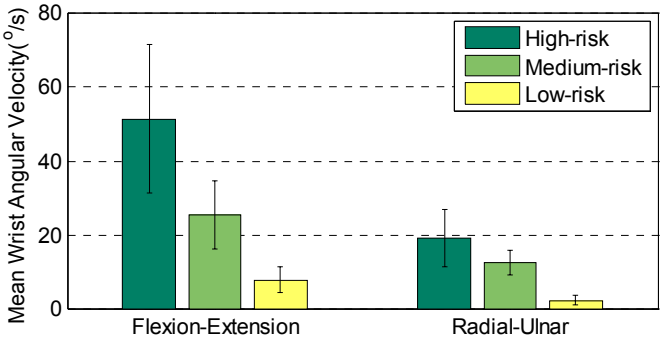

(b) Mean wrist angular velocities of F/E and radial-ulnar movements.

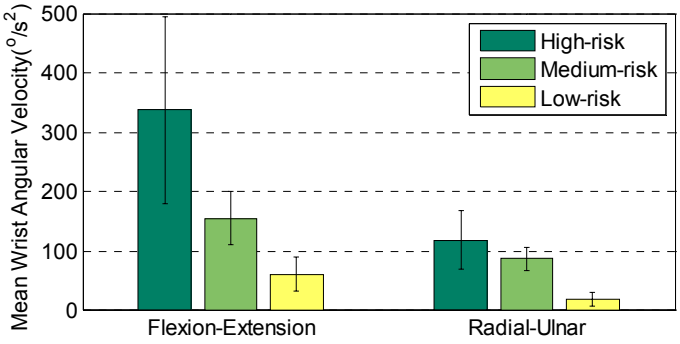

(c) Mean wrist angular accelerations of F/E and radial-ulnar movements.

Figure 5.4 Mean wrist angles, angular velocities, and angular accelerations for high-risk, medium-risk, and low-risk jobs.

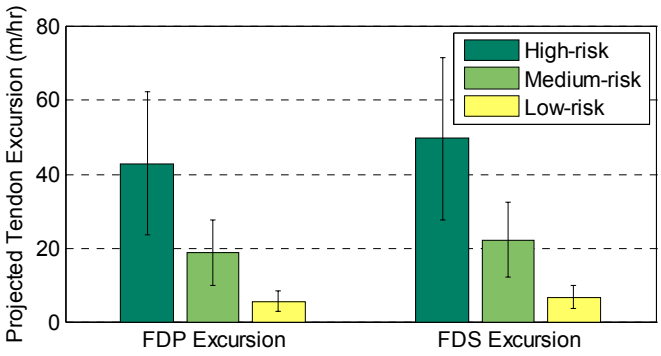

Figure 5.5 Normalized cumulative tendon excursions of FDP and FDS tendons for high-risk, medium-risk, and low-risk jobs.

5.4 DISCUSSION

Marras and Schoenmarklin (1993) found that the mean, maximum, minimum, and differences of the wrist velocity and acceleration variables significantly differentiated MSD risk levels, but that wrist angle variable did not. Our study indicated that only mean angular velocity and mean angular acceleration of the wrist movements in both F/E and R/U were significantly different across the risk groups and corresponded to the risk of MSDs. These discrepancies can be explained by several reasons. First, Marras's study dichotomized the risk of MSDs as high risk and low risk, while we classified the risk of MSDs as high-, medium-, and low-risk jobs. This difference in classification of the jobs may have large effects on the results of ANOVA tests, as it changes degrees of freedom of the analysis. Modeling more levels of an exposure tends to decrease the probability of significance (Hagberg 1992). However, examination of the intermediate level of the risk helps to quantify exposures more precisely. Secondly, the discrepancies might be caused by the characteristics of the jobs examined. For example, two medium-risk jobs showed higher maximum velocity (180 º/s each) than two high-risk jobs (160 º/s and 120 º/s), but the medium-risk jobs reached their maximum velocities much less frequently (2.7 times/minute and 0.38 times/minute, respectively) than the high-risk jobs did (17.1 times/minute and 13.7 times/minute). A job that has the largest maximum (or the smallest minimum) velocity or acceleration for a moment may not entail high velocity or acceleration for the rest of the time, because the maximum and minimum values can be obtained for a very short period during an entire job. Thirdly, the experimental methods were different. Marras and Schoenmarklin used an electromechanical goniometer to measure wrist angles directly, while we chose a video-based observational method. The observational method we used in this study may have missed some of dynamic

characteristics at high frequency, because observation frequency was lower than that of direct measurement. However, it is not possible to use goniometer to retrospectively analyzed video recordings.

Comparison of mean velocities and accelerations between Marras' study and this study gives more quantitative information. In Marras' study, mean velocities in F/E direction were 42.2 ± 11.7º/s and 28.7 ± 7.6º/s for high-risk and low-risk jobs, respectively. In this study, mean velocities in F/E direction were 51.4 ± 20.0º/s for high-risk job, 25.5 ± 9.3º/s for medium-risk jobs, and 7.9 ± 3.5º/s for low-risk jobs. For acceleration in F/E direction, mean acceleration of high-risk and low-risk jobs was 824 ± 266º/s^2 and 494 ± 156º/s^2 in Marras' study. In our study, mean accelerations in F/E direction were 338 ± 158º/s^2, 156 ± 45º/s^2, and 60 ± 29º/s^2 for high-, medium-, and low-risk jobs, respectively. Marras' study shows higher values, especially in acceleration. These differences seem to be caused by the difference in job classification and the measurement method. In the time-based analysis, a 0.25-second interval was used for this study. According to the Nyquist-Shannon sampling theorem, this sampling rate (4Hz) can completely capture the motion up to 2 Hz without aliasing (Shannon 1949). Even though the peak frequency component ranges from 0.48 to 2.47 Hz in our daily living activities (Mann, Werner et al. 1989), there might have been the wrist motion at high frequency which our method could not capture.

Normalized cumulative tendon excursion data are comparable to the data from Moore et al. (Moore, Wells et al. 1991). They calculated tendon excursions of FDP and FDS using the same model (Armstrong and Chaffin 1978) we used, and averaged over FDP and FDS tendons of index and middle fingers. In their study, average normalized cumulative tendon excursions for low repetition jobs were 19.1 m/hr, and those for high repetition jobs were 73.2 m/hr. In our study, average normalized cumulative tendon

excursions were 46.3 m/hr for high-risk jobs, 20.6 m/hr for medium-risk job, and 6.2 m/hr for low-risk jobs. The differences between these two studies can be explained by (1) the sampling frequency as mentioned above, and (2) inclusion of finger motion. Moore et al. computed tendon excursion not only by the wrist motions but also by the index and middle finger motions, and thus resulted in higher estimated tendon excursions.

The wrist angles did not differentiate the risk of MSDs correctly as shown in Figure 5.4. In our study, some high-risk jobs such as band welding or handle assembly jobs included smaller F/E (40º for each) and R/U (25º and 16º, respectively) angles than some of the medium-risk (F/E:75º~95º, R/U: 35º~45º) and low-risk jobs (F/E: 30º~90º, R/U: 15º~30º) as shown in Table 5.3. But repetition levels of these jobs (8.5 and 8.8 repetition ratings respectively) were notably higher than other medium-risk (repetition rating: 5.3~6.4) or low-risk jobs (repetition rating: 1.6~2.9). Also, in some of the medium-risk (office panel upholstery, small drum cover glue, spark plug transfer) and low-risk jobs (NC machine operation), the repetition level was not as high as in high-risk jobs, but the range of motions was larger than in high-risk jobs for some time intervals (Table 5.3). Figure 5.6 shows the plot of mean velocities vs. maximum ROMs (range of motions) in F/E and R/U wrist motions. Comparing medium- and high-risk jobs, the maximum ROM decreased as mean velocity increased. Workers might not have enough time to achieve extreme ROMs at high repetition, whereas they could use greater ROMs at medium repetition. At low repetition jobs, workers seems not have used their hand much, and consequently did not have exposure to high ROMs. Therefore, the magnitude of angles is not effective to indicate the risk level of MSDs. This observation emphasizes the importance of the role of frequency components in velocity and acceleration which differentiated the risk of MSDs significantly.

Table 5.3. Ranges of motion in F/E and R/U movement of the wrist for the jobs examined in this study

MSD risk level	Job	Maximum ROM (F/E)	Maximum ROM (R/U)
High-risk	band welding	40°	25°
	handle assembly	40°	16°
	platinum spark plug weld	70°	20°
	spark plug transfer B	80°	10°
	Pooled	80°	25°
Medium-risk	office panel upholstery	95°	45°
	small drum cover glue	80°	40°
	spark plug transfer	75°	35°
	Pooled	95°	45°
Low-risk	machine loading	35°	20°
	NC machine operation	95°	30°
	Injection molding machine operator	30°	15°
	Pooled	95°	30°

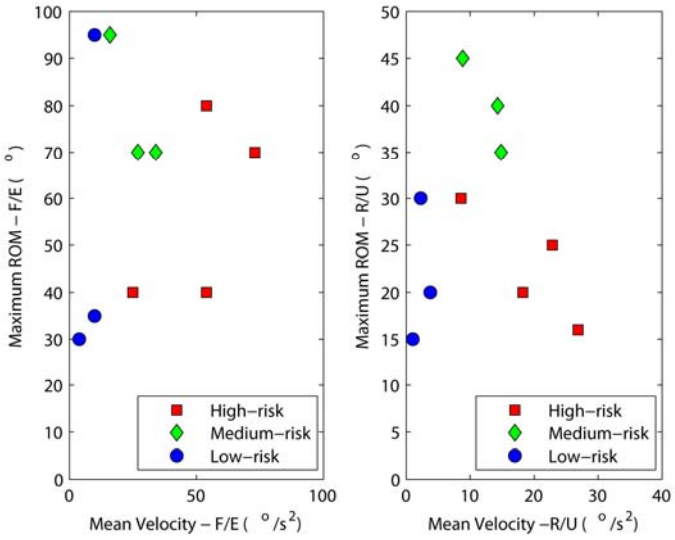

Figure 5.6 Plot of mean velocity vs. maximum ROM (range of motion) in F/E and R/U wrist motion

Consideration of biomechanical aspects of the dependent variables that we used in this study give more insight into the pathomechanism of MSDs. Wrist angle affects the resultant force on flexor tendons (Armstrong and Chaffin 1979). Increase of resultant force causes increase of friction force on the tendon, because the normal force on the tendon increases. The histogram of the wrist angle (Figure 5.1) can be used to investigate the effect of the static posture on MSDs. Wrist angular velocity is closely related to tendon excursion at the wrist as shown by Eq. (5.4). Therefore, the velocity indicates how much the tendon is exposed to shear force and friction force during the job period. Wrist angular acceleration is related to the tension force exerted on the tendon. According to the model by Schoenmarklin and Marras (1990), tension force is determined by the curvature of the wrist, mass and inertia of the hand, distance from the wrist to the center of the hand, and the angular acceleration of the wrist joint. As the tension force is proportional to the moment inertia of the hand and angular acceleration, the higher repetition jobs (which has higher acceleration) would require more tendon loads than the lower repetition jobs. Also, as tension force is proportional to resultant force according to the biomechanical wrist model by Armstrong (1979), wrist angular acceleration affects the resultant force eventually.

5.5 LIMITATIONS AND FUTURE RESEARCH

There are some limitations of this study. Time-based analysis enables the user to analyze the job repeatedly without interference with workers' activities. However, the resolution of the video and the parallax by the camera angle can affect the results (Lau, 2007). Using multiple synchronized cameras can be an effective solution for the parallax problem. Another limitation of using the time-based analysis is the sampling rate. As

the time-based analysis requires a large amount of time, the proper sampling rate should be chosen to avoid aliasing effect.

We observed the wrist angles, but for more detailed analysis, the finger movements need to be considered as well. The finger movements cannot be easily measured without using special equipment such as an electromechanical goniometer or position markers. An alternative approach is to develop models using laboratory data that can be used to predict MCP (metacarpophalangeal) , PIP (proximal interphalangeal), and DIP (distal interphalangeal) joint angles of the hand (Choi and Armstrong 2007). Such models can then be used to construct motion sequences based on descriptions of work elements and work objects. For example, a task might involve reaching for a cylindrical part 25 mm in diameter and positioning it in a box for shipping. The work elements for this task can be predicted using a predetermined time system such as MTM: Reach, grasp, move, and position (e.g., R12B, G1C1, M12B, P1S, RL1). The MCP, PIP and DIP joint angles, in “reach” and “grasp” of the part, can be predicted from previous laboratory simulations. During the “move” and “position” the finger position is fixed. During the release the inter-digit angles decrease slightly, but this is not significant. The hand then returns to the resting position. Future work will entail conducting a series of laboratory simulations to populate a database with joint angles for generic tasks.

5.6 CONCLUSIONS

- Mean wrist angular velocity and mean wrist angular acceleration differentiated the risk of MSDs significantly and correctly, while mean wrist angle did not.
- Normalized cumulative tendon excursion of both FDP and FDS tendons significantly differentiated the risk levels of MSDs.
- Frequency components play a more important role in magnifying and lessening the velocity and acceleration than does magnitude of angle.
- Observational method can be used to assess the risk level with minimum equipment and without interference with worker's activities, but the sampling rate should be carefully chosen to avoid aliasing.

5.7 REFERENCES

Armstrong, T. J., W. A. Castelli, F. G. Evans, et al. (1984). "Some histological changes in carpal tunnel contents and their biomechanical implications." J Occup Med **26**(3): 197-201.

Armstrong, T. J. and D. B. Chaffin (1978). "An inverstigation of the relationship between displacements of the finger and wrist joints and the extrinsic finger flexor tendons." Journal of biomechanics **11**: 119-128.

Armstrong, T. J. and D. B. Chaffin (1979). "Some biomechanical aspects of the carpal tunnel." J Biomech **12**(7): 567-70.

Armstrong, T. J., W. M. Keyserling, D. C. Grieshaber, et al. (2003). Time based job analysis for control of work related musculoskeletal disorders. 15th Congress of the Internatinal Ergonomics Association, Seoul, Korea.

Barnhart, S., P. A. Demers, M. Miller, et al. (1991). "Carpal tunnel syndrome among ski manufacturing workers." Scand J Work Environ Health **17**(1): 46-52.

Chiang, H. C., S. S. Chen, H. S. Yu, et al. (1990). "The occurrence of carpal tunnel syndrome in frozen food factory employees." Gaoxiong Yi Xue Ke Xue Za Zhi **6**(2): 73-80.

Choi, J. and T. J. Armstrong (2007). Quantitative analysis of finger movements during reaching and grasping tasks. ASB annual meeting, Stanford, CA.

Feldman, R. G., P. H. Travers, J. Chirico-Post, et al. (1987). "Risk assessment in electronic assembly workers: carpal tunnel syndrome." J Hand Surg [Am] **12**(5 Pt 2): 849-55.

Fuchs, P. C., P. A. Nathan and L. D. Myers (1991). "Synovial histology in carpal tunnel syndrome." J Hand Surg [Am] **16**(4): 753-8.

Gell, N., R. A. Werner, A. Franzblau, et al. (2005). "A longitudinal study of industrial and clerical workers: incidence of carpal tunnel syndrome and assessment of risk factors." J Occup Rehabil **15**(1): 47-55.

Goldstein, S. A., T. J. Armstrong, D. B. Chaffin, et al. (1987). "Analysis of cumulative strain in tendons and tendon sheaths." J Biomech **20**(1): 1-6.

Hagberg, M. (1992). "Exposure variables in ergonomic epidemiology." Am J Ind Med **21**(1): 91-100.

Hagberg, M., H. Morgenstern and M. Kelsh (1992). "Impact of occupations and job tasks on the prevalence of carpal tunnel syndrome." Scand J Work Environ Health **18**(6): 337-45.

Keyserling, W. M., D. S. Stetson, B. A. Silverstein, et al. (1993). "A checklist for evaluating ergonomic risk factors associated with upper extremity cumulative trauma disorders." Ergonomics **36**(7): 807-31.

Latko, W. A., T. J. Armstrong, A. Franzblau, et al. (1999). "Cross-sectional study of the relationship between repetitive work and the prevalence of upper limb musculoskeletal disorders." Am J Ind Med **36**(2): 248-59.

Leclerc, A., M. F. Landre, J. F. Chastang, et al. (2001). "Upper-limb disorders in repetitive work." Scand J Work Environ Health **27**(4): 268-78.

Mann, K. A., F. W. Werner and A. K. Palmer (1989). "Frequency spectrum analysis of wrist motion for activities of daily living." Journal of Orthopaedic Research **7**(2): 304-306.

Marklin, R. W. and J. F. Monroe (1998). "Quantitative biomechanical analysis of wrist motion in bone-trimming jobs in the meat packing industry." Ergonomics **41**(2): 227-37.

Marras, W. S. and R. W. Schoenmarklin (1993). "Wrist motions in industry." Ergonomics **36**(4): 341-51.

McCormack, R. R., Jr., R. D. Inman, A. Wells, et al. (1990). "Prevalence of tendinitis and related disorders of the upper extremity in a manufacturing workforce." J Rheumatol **17**(7): 958-64.

Moore, A., R. Wells and D. Ranney (1991). "Quantifying exposure in occupational manual tasks with cumulative trauma disorder potential." Ergonomics **34**(12): 1433-53.

Moore, J. S. (2002). "Biomechanical models for the pathogenesis of specific distal upper extremity disorders." Am J Ind Med **41**(5): 353-69.

Osorio, A. M., R. G. Ames, J. Jones, et al. (1994). "Carpal tunnel syndrome among grocery store workers." Am J Ind Med **25**(2): 229-45.

Phalen, G. S. (1966). "The carpal-tunnel syndrome. Seventeen years' experience in diagnosis and treatment of six hundred fifty-four hands." J Bone Joint Surg Am **48**(2): 211-28.

Rempel, D., L. Dahlin and G. Lundborg (1999). "Pathophysiology of nerve compression syndromes: response of peripheral nerves to loading." J Bone Joint Surg Am **81**(11): 1600-10.

Schoenmarklin, R. W. and W. S. Marras (1990). A dynamic biomechanical model of the wrist joint. Proceedings of the 34th Annual Meeting of the Human Factors Society, Santa Monica, CA, USA.

Serina, E. R., R. Tal and D. Rempel (1999). "Wrist and forearm postures and motions during typing." Ergonomics **42**(7): 938-51.

Shannon, C. E. (1949). Communication in the presence of noise. Proc. Institute of Radio Engineers.

Silverstein, B. A., L. J. Fine and T. J. Armstrong (1986). "Hand wrist cumulative trauma disorders in industry." Br J Ind Med **43**(11): 779-84.

Silverstein, B. A., L. J. Fine and T. J. Armstrong (1987). "Occupational factors and carpal tunnel syndrome." Am J Ind Med **11**(3): 343-58.

Sommerich, C. M., W. S. Marras and M. Parnianpour (1996). "A quantitative description of typing biomechanics." Journal of Occupational Rehabilitation **6**(1): 33-54.

Wells, R., A. Moore and P. Keir (1994). Biomechanical models of the hand. Proc. Marconi Keyboard Research Conference.

Wells, R., A. Moore, J. Potvin, et al. (1994). "Assessment of risk factors for development of work-related musculoskeletal disorders (RSI)." Appl Ergon **25**(3): 157-64.

Wren, T. A., G. S. Beaupre and D. R. Carter (1998). "A model for loading-dependent growth, development, and adaptation of tendons and ligaments." J Biomech **31**(2): 107-14.

CHAPTER 6

CONCLUSIONS

The overall purpose of this work was to develop a 3-D kinematic model of the hand that can predict hand posture and hand space envelope, based on a contact algorithm and proper implementation of finger movements. In addition, the association between tendon excursion and the risk of MSDs was examined.

6.1 SUMMARY OF MAJOR FINDINGS AND DISCUSSION

1) A 3-dimensional kinematic model of the hand to predict hand posture was developed using a contact algorithm. The model gave a reasonable prediction of hand posture for both power grip (R^2 = 0.76) and pulp pinch grip (R^2 = 0.88) (Chapter 2).

The 3-D kinematic model developed in this study was found to reasonably predict the hand posture for both power and pinch grip. Application of the "variable rotation algorithm," where finger joints were rotated at the observation-based rate, improved the accuracy of the model by 20% on average, compared to application of the "constant rotation algorithm," where finger joints were rotated at constant rate. Only the power grip posture has been predicted in the earlier model, by modeling finger movements with flexion only (Buchholz and Armstrong 1992; Endo and Kanai 2006; Miyata, Kouchi et al. 2006). The optimization-based model was unable to predict the posture of thumb and

pinch grip posture, because its objective function was not applicable to thumb and pinch grip (Lee and Zhang 2005). Pinch grip posture and thumb posture in both power and pinch grip were predicted in this study by applying a "variable rotation algorithm." The sensitivity study by simulation revealed that finger posture is more sensitive to object size (sensitivity measure = 47.8), orientation (7.4), and location (6.9) than to hand size (4.7) and skin deformation (1.7).

The predicted posture can be used as the basic data to predict hand strength. Many kinetic models (Chao, Opgrande et al. 1976; Lee and Rim 1990; Valero-Cuevas, Zajac et al. 1998; Sancho-Bru, Perez-Gonzalez et al. 2003) have been developed to predict the maximum force in certain grasps, but these studies did not include the validation of hand posture. Strength prediction without sufficient validation of hand posture may lead to inaccurate results, because muscle tension is significantly affected by the muscle length in isometric exertion.

2) Hand space envelopes during a hose placement task were estimated using the kinematic model of the hand. The simulation results show good agreement with measured data with an average 17% underestimation of sectional areas. The simulated space envelopes were affected by grip type (pinch grip requires 72% more sectional areas than power grip), method (rotation method requires 26% more sectional areas than straight method), and hand size (95% male hand requires 44% more sectional areas than 5% female hand) (Chapter 3).

The hand space envelope is useful information for designing the work place and work objects so that minimum interference with obstructions occur. The hand space

envelope is affected by hand size and grip type, because these change the hand posture when grasping work objects. The space envelope is also affected by behavioral characteristics: for example, amplitude of rotation angle and frequency of rotation in the hose placement task. In this task, the behavioral aspect can be influenced by the required force, lubrication condition, and hand strength. The more force that is required, the larger the amplitude of rotation angle, and the more frequently rotation occurs. Therefore, consideration of biomechanical factors during certain manual tasks will be helpful to model behavioral features as accurately as possible.

3) Finger movements during grasping differently sized objects were characterized quantitatively using spatial and temporal variables, which can be applied to the model that predicts hand posture using a contact algorithm (Chapter 4).

Object size changes both spatial and temporal variables during reaching and grasping movements. Power grasp uses all joints of four fingers and flexion-extension of MCP and CMC joints of the thumb to adjust the hand to different object sizes. Pinch grasp uses MCP joints of four fingers and thumb CMC joints to adjust the hand to different object sizes. During grasping movements, humans change the velocities of joints as the object size changes, which reduces the difference in time to complete grasping. These spatial and temporal variables can characterize the finger movement during reaching and grasping. Linear curve fitting with measured spatial and temporal variables defined in this study was able to explain 86% - 93% of the variability of velocities on average.

4) The normalized cumulative tendon excursion of both FDP (flexor digitorum profundus) and FDS (flexor digitorum superficialis) tendons significantly differentiated the risk levels of MSDs (musculoskeletal disorders) (Chapter 5).

Mean wrist angular velocity and mean wrist angular acceleration differentiated the risk of MSDs significantly and correctly, while mean wrist angle did not. This was because frequency components play a more important role in magnifying and lessening the velocity and acceleration than does magnitude of angle. Cumulative tendon excursion is closely related to the angular velocity components, and it also captures not only the peak wrist angle and frequency but also the duration of the job, which should be considered when assessing a job. The cumulative tendon excursion gives more physically meaningful values than velocity or acceleration component alone, because it is related to friction and wear that may contribute to MSDs.

6.2 DISCUSSION OF MAJOR FINDINGS

The goal of this study was to develop a tool that can be used for ergonomics analyses. To illustrate the use of the outcomes of this research, two job exemplars were analyzed.

6.2.1 Hose placement job

In this job, the workers are assumed to be trying to install hose onto the flange of the engine in an automobile plant. The worker starts with the hand in a resting posture then reaches for and grasps the hose. Then (s)he places the hose onto the flange using the rotation method (Chapter 3). There exists an obstruction at 40 mm in the medial direction from the center of the flange on which the hose is placed. Simulation of this job was performed for two workers, 5% female and 95% male hand sizes (Garrett 1971), two different hose sizes (D:25 mm and D:60 mm), and two grip types (power grip and pinch grip).

- **Hand posture**

Predicted hand postures for the above conditions are shown in Table 6.1. The results were in good agreement with the sensitivity study in Chapter 2. Increasing object size decreased joint angles and increasing hand size increased joint angles. Figure 6.1 shows the predicted hand postures for two different hand sizes (5% female and 95% male), object sizes (D: 25 mm and D: 60 mm), and grip types (power grip and pinch grip).

Table 6.1 Predicted hand postures (°) for two different hand sizes (5% female and 95% male), object sizes (D: 25 mm and D: 60 mm), and grip types (power grip and pinch grip)

Hand Size	Object Size	Grip Type	Index			Middle			Ring		
			MCP	PIP	DIP	MCP	PIP	DIP	MCP	PIP	DIP
5% Female	25 mm	Power	24	48	60	49	93	43	61	84	51
95% Male	25 mm	Power	42	96	46	80	89	49	83	84	50
5% Female	60 mm	Power	20	21	8	31	39	34	40	47	28
95% Male	60 mm	Power	27	30	52	53	65	39	63	56	37
5% Female	25 mm	Pinch	48	5	25	51	19	17	49	27	7
95% Male	25 mm	Pinch	67	0	18	78	1	16	69	19	18

Hand Size	Object Size	Grip Type	Little			Thumb					
			MCP	PIP	DIP	IP	MCP FE	MCP AA	CMC FE	CMC AA	CMC PS
5% Female	25 mm	Power	65	68	42	53	41	5	37	7	-91
95% Male	25 mm	Power	74	77	46	51	48	-3	36	33	-109
5% Female	60 mm	Power	50	28	34	43	32	11	21	8	-86
95% Male	60 mm	Power	54	39	45	49	40	2	20	32	-107
5% Female	25 mm	Pinch	55	6	25	10	19	11	38	6	-99
95% Male	25 mm	Pinch	74	11	22	9	13	6	35	26	-111

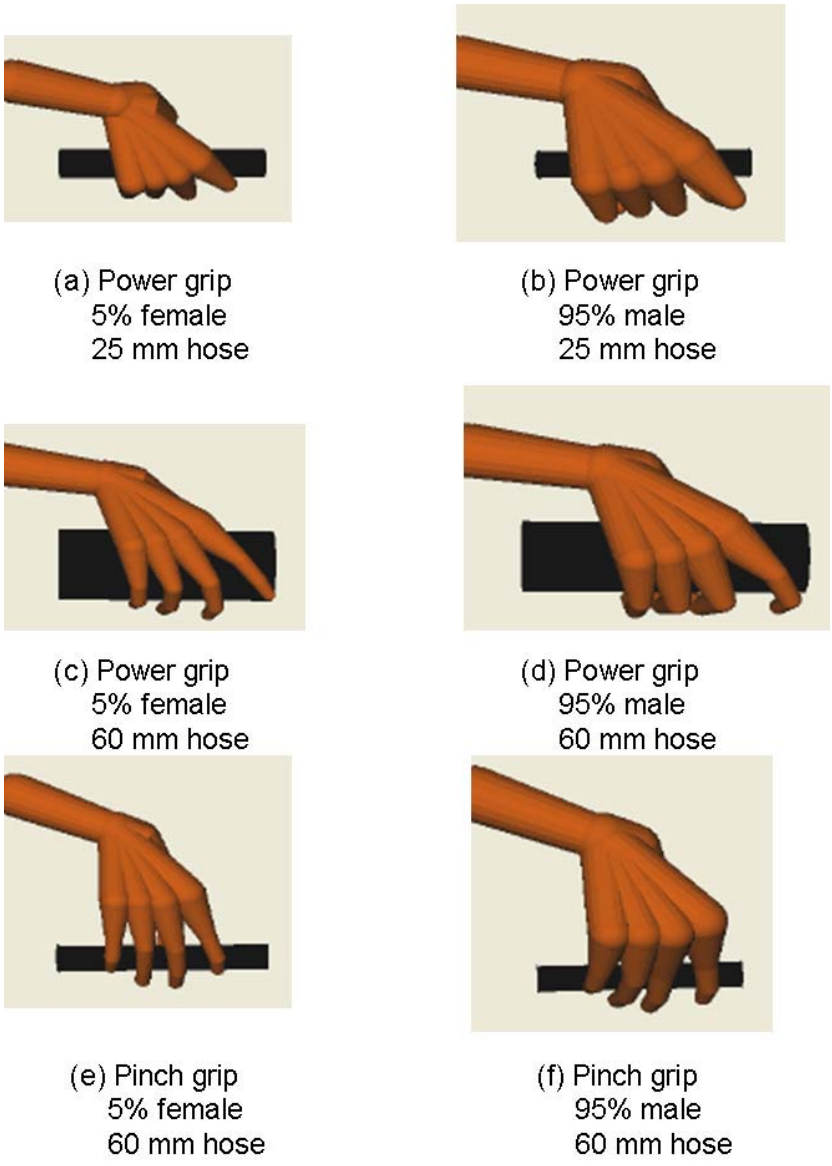

Figure 6.1 Predicted postures for two different hand sizes (5% female and 95% male), object sizes (D: 25 mm and D: 60 mm), and grip types (power grip and pinch grip)

- **Hand space envelope**

Hand space envelopes were estimated for the above conditions based on predicted postures. As observed in Chapter 3, increasing hand size was associated with an increasing hand space envelope over all ranges (Figure 6.2). Comparison of Figure 6.2 and Figure 6.3 shows the effect of object size on grasp envelope. Figure 6.4 shows the hand space envelope when using the pulp pinch grip. As observed in Chapter 3, the pinch grip requires less space in the medial direction than the power grip. The obstruction, located 40 mm in the medial direction from the center of the flange, may force the workers to perform the task without interference or to change the grip type. With the power grip (Figure 6.2), only workers whose hand sizes are less than a 5% female hand size can perform the task, and even then, only barely. But there is a high possibility that the hand will interfere with the obstruction during the task if the worker moves the hand in the medial – lateral direction to increase the push force. With a hose of 60 mm diameter, almost no one can perform this task, because the hand interferes with the obstruction at least 5 mm. Then some workers with small hand size may change the hose placement method from the rotation method to the straight method to minimize the space taken up by the hand. But the straight method requires more axial force than rotation method, and thus the workers will have more difficulty with this job. Use of pinch grip will be the best choice in this situation to avoid the obstruction (Figure 6.4). The pinch grip enables workers with a 95% male hand size to perform the task without interference with the obstruction. However, use of pinch grip decreases the grip strength, which will decrease the friction force that is needed to push the hose onto the flange. Decreased hand strength may lead to high risk on the job because worker will have more chance to slip the grip object.

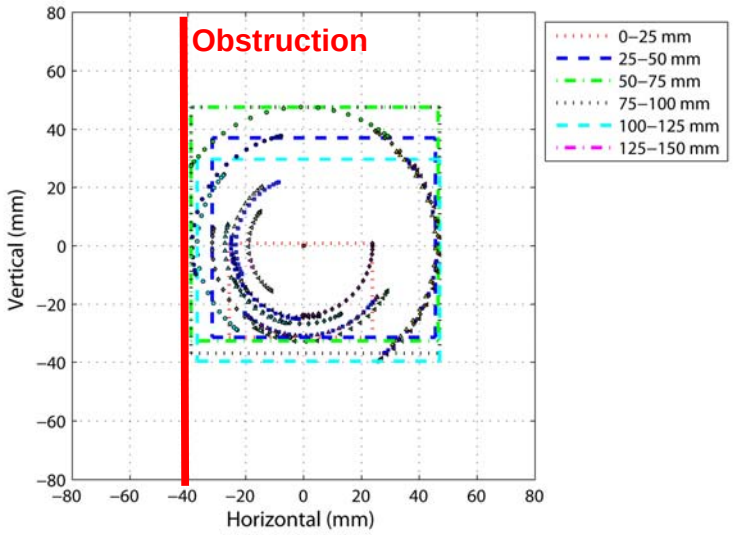

(a) Power grip, 5% female, 25 mm hose

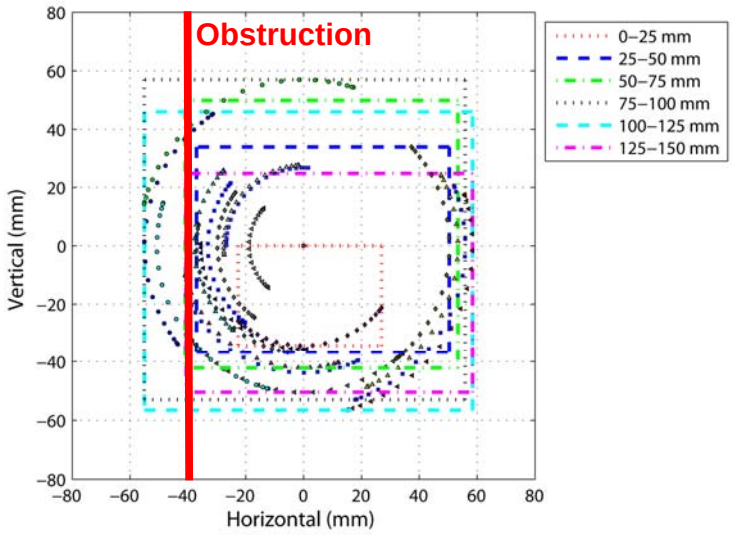

(b) Power grip, 95% male, 25 mm hose

Figure 6.2 Hand space envelope for 5% female and 95% male hand sizes with 25 mm hose in power grip

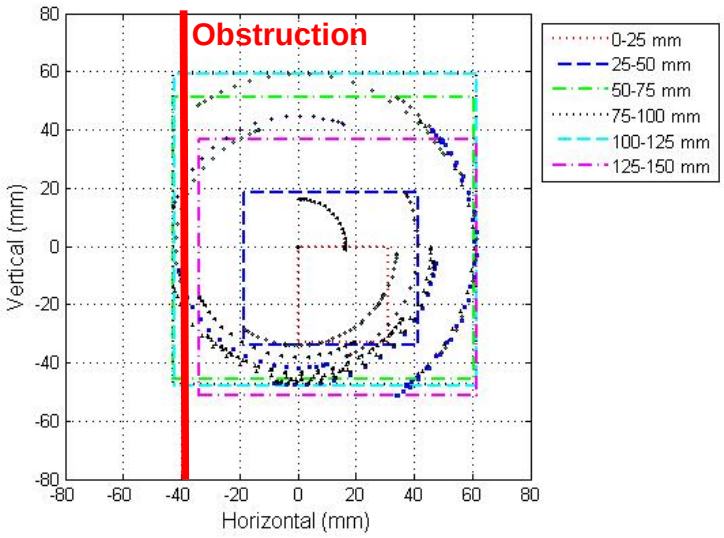

(a) Power grip, 5% female, 60 mm hose

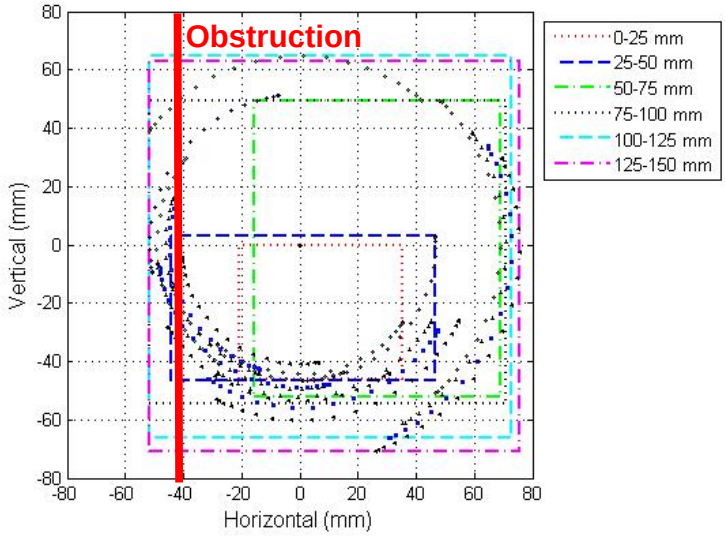

(b) Power grip, 95% male, 60 mm hose

Figure 6.3 Hand space envelope for 5% female and 95% male hand sizes with 60 mm hose in power grip

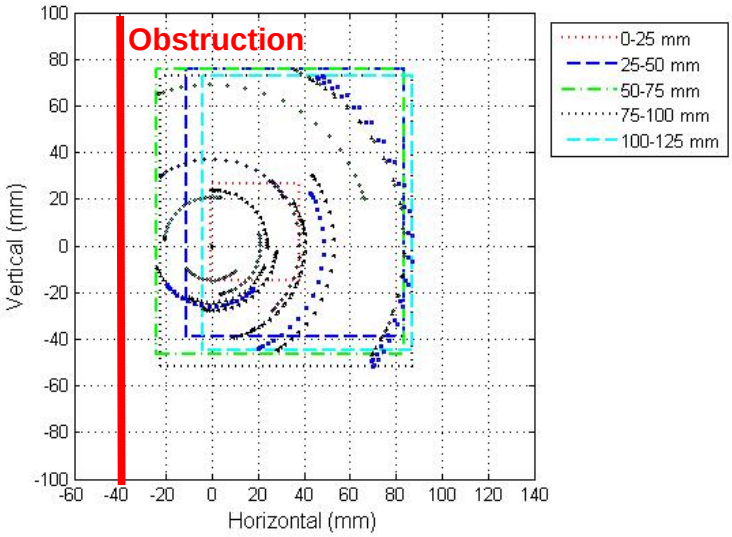

(a) Pinch grip, 5% female, 25 mm hose

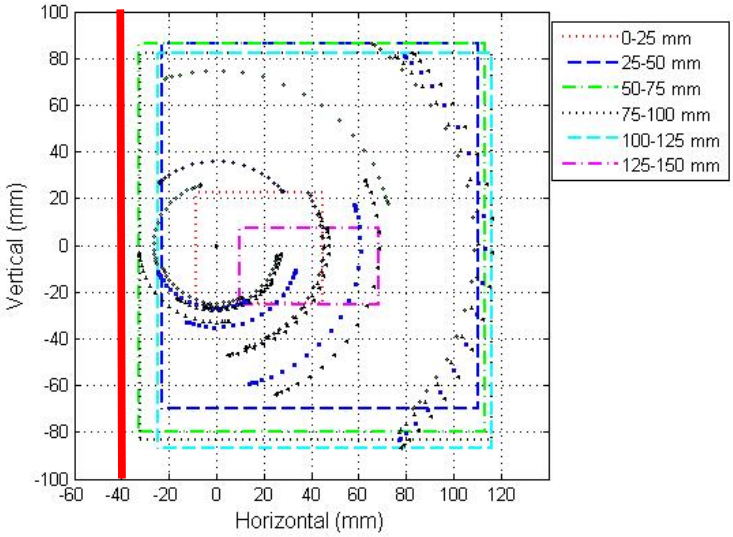

(b) Pinch grip, 95% male, 25 mm hose

Figure 6.4 Hand space envelope for 5% female and 95% male hand sizes with 25 mm hose in pinch grip

Table 6.2 Sectional areas along the axis of the hose

Distance from the end of the hand (mm)	Power (mm^2)		Power (mm2)		Pinch (mm2)	
	25 mm hose		60 mm hose		25 mm hose	
	5% female	95% male	5% female	95% male	5% female	95% male
0-25	2169	2317	1985	3313	2092	2711
25-50	5283	6170	3127	5367	11006	20881
50-75	6842	8674	10004	8581	13154	24252
75-100	7258	12200	11118	12731	13613	24626
100-125	5809	11619	11130	16335	11711	23784
125-150	772	7437	8412	16977	0	2115
Average	4689	8070	7629	10551	8596	16395

- **Tendon excursion during grasping**

Based on the findings, cumulative tendon excursion can be estimated using the model. To calculate the cumulative tendon excursions, we need to know the finger joint angles at rest posture, at maximum opening, and at final grasping. The average finger joint angles at the rest posture are shown in Table 6.3. Open angles can be obtained using the Table 4.3 and Table 4.4 in Chapter 4. To calculate tendon displacement at finger joints, the empirical equations by Armstrong et al. (1978) were used. Cumulative tendon excursion was calculated by the following equation.

$$\text{Cumulative tendon excursion} = |TD_{open} - TD_{initial}| + |TD_{final} - TD_{open}| \quad (6.1)$$

, where TD : Tendon Displacement

$TD_{initial}$: Tendon Displacement at rest posture

TD_{open} : Tendon Displacement at open posture

TD_{final} : Tendon Displacement at final posture

Cumulative tendon excursion for the various conditions are shown in Table 6.4. On average, power grasping needs almost two times more tendon excursions than pinch grasping. For the same object size with same grip type, tendon excursions of 95% male were 30% larger than those of 5% female. As the object size increased, the tendon excursion decreased.

The workers with 5% female hand size requires smaller tendon excursion, because (1) the radius of curvature at each joint was smaller than 95% male, and (2) joint angles at the final posture were significantly larger than 95% male. It is also

expected that 5% female has smaller tendon excursion at the wrist because the thickness of 5% female wrist is smaller. However, the normal supporting force acting on the tendon is inversely proportional to the thickness of the wrist (Armstrong and Chaffin 1979). The trade-off between tendon excursion and the normal force on the tendon needs to be investigated.

Pinch grasping requires much smaller tendon excursion than power grasping. But the reduction of grip strength in pinch grip may cause a larger force on the tendon and muscles.

Table 6.3 Averages and standard deviations of finger joint angles (°) at rest posture (16 subjects, 168 trials)

	MCP	PIP	DIP
Index	33.6±10.2	33.4±10.3	13.6±5.9
Middle	34.0±12.9	35.7±12.2	13.2±8.6
Ring	29.4±9.5	39.0±12.9	15.1±7.6
Little	29.1±7.5	33.8±11.9	19.5±10.3

Table 6.4 Cumulative tendon excursions for FDP and FDS tendons (mm)

Hand Size	Object Size	Grip Type	FDP Index	Middle	Ring	Little	Average
5% Female	25 mm	Power	5.5	13.4	12.3	10.3	10.4
95% Male	25 mm	Power	10.7	13.6	14.0	12.1	12.6
5% Female	60 mm	Power	2.8	7.9	8.2	6.7	6.4
95% Male	60 mm	Power	4.3	10.1	11.1	8.3	8.4
5% Female	25 mm	Pinch	4.5	4.0	4.5	5.5	4.7
95% Male	25 mm	Pinch	6.6	7.7	5.9	7.2	6.8
Hand Size	Object Size	Grip Type	FDS Index	Middle	Ring	Little	Average
5% Female	25 mm	Power	6.0	13.6	12.6	10.5	10.7
95% Male	25 mm	Power	10.3	14.1	14.6	12.3	12.8
5% Female	60 mm	Power	2.8	8.7	8.6	7.3	6.8
95% Male	60 mm	Power	5.0	10.5	11.7	8.9	9.0
5% Female	25 mm	Pinch	4.6	4.2	4.4	5.8	4.7
95% Male	25 mm	Pinch	6.7	8.0	6.4	7.7	7.2

6.2.2 Insulator placement

The second example is 'insulator placement' job in the spark plug manufacturing plant. The video clip of this job was obtained from the study by Latko et al. (Latko, Armstrong et al. 1997; Latko, Armstrong et al. 1999). The objective of this job was to put the insulators on the pins which are moving in the lateral direction. The worker approached and grasped multiple insulators from the box, moved the insulators about 20 cm forward, and put those insulators on the pins. Five thousand insulators were placed on the pins every hour. Figure 6.5 shows the screenshots of the job. For analysis of the job, we assumed that the worker's hand size was 50% female and the distance between the pins was approximately 7 cm based on our observation of the video.

Figure 6.5 Insulator placement job. The worker grasped the insulators and put them on the pins moving in lateral direction

- **Posture prediction**

As the model could not accommodate multiple objects, we assumed a larger object size can represent multiple objects. The object shape was assumed to be a cylindrical shape and its diameter was assumed to be 25 mm. The object was placed so

that the long axis of the object was perpendicular to the palm. The predicted posture is shown in Figure 6.6. As the contacts were detected for only the index and middle finger, the ring and little fingers were flexed until they made contact with the palm or reached the maximum range of motions of each joint.

Figure 6.6 Predicted posture by the 3-D kinematic model during grasping an insulator.

Table 6.5 Joint angles(°) in predicted posture by the 3-D kinematic model

	MCP	PIP	DIP
Index	64	2	24
Middle	58	14	24
Ring	90	81	56
Little	90	80	64
Thumb	IP	MCPFE	MCPAA
	10	18	9
	CMCFE	CMCAA	CMCPS
	38	12	-103

- **Space envelope**

The space envelope was calculated from the predicted posture. As the hand moved not only in the axial direction of the pins but also in other directions slightly, we assumed 10º rotations as we did in Chapter 3.

Figure 6.7 shows the space envelope along the axis of the insulator. As the worker grasped the insulator using three fingers (thumb, index, and middle fingers), the least space was required at 0~25 mm range. As the distance from the end of the finger tips becomes larger, more space was required, because of the palm areas. The distance between the pins was assumed to be 7 cm. Pins on either side were regarded as obstructions. The maximum lateral dimension is very close to the obstruction, which may interfere with the hand during the task. But the placement of the insulator on the pins does not require larger translation in the axial direction. If we assume that the hand moved about 3 cm in axial direction to place the insulator on the pins, we need only look at the space envelope in the 0~30 mm range. The predicted space envelope shows that this job does not have interference from obstructions at 0~50mm range. Therefore, this task can be performed without any interference from obstructions.

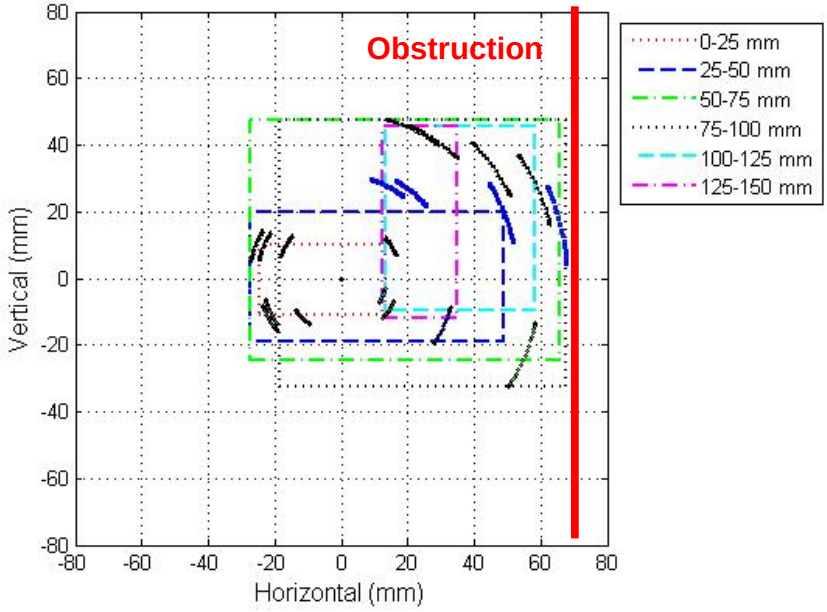

Figure 6.7 Hand space envelope during 'insulate glaze' job.

- **Tendon excursion**

The cumulative tendon excursion at the wrist for this job was calculated in Chapter 5. Now we can estimate tendon excursions at finger joints, based on the predicted hand posture. Figure 6.8 shows that the worker grasped the insulators twice during this time frame.

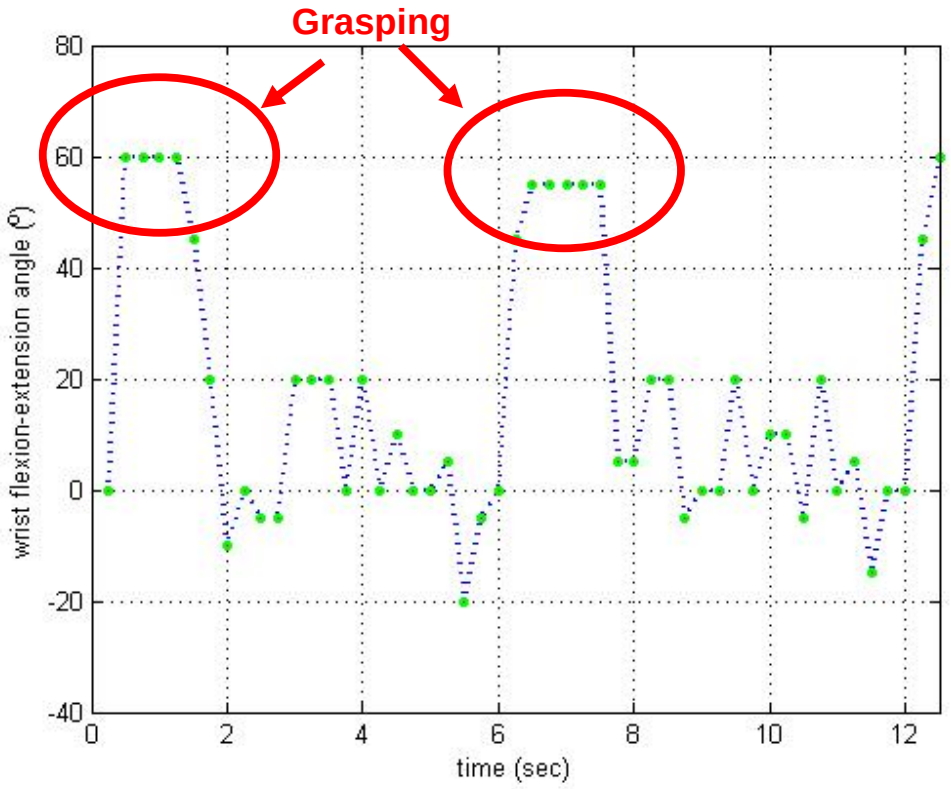

Figure 6.8 Time-based analysis of the wrist angle during 'insulate glaze' job. The worker grasped the insulators at the time marked by two circles.

Table 6.6 shows the estimated cumulative tendon excursions of FDP and FDS tendons during the 'insulate glaze' job. The tendon excursion by the wrist movement is larger than the tendon excursion at the finger joints. However, the tendon excursions at some fingers is about 52 to 56 % of the tendon excursions at the wrist. We simplified the grasping procedure to be able to simulate the final posture, but the worker grasped multiple objects and used the fingers while placing the insulators on the pins. Inclusion of all these finger movements will increase tendon excursions at the fingers. Analysis of tendon excursion without observing finger movement may not correctly estimate total tendon excursions. Therefore, it is necessary to investigate the tendon excursions by the finger movements as well as by the wrist movements to obtain more accurate results.

Table 6.6 Cumulative tendon excursions during the observed time frame (mm)

		MCP	PIP	DIP	Sum	Wrist
FDP	Index	9.8	6.0	0.8	16.6	51.9
	Middle	11.4	4.2	1.0	16.6	-
	Ring	15.1	11.8	2.2	29.1	-
	Little	12.6	13.1	2.4	28.1	-
		MCP	PIP	DIP	Sum	Wrist
FDS	Index	11.6	4.7	1.4	17.7	59.1
	Middle	13.5	3.3	1.7	18.5	-
	Ring	17.9	9.2	3.9	31.1	-
	Little	14.9	10.3	4.4	29.5	-

6.3 SUGGESTIONS FOR FUTURE RESEARCH

6.3.1 Kinematics model

To predict various hand postures such as tip pinch grip or two or three finger pinch grips, the model will require flexion-extension and pronation-supination of the fourth and fifth metacarpal phalanges about long axis of the third metacarpal phalanx.

The kinematic structure of our hand model is not perfectly congruent with the anatomic structure of the hand. First, four metacarpals in the palm are placed in parallel, but they were modeled as four bones spreading from the wrist. Many kinematic models (Buchholz and Armstrong 1992; Lee and Zhang 2005; Abdel-Malek, Yang et al. 2006) used the same kinematic structure as this model. Such kinematic structure enables the model to have scalability based on the external hand size such as hand length and hand breath, because the model used anthropometric data by Buchholz (1992) who modeled hand anthropometry as a function of external hand measurement. Second, the CMC joints of the second and fourth digits were not modeled in this study. Those joints enable the hand to change its shape to make the transverse arch during tip pinch posture or in grasping spherical objects. Savescu et al.(2005) added two more degrees of freedom in their hand model to represent the transverse arch of the hand. This can lead to better prediction of hand posture during tip pinch or grasping a spherical shaped object, but doesn't seem to have much effect on the hand posture during grasping cylindrical objects. To predict various hand postures such as tip pinch grip or two or three finger pinch grips, a model including more degrees of freedom will be necessary.

Hand posture predictions might be improved by using a real hand shapes instead of simplified description of hand segments with truncated cones.

For simple and reasonable representation of the hand shape, hand segments were modeled as truncated cones. These simplified depiction of the hand shape is not perfectly congruent with the real hand shapes, particularly in the thenar palm area. The model can be improved by importing the scanned surface data of the hand as an array of points. The contact algorithm can still be used with the imported surface data to predict hand postures. Also, it would improve aesthetics and fidelity of the model.

Hand posture during grasping unconstrained object can be predicted by modification of the code of hand model using a forward kinematics.

Subjects in our experiments grasped space-fixed and vertically located objects, and the model was developed based on these data. If the objects are not fixed in space or their orientation are in other directions, the resultant hand postures can be different from our results. To predict the hand posture more accurately in such situations, modification of the hand model is required. Using a forward kinematics based on the information of contact points between hand segments and object and the finger joint angle profile, the movement direction of object can be calculated. The object will be moved in calculated direction until it meets another constraint such as the palm or opposing thumb. It is also needed to perform the experiments to see how removal of object constraints affects predicted hand postures. Grasping a non-constrained object can also change the object location and orientation with respect to the hand, which ultimately influence the grip posture.

A study should be performed to determine how well the model predicts hand postures in other shapes of objects.

Only cylindrical objects were used to validate the model. Other object shapes can be used in this contact-based model if the surface information can be imported into the model as an array of points. Current model has a function that can predict the hand postures during grasping rectangular and ellipsoidal objects, but they have not been validated through experiments. More experimental studies to validate the use of other object shapes will improve the model's application to broader situations.

Dynamic space envelope, which is the space required during reach and grasp, can be predicted by use of the kinematic model.

One of the potential extensions of hand space envelope study is to estimate the dynamic space envelope, which means the required space during reaching and grasping. Chapter 3 focused on the hand space envelopes after grasping was completed, but the space required during reach and grasp procedure is also important to improve work environment minimizing interference with obstructions. To estimate the dynamic space envelope, appropriate modeling of behavioral characteristics of the hand - such as finger joint angle, wrist trajectory, and wrist angle as a function of hand size, grip type, and object properties - need to be explored first. Based on these data, the dynamic space envelopes can be estimated using the kinematic model in a similar way as the study in chapter 3.

Tendon excursions not only by the wrist movement but also by finger movement should be included to assess the risk of MSDs by tendon excursions.

Observation was made only for the wrist angles in time-based analysis (Chapter 5), but for more detailed analysis of tendon excursion, the finger movements also need to be considered as shown in Chapter 6. The finger movements cannot be easily measured without using special equipment such as an electromechanical goniometer or position markers. An alternative approach is to develop models using laboratory data that can be used to predict MCP (metacarpophalangeal), PIP (proximal interphalangeal), and DIP (distal interphalangeal) joint angles of the hand (Choi and Armstrong 2007). Such models can then be used to construct motion sequences based on descriptions of work elements and work objects.

6.3.2 Biomechanical model

Addition of friction force and hand grip kinetics can improve the model's applicability.

Contact-based model may not be sufficient to predict the hand posture for some tasks. For example, hand posture during holding a cylindrical object vertically cannot be predicted by contact-based model only, because the friction force is acting to keep the object from sliding out of the hand. To predict friction force, hand grip kinetics is necessary because the friction forces are dependent on the normal forces acting on hand segments. As discussed in chapter 2, forces acting on the hand segments can change the joint angles of fingers, particularly in DIP joints. Inclusion of friction force and

hand grip kinetics in the model will be necessary to predict hand postures in more realistic situations.

Hand posture during grasping unconstrained object can be predicted by modification of the code of hand model, considering force equilibrium during grasping.

Subjects in our experiments grasped space-fixed and vertically located objects, and the model was developed based on these data. If the objects are not fixed in space or their orientation are in other directions, the resultant hand postures can be different from our results. To predict the hand posture more accurately in such situations, modification of the hand model is required to include force equilibrium during grasping. It is also needed to perform the experiments to see how removal of object constraints affects predicted hand postures. Grasping a non-constrained object can also change the object location and orientation with respect to the hand, which ultimately influence the grip posture.

To predict hand postures grasping non-constrained objects, the biomechanical aspects of the hand and the force equilibrium between the gripping object and hand need to be considered.

Prediction of hand posture for non-constrained objects may result in different results, because the gripping object can be moved during grasping. To better predict hand posture for non-constrained objects, the biomechanical aspects of the hand and force equilibrium during grasping process should be considered. First, a forward

dynamic model describing finger movements during grasping needs to be developed. Then consideration of force equilibrium between objects and hand, the movement of the object can be determined throughout the grasping process. The object will be moved to the direction to which the resultant force is acting until it meets another constraints such as the palm or the thumb.

Empirical studies of the relationship between external load and tendon forces can be used to enhance the kinematic model for study of musculoskeletal disorders.

Through chapter 5 and chapter 6, tendon excursions at the wrist and at each finger were investigated. As mentioned in chapter 5, tendon excursion is an important parameter used in the most popular model (tenosynovitis) for pathogenesis of MSDs. However, many other factors – friction, tension force, contact pressure, and heating on the tendon – are also used in different models of pathogenesis of MSDs (Jessurun, Hillen et al. 1987; Cobb, An et al. 1994; Szabo, Bay et al. 1994; Cobb, An et al. 1995; Rempel, Dahlin et al. 1999). It was not possible to include such frictions and other forces with the kinematic model of the hand. However, it may be possible to determine an empirical relationship between external forces and tendon forces that can be used with kinematic model (Chao, Opgrande et al. 1976; Armstrong 1982; Valero-Cuevas, Zajac et al. 1998; Dennerlein 2005).

Gender difference can be investigated through supplemental experiments and development of kinetic model.

This study did not address gender difference directly. Gender difference is an important aspect that needs to be considered in the study of human subjects. Previous studies have not shown a gender difference above and beyond hand size (both hand length and hand breadth) and hand strength. The kinematic model suggested in this study can partly address gender difference from the aspect of hand size, but cannot be applied to explore the difference caused from the hand strength. Supplemental experiments and development of kinetic model of the hand will enable for us to investigate gender difference caused by hand size and hand strength.

Use of deformable hand might improve the accuracy of the model particularly at DIP joints of the fingers.

All the solutions in this study were based only on kinematics with rigid body modeling of hand segments. But contact between hand and grip object causes skin deformations particularly at the distal phalanges, which can affect the DIP joint angles at final hand posture. Soft tissues such as skin is nonlinear and viscous (Zheng and Mak 1996; Rubin, Bodner et al. 1998). Palmar tissue of the hand is initially very compliant and reaches a large deformation at low load. Combined use of the kinematic model with skin deformation model from mechanical properties of the soft tissue (Serina, Mockensturm et al. 1998; Mazza, Papes et al. 2005) might lead to better prediction of hand postures, particularly in DIP joints which were found to be the most sensitive to the force.

6.4 REFERENCES

Abdel-Malek, K., J. Yang, T. Marler, et al. (2006). "Towards a new generation of virtual humans." Int. J. Human Factors Modelling and Simulation **1**(1): 2-39.

Armstrong, T. J. (1982). Development of biomechanical hand model for study of manual activities. Anthropometry and Biomechanics: Theory and Application. K. K. Easterby R., Plenum.

Armstrong, T. J. and D. B. Chaffin (1978). "An inverstigation of the relationship between displacements of the finger and wrist joints and the extrinsic finger flexor tendons." Journal of biomechanics **11**: 119-128.

Armstrong, T. J. and D. B. Chaffin (1979). "Some biomechanical aspects of the carpal tunnel." J Biomech **12**(7): 567-70.

Buchholz, B. and T. J. Armstrong (1992). "A kinematic model of the human hand to evaluate its prehensile capabilities." J Biomech **25**(2): 149-62.

Buchholz, B., T. J. Armstrong and S. A. Goldstein (1992). "Anthropometric data for describing the kinematics of the human hand." Ergonomics **35**(3): 261-73.

Chao, E. Y., J. D. Opgrande and F. E. Axmear (1976). "Three-dimensional force analysis of finger joints in selected isometric hand functions." J Biomech **9**(6): 387-96.

Choi, J. and T. J. Armstrong (2007). Quantitative analysis of finger movements during reaching and grasping tasks. ASB annual meeting, Stanford, CA.

Cobb, T. K., K. N. An and W. P. Cooney (1995). "Effect of lumbrical muscle incursion within the carpal tunnel on carpal tunnel pressure: a cadaveric study." J Hand Surg [Am] **20**(2): 186-92.

Cobb, T. K., K. N. An, W. P. Cooney, et al. (1994). "Lumbrical muscle incursion into the carpal tunnel during finger flexion." J Hand Surg [Br] **19**(4): 434-8.

Dennerlein, J. T. (2005). "Finger flexor tendon forces are a complex function of finger joint motions and fingertip forces." J Hand Ther **18**(2): 120-7.

Endo, Y. and S. Kanai (2006). An Application of a Digital Hand to Ergonomic Assessment of Handheld Information Appliances. Digital Human Modeling for Design and Engineering Conference, Lyon, France.

Garrett, J. W. (1971). "The adult human hand: some anthropometric and biomechanical considerations." Hum Factors **13**(2): 117-31.

Jessurun, W., B. Hillen, F. Zonneveld, et al. (1987). "Anatomical relations in the carpal tunnel: a computed tomographic study." J Hand Surg [Br] **12**(1): 64-7.

Latko, W. A., T. J. Armstrong, J. A. Foulke, et al. (1997). "Development and evaluation of an observational method for assessing repetition in hand tasks." Am Ind Hyg Assoc J **58**(4): 278-85.

Latko, W. A., T. J. Armstrong, A. Franzblau, et al. (1999). "Cross-sectional study of the relationship between repetitive work and the prevalence of upper limb musculoskeletal disorders." Am J Ind Med **36**(2): 248-59.

Lee, J. W. and K. Rim (1990). "Maximum finger force prediction using a planar simulation of the middle finger." Proc Inst Mech Eng [H] **204**(3): 169-78.

Lee, S. W. and X. Zhang (2005). "Development and evaluation of an optimization-based model for power-grip posture prediction." J Biomech **38**(8): 1591-7.

Mazza, E., O. Papes, M. B. Rubin, et al. (2005). "Nonlinear elastic-viscoplastic constitutive equations for aging facial tissues." Biomech Model Mechanobiol **4**(2-3): 178-89.

Miyata, N., M. Kouchi and M. Mochimaru (2006). Posture Estimation for Design Alternative Screening by DhaibaHand - Cell Phone Operation. Digital Human Modeling for Design and Engineering Conference, Lyon, France.

Rempel, D., L. Dahlin and G. Lundborg (1999). "Pathophysiology of nerve compression syndromes: response of peripheral nerves to loading." J Bone Joint Surg Am **81**(11): 1600-10.

Rubin, M. B., S. R. Bodner and N. S. Binur (1998). "An elastic-viscoplastic model for excised facial tissues." J Biomech Eng **120**(5): 686-9.

Sancho-Bru, J. L., A. Perez-Gonzalez and G. J. Giurintano (2003). "A 3d biomechanical model of the hand for power grip." ASME **125**: 78-83.

Savescu, A. and L. Cheze (2005). Numerical model of the thumb. Digital Human Modeling for Design and Engineering Conference, Iowa city, IA.

Serina, E. R., E. Mockensturm, C. D. Mote, Jr., et al. (1998). "A structural model of the forced compression of the fingertip pulp." J Biomech **31**(7): 639-46.

Szabo, R. M., B. K. Bay, N. A. Sharkey, et al. (1994). "Median nerve displacement through the carpal canal." J Hand Surg [Am] **19**(6): 901-6.

Valero-Cuevas, F. J., F. E. Zajac and C. G. Burgar (1998). "Large index-fingertip forces are produced by subject-independent patterns of muscle excitation." J Biomech **31**(8): 693-703.

Zheng, Y. P. and A. F. Mak (1996). "An ultrasound indentation system for biomechanical properties assessment of soft tissues in-vivo." IEEE Trans Biomed Eng **43**(9): 912-8.

Appendices

Appendix A

Figure A.1 shows the GUI of the model. It consists of five parts: hand data input, posture input, object data input, grip type input, and 3-D graphical displays from four different viewpoints. In the hand data input part, the length of hand segments can be entered for each hand segment or predicted based on work by Buchholz, which models the hand anthropometry as a function of external hand measurements such as a hand length and a hand breadth (Buchholz, Armstrong et al. 1992). The percentile value of male or female can be chosen to accommodate the specified percent of the population. The object data input parts were designed so that the user can specify object shape, object size, object location, and object orientation. In posture input parts, the user can directly input joint angles of all joints, import joint angle profile, or choose to use the posture prediction algorithm. The grip type input parts enable the user to select grip types (e.g., power grip, pulp pinch grip) as needed. In 3-D graphical displays, the user can rotate and translate the displayed hand to desired orientations and locations.

Figure A.2 shows the structure of the hand model. The model is comprised of five modules. Hand data, object data, and posture data are input in the data input module. In the main module, the program determines mesh size, applies finger motion algorithm, and calculates the distances between hand segments and object using a contact algorithm. All matrix calculation including homogeneous transformation are processed in the mathematical module. The graphical display module is implemented for graphical display using OpenGL graphic function. The results of simulation are exported or displayed through the data output module.

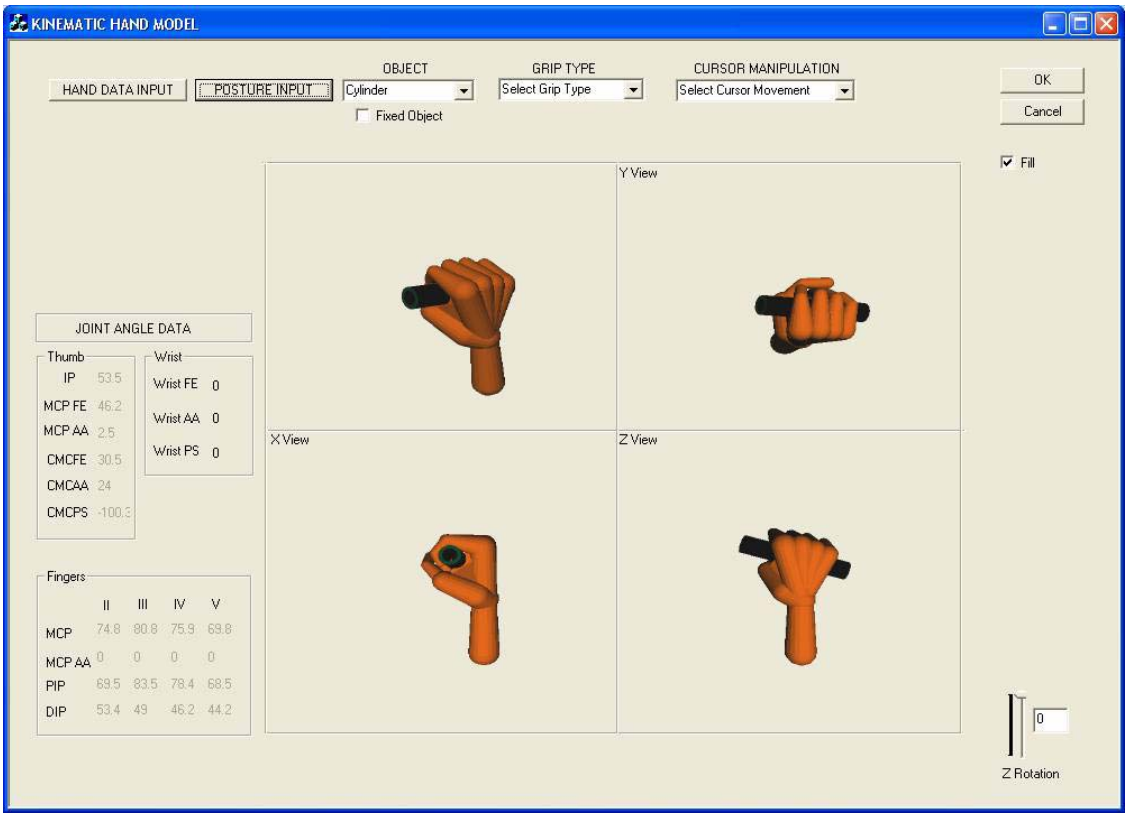

(a) Main GUI of hand model

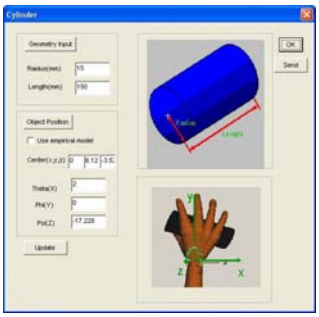

(b) Object data input

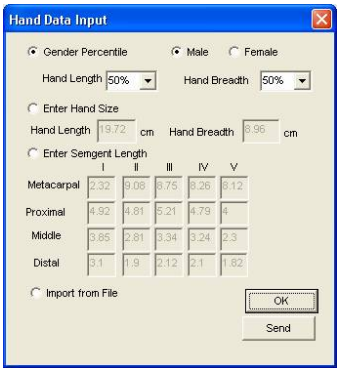

(c) Hand data input

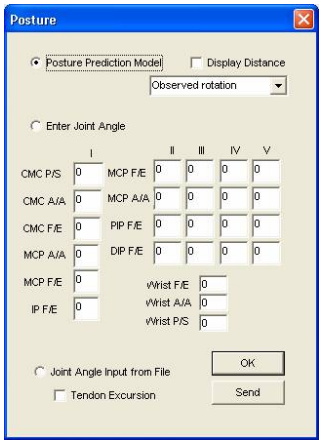

(d) Posture data input

Figure A.1 Graphical user interface (GUI) of the hand model. The model was implemented in visual C++ ® environment with OpenGL graphic function. (a) Main GUI of the hand model (b) object data input part (c) hand data input part (d) hand posture data input part

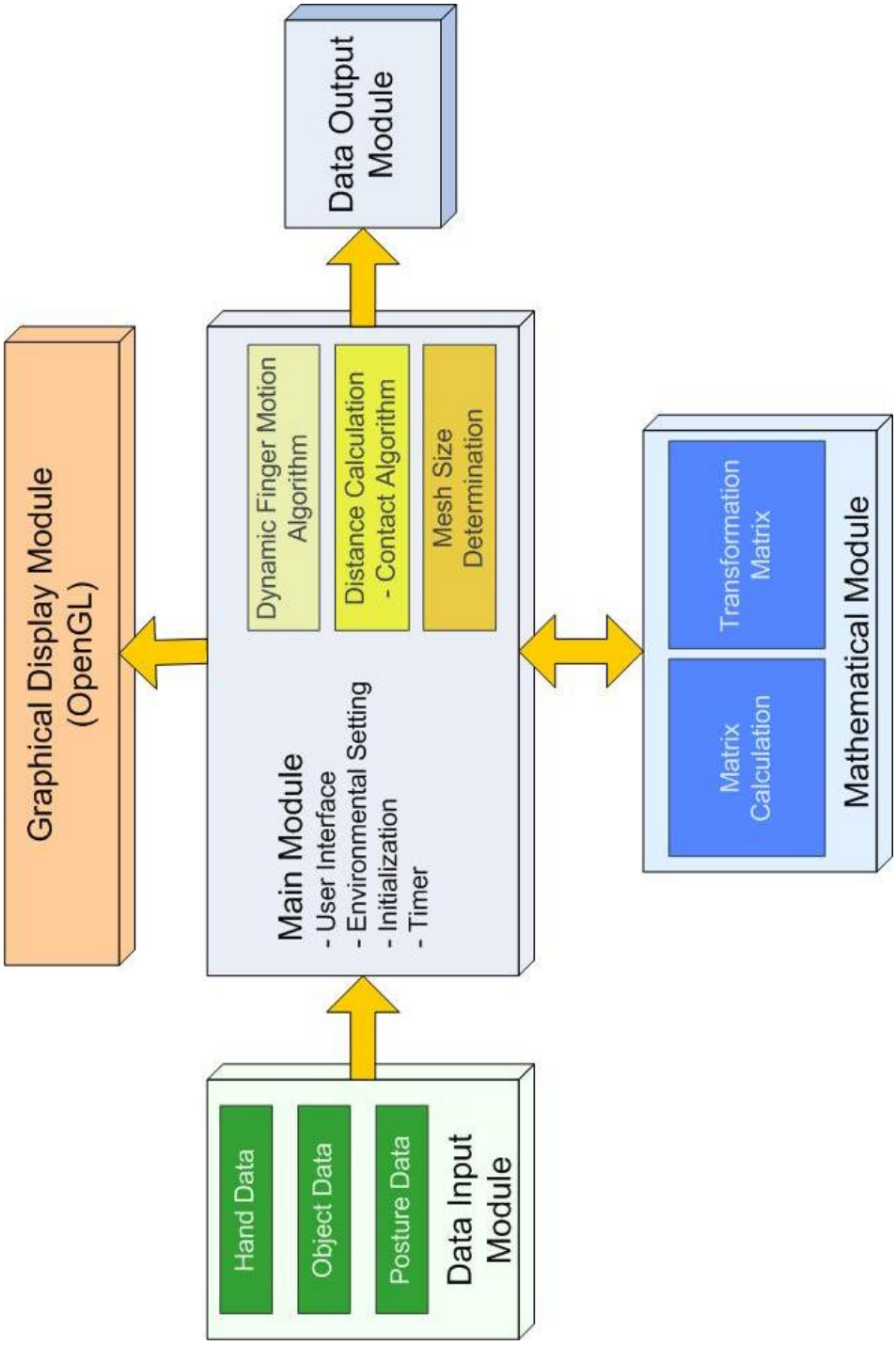

Figure A.2 The structure of the hand model. The program is comprised of five modules – data input module, main module, mathematical module, graphical display module, and data output module. Hand data, object data, and posture data are input in the data input module.

Mesh size

In using a minimum distance method, computation speed relies heavily on the number of meshes on the object surface and the hand. There is a trade-off between accuracy and speed. As the number of meshes gets larger, the accuracy of prediction gets better. On the other hand, as the number of meshes gets smaller, the computation speed decreases. To improve both the computation speed and accuracy, variable mesh sizes were applied to the model. Two methods were used to determine the number of meshes. First, the number of meshes in the object surface was modeled as a function of object size – in a cylindrical object, the number of meshes is dependent on the cylinder's diameter and length. Secondly, as the distance between a hand segment and object surface gets closer, the number of meshes on the hand segment increases.

Appendix B

Table B.1 Spatial variables during power grasp (Chapter 4)

Spatial Variables	Finger	Index			Middle			Ring		
	Joint	MCP	PIP	DIP	MCP	PIP	DIP	MCP	PIP	DIP
Initial		32.5±9.9	33.0±10.1	13.7±5.7	31.5±13.6	35.7±11.1	13.0±8.2	27.9±9.7	38.7±12.0	14.6±7.7
Open Angle	Lg (D:114 mm)	19.4±6.5*	15.1±6.5	6.5±3.6	8.1±5.2	18.3±8.9	4.9±2.7	8.8±4.4	13.5±7.3	5.5±3.1
	Med (D: 60 mm)	19.9±7.3*	24.1±8.5	8.7±4.8	12.2±7.4	25.9±10.5	7.0±3.8	14.4±6.2	24.1±10.2	7.4±3.4
	Sm(D: 26 mm)	22.3±6.7*	24.6±9.7	9.1±5.0	15.9±8.9	26.4±11.5	7.4±5.5	16.4±6.5	28.0±11.2	8.8±5.3
Final Angle	Lg (D:114 mm)	25.9±9.0	29.3±6.6	20.8±5.4	22.2±10.6	28.4±8.2	22.7±8.1	22.2±7.7	23.9±7.6	20.2±8.5
	Med (D: 60 mm)	38.6±12.2	54.6±7.1	29.9±5.6	48.9±8.4	48.2±7.9	35.0±9.9	45.2±8.9	44.5±9.1	33.4±8.8
	Sm(D: 26 mm)	71.2±6.8	79.7±5.9	44.4±9.9	79.9±4.8	80.0±5.7	52.1±8.8	73.4±5.0	80.1±6.9	52.3±6.0
Spatial Variables	Finger	Little			Thumb					
	Joint	MCP	PIP	DIP	IP	MCPFE	MCPAA	CMCFE	CMCAA	CMCPS
Initial		28.6±7.6	33.2±11.3	19.1±9.8	13.9±5.7	17.6±9.2	8.8±6.3	28.6±10.4	12.8±10.3	-89.6±7.8
Open Angle	Lg (D:114 mm)	14.1±7.8	9.6±6.7	9.3±5.1*	10.7±4.1*	3.6±7.5	14.1±6.8*	-5.0±5.9	25.0±8.4*	-88.2±9.8*
	Med (D: 60 mm)	21.3±6.7	18.5±8.2	10.2±5.0*	10.7±3.8*	5.9±6.9	15.1±6.9*	9.9±15.9	17.3±15.4*	-85.4±10.7*
	Sm(D: 26 mm)	23.5±6.1	21.1±8.7	11.1±6.3*	9.1±2.8*	11.4±6.9	13.0±7.2*	14.3±11.6	19.1±9.8*	-88.6±8.6*
Final Angle	Lg (D:114 mm)	20.2±9.1	15.3±10.5	24.3±11.9	26.4±6.6	13.7±13.8	17.7±8.7	-8.7±13.0	22.0±10.4*	-86.7±20.0
	Med (D: 60 mm)	40.7±13.3	34.3±10.8	32.3±9.2	49.9±10.9	13.0±12.4	15.5±7.7	20.1±6.5	17.5±12.5*	-96.8±14.6
	Sm(D: 26 mm)	69.8±7.4	61.1±9.0	55.2±6.9	51.0±16.2	30.6±13.2	10.2±8.5	38.2±4.5	16.0±8.4*	-106.7±6.5

Table B.2 Spatial variables during pinch grasp (Chapter 4)

Spatial Variables	Finger	Index			Middle			Ring		
	Joint	MCP	PIP	DIP	MCP	PIP	DIP	MCP	PIP	DIP
Initial		32.6±13.5	27.6±8	11.1±4.1	35.3±12.4	27.6±12.3	8.9±6.2	31.3±7.8	30.6±12.3	11.2±4.3
Open Angle	Lg (D:114 mm)	18.4±8.4	15.2±8.1	6.7±3.6	11.7±4.9	12.9±8.7	5.7±4.1	13.4±4.3	10.9±8.2	7.3±3.4
	Med (D: 60 mm)	29.0±6.5	14.8±8.1	6.5±2.7	27.8±7.9	14.5±10.2	5.2±2.5	27.1±5.1	12.4±7.8	6.5±3.5
	Sm(D: 26 mm)	36.4±7.3	18.9±10.4	8.5±2.4	37.8±7.3	17.1±13.7	6.2±3.3	33.1±5.6	22.3±10.8	8.4±2.4
Final Angle	Lg (D:114 mm)	28.0±13.2	23.3±5.2	15.8±4.9	23.4±14.7	19.7±7.4	13.9±8.8	26.3±7.2	12.8±9.2	11.9±5.5
	Med (D: 60 mm)	42.0±9.6	22.9±11.2	19.3±6.7	47.2±8.7	15.5±9.2	14.4±7.4	47.2±6.9	11.3±7.3	10.4±4.3
	Sm(D: 26 mm)	56.5±9.4	17.6±11.5	18.6±9.6	59.5±12.0	19.8±18.6	15.0±8.1	53.6±8.4	27.1±14.9	10.9±2.5
Spatial Variables	Finger	Little			Thumb					
	Joint	MCP	PIP	DIP	IP	MCPFE	MCPAA	CMCFE	CMCAA	CMCPS
Initial		33.1±8.6	21.8±9.9	12.9±7.7	13.1±5.1	12.8±12.3	1.6±13.4	-44.4±17.1	12.7±12	-93.7±13.3
Open Angle	Lg (D:114 mm)	23.6±7.5	6.4±3.6	7.8±4.3	10.1±5.3	5.0±12.0	9.5±9.6	-34.5±12.3	19.8±11.0	-86.7±10.0
	Med (D: 60 mm)	32.7±5.9	4.1±2.6	6.5±3.2	9.6±2.9	7.4±10.7	4.6±12.5	-39.8±17.3	24.6±15.3	-90.7±10.5
	Sm(D: 26 mm)	38.4±5.9	8.1±4.2	10.0±7.3	10.8±5.4	5.2±14.7	5.2±11.5	-37.8±13.2	29.7±13.7	-108.5±10.1
Final Angle	Lg (D:114 mm)	32.4±6.8	10.2±5.4	12.1±11.4	14.5±7.2	10.4±11	8.6±10.3	-17.1±15.3	17.8±11.4	-87.7±9.7
	Med (D: 60 mm)	48.2±6.6	6.1±4.4	10.6±5.7	14.6±6.8	11.9±9.1	-3.1±16.0	-31.6±17.2	20.6±12.9	-100.0±10.7
	Sm(D: 26 mm)	59.1±5.0	10.2±5.6	21.4±14.2	17.6±6.4	7.9±14.6	4.7±15.2	-34.8±11.2	27.2±11.8	-122.1±13.6

Table B.3 Velocity variables during power grasp (Chapter 4)

Spatial Variables	Finger	Index			Middle			Ring		
	Joint	MCP	PIP	DIP	MCP	PIP	DIP	MCP	PIP	DIP
Minimum Velocity	Lg (D:114 mm)	-71.6±49.7	-70.4±44.7	-35.6±25.3	-116.1±67.6	-64.3±44.0	-34.7±30.7*	-91.7±64.2	-88.2±53.2	-43.4±37.3
	Med (D: 60 mm)	-49.7±49.3	-42.7±43.4	-27.4±30.5	-72.8±60.7	-44.5±47.7	-30.2±35.0*	-53.6±54.9	-52.7±49.4	-29.7±30.6
	Sm(D: 26 mm)	-41.2±34.5	-34.0±28.4	-22.2±16.6	-65.2±44.9	-34.5±31.1	-25.7±27.1*	-50.7±41.3	-45.1±29.8	-27.2±22.5
Maximum Velocity	Lg (D:114 mm)	34.8±15.5	66.2±28.9	48.9±20.5	58.6±22.8	62.0±38.5	74.1±22.4	57.8±30.9	64.7±36.7	59.5±22.5
	Med (D: 60 mm)	81.2±49.3	122.3±36.9	81.0±24.2	148.4±53.5	100.3±52.9	114.8±55.8	133.2±46.4	105.6±59	114.9±61.4
	Sm(D: 26 mm)	183.0±50.6	230.6±49.9	133.9±50.0	228.8±61.0	227.7±66.1	162.7±62.1	211.7±47.4	219.7±69	159.6±56.1
Spatial Variables	Finger	Little			Thumb					
	Joint	MCP	PIP	DIP	IP	MCPFE	MCPAA	CMCFE	CMCAA	CMCPS
Minimum Velocity	Lg (D:114 mm)	-61.0±41.2	-87.8±52.7	-50.1±44.3*	-13.8±25.3*	-38.6±29.1	25.8±11.9	-89.8±23.3	30.0±18.4*	35.2±19.9
	Med (D: 60 mm)	-32.2±33.4	-56.1±52.1	-41.1±50.3*	-18.3±13.5*	-36.7±28.0	21.0±8.7	-68.8±23.6	38.9±13.7*	22.4±30.0
	Sm(D: 26 mm)	-25.3±31.3	-47.6±33.0	-32.1±33.2*	-21.1±17.9*	-7.0±28.5	11.1±6.1	-39.4±18.0	26.9±14.9*	10.7±11.1
Maximum Velocity	Lg (D:114 mm)	31.7±26.3	40±34.3	58.6±35.7	71.0±35.0	27.5±31.8	-5.9±7.5	9.7±10.9	-17.5±14.1*	-15.9±27.4
	Med (D: 60 mm)	90.0±38.8	84.4±46.6	92.7±43.1	138.4±62.1	28.9±16.2	-5.0±5.2	30.0±30.0	-9.3±7.2*	-45.7±47.1
	Sm(D: 26 mm)	170.4±39.4	181.7±70.4	171.8±70.6	159.2±64	67.4±36.7	-15.4±11.8	83.4±45.5	-16.0±10.4*	-55.9±27.9

Table B.4 Velocity variables during pinch grasp (Chapter 4)

Spatial Variables	Finger	Index			Middle			Ring		
	Joint	MCP	PIP	DIP	MCP	PIP	DIP	MCP	PIP	DIP
Minimum Velocity	Lg (D:114 mm)	-33.3±31.8	-45.4±31.9	-25.3±21.4	-63.8±32.9	-54.7±44.1	-21.7±22.9	-46.1±32.4	-71.4±47.3	-23.0±18.0
	Med (D: 60 mm)	-17.6±12.4	-38.5±32.3	-21.4±21.7	-20.5±12.7	-38.2±34.8	-18.1±23.3	-14.8±11.2	-42.4±36.7	-14.1±15.2
	Sm(D: 26 mm)	-16.1±8.6	-31.7±28.4	-13.4±18.2	-17.8±13.2	-33.5±28	-11.4±20.8	-15.3±12.9	-32.8±31.2	-10.5±12.5
Maximum Velocity	Lg (D:114 mm)	24.7±22.4	43.1±30.7	34.7±12.6	32.9±22.3	42.0±28.3	31±22.6	34.9±19.4	20.9±18.1	16.4±11.3
	Med (D: 60 mm)	34.8±20.6	60.6±28.0	60.6±17.7	54.9±23.8	35.5±24.0	34.1±28.8	54.5±23.4	8.4±6.7	18.0±15.9
	Sm(D: 26 mm)	54.2±21.7	27.9±23.9	41.5±27.7	64.7±22.0	35.2±28.7	35.9±28.1	66.8±20.5	26.0±19.4	11.8±9.1
Spatial Variables	Finger	Little			Thumb					
	Joint	MCP	PIP	DIP	IP	MCPFE	MCPAA	CMCFE	CMCAA	CMCPS
Minimum Velocity	Lg (D:114 mm)	-24.8±24.7	-64.2±38.9	-30.1±31.8	-27.8±17	-31.8±34.8	35.0±29.5	-10.7±24.8	26.6±10.7	24.3±20.1
	Med (D: 60 mm)	-9.3±12.0	-31.5±25.1	-13.7±23.5	-9.1±13.1	-23.0±29.2	21.2±20	-11.1±22.7	22.3±6.6	11.2±17.3
	Sm(D: 26 mm)	-6.4±11.4	-33.4±23.2	-13.7±15.2	-6.6±16.6	-20.4±23.7	7.8±18.2	-12.5±29.8	21.0±8.4	4.8±17.7
Maximum Velocity	Lg (D:114 mm)	24.6±13.6	13.7±14.1	14.3±24.1	19.5±18.5	23.9±24.4	-10.5±15	71.7±41.9	-7.7±4.7	-10.3±10.9
	Med (D: 60 mm)	40.2±16.1	13.3±12.3	14.0±11.4	16.4±16.5	17.7±14.1	-28±29.4	46.5±37.0	-12.2±10.5	-27.4±12.7
	Sm(D: 26 mm)	53.6±14.2	13.4±10.4	40.7±40.1	27.2±17.4	14.4±10.1	-26.3±32.7	44.2±35.7	-8.9±6.8	-35.9±12.8

Table B.5 P-values for spatial variables. The effect tested was the object size (Chapter 4)

Finger	Joint	Power				Pinch			
		Open	Final	Min	MaX	Open	Final	Min	MaX
Index	MCP	0.1192	0.0000	0.0072	0.0000	0.0000	0.0000	0.0686	0.0049
	PIP	0.0000	0.0000	0.0001	0.0000	0.4539	0.2680	0.5354	0.0196
	DIP	0.0236	0.0000	0.0461	0.0000	0.2129	0.3567	0.3472	0.0019
Middle	MCP	0.0000	0.0000	0.0002	0.0000	0.0000	0.0000	0.0000	0.0024
	PIP	0.0005	0.0000	0.0043	0.0000	0.6011	0.5381	0.2905	0.7439
	DIP	0.0176	0.0000	0.4136	0.0000	0.7825	0.9391	0.5147	0.8855
Ring	MCP	0.0000	0.0000	0.0009	0.0000	0.0000	0.0000	0.0004	0.0014
	PIP	0.0000	0.0000	0.0000	0.0000	0.0051	0.0009	0.0372	0.0157
	DIP	0.0012	0.0000	0.0375	0.0000	0.3456	0.6234	0.1124	0.4557
Little	MCP	0.0000	0.0000	0.0000	0.0000	0.0000	0.0000	0.0185	0.0000
	PIP	0.0000	0.0000	0.0003	0.0000	0.0198	0.0550	0.0088	0.9940
	DIP	0.3553	0.0000	0.1577	0.0000	0.1999	0.0342	0.1417	0.0226
Thumb	IP	0.3884	0.0000	0.5842	0.0003	0.8105	0.4613	0.0012	0.3053
	MCPFE	0.0119	0.0006	0.0052	0.0006	0.8369	0.6807	0.5781	0.3883
	MCPAA	0.7135	0.0478	0.0002	0.0030	0.4304	0.0731	0.0197	0.1389
	CMCFE	0.0002	0.0000	0.0000	0.0000	0.5864	0.0072	0.9842	0.1154
	CMCAA	0.1904	0.2826	0.1001	0.1026	0.1799	0.1460	0.2230	0.2655
	CMCPS	0.6143	0.0023	0.0134	0.0108	0.0000	0.0000	0.0270	0.0000